

# Wind- and stack-assisted mechanical ventilation with heat recovery and night cooling

**Hviid, Christian Anker; Svendsen, Svend**

*Publication date:*
2012

*Document Version*
Publisher's PDF, also known as Version of record

# Wind- and stack-assisted mechanical ventilation with heat recovery and night cooling

## PSO project 339-24

**Christian Anker Hviid**
**Svend Svendsen**

Report R-282

Department of Civil Engineering
Technical University of Denmark

2012

Wind- and stack-assisted mechanical ventilation with heat recovery and night cooling
PSO project 339-24

Printed by DTU Byg
Department of Civil Engineering
Technical University of Denmark
ISBN: 9788778773678
ISSN: 1601-2917

# Preface

The report is the result of PSO project 339-24 'Naturlig ventilation med varmegenvinding og natkøling' (in Danish: 'Natural ventilation with heat recovery and night cooling'). It constitutes the practical implementation of multiple theoretical studies carried out in theses on master and Ph.D. level performed at the department. The core concept, the heat recovery unit, is designed for system purely naturally driven, hence the project title refers to natural ventilation. However, because of implementation compromises and market penetrability, the full scale system is based on a mixture of natural and forced ventilation, hence the report title was changed to to the more accurate 'Wind- and stack-assisted mechanical ventilation with heat recovery and night cooling'.

Project partners:

Christian Anker Hviid, Ass. Prof., DTU Byg / ALECTIA

Svend Svendsen, Prof., DTU Byg

Lars D. Christoffersen, forskningschef, ALECTIA

Dennis Naldal Jensen, R&D, Dantherm

# Acknowledgements

The project was initiated by professor Svend Svendsen, DTU Byg and gratefully funded by Dansk Energi, Rosenørns Allé 9, 1970 Frederiksberg C in conjunction with the participants in the project. Also significant funding came Campus Service at DTU and for that I wish to extend sincere thanks to Freddy Mortensen and Tommy Plesner. Dantherm provided the most crucial part of the system — namely the heat exchangers — after numerous discards of exchanger designs. For their patience a special thanks is extended to Dennis Naldal Jensen and Orla Sørensen from Dantherm.

# Abstract

The dual-sided issue of indoor environment and energy consumption have become increasingly important in building design. One possible solution is to ventilate by passive means, such as by stack effect and wind pressure, but this requires the development of new concepts and components. Here we have presented the outline of a heat recovery concept suitable for stack and wind-assisted mechanical ventilation systems with total system pressure losses of 74 Pa.

The heat recovery concept is based on two air-to-water exchangers connected by a liquid loop powered by a pump. The core element of the concept, a prototype of a heat exchanger, was developed based on design criteria about pressure drop, efficiency and production concerns. The exchanger is based on banks of plastic tubing cris-crossing the airflow, thus creating approximate counterflow between air and water. Round PE plastic tubing is used. The tubing is commonly used for water-based floor-heating systems. Oval or even wing shaped tubes may have better heat transfer and lower drag coefficient, but round tubes require less meticulous production procedures. The tubing used here is mass-produced, cheap, and flexible but the current design does require many fittings.

Multiple design proposals were modeled and investigated to determine the optimal solution with respect to pressure drop, heat transfer, and production feasibility. Software models were developed to simulate the temperature distribution within the tube bank.

The final design involves two parallel tubes cris-crossing the air fixated in a 'radiator' by tube bending brackets and spacers. The radiators are stacked in a staggered grid to force a more tortuous airflow and generate as much heat transfer as possible.

The performance was confirmed by comparing the pressure drop and heat transfer measured on a section with numerical fluid calculations and literature sources. The measurements and calculations agree reasonably well.

A full scale implementation was achieved in a part of building 118 at Dept. of Civil Eng., Tech. Univ. of Denmark. In this building the system supplies offices and two teaching rooms with fresh air. The mean specific fan power (SFP, in Danish: SEL-værdi) is measured to be approx. 240 $J/m^3$. The SFP of the entire system including fans, pump and controls is measured to be approx. 600-700 $J/m^3$. The total heat recovery efficiency of the system was measured to be 63%.

Night cooling is implemented in the CTS-system, which means that the building is cooled at night in warm summer periods based on the temperature sensor in a critical room. With the extremely low fan power consumption, the cooling is practically free.

# Resumé

Indeklima og energiforbrug er blevet stadig vigtigere i bygningsdesign, men de to aspekter er modsatrettede med konventionel teknologi. En mulig løsning er at ventilere passivt, det vil sige med tørre udnyttelse af opdrift og vindtryk, men det kræver udvikling af nye koncepter og komponenter. Her præsenterer vi et varmegenvindingskoncept, som er egnet til opdrift- og vindassisterede mekaniske ventilationsanlæg. Det implementerede ventilationsanlæg har et samlet systemtryktab på blot 40 Pa

Varmegenvindingenskonceptet er baseret på to luft-til-vand-varmevekslere, som er forbundet med et pumpedrevet væskekredsløb. Det centrale element i konceptet, en varmevekslerprototype, er blevet udviklet baseret på designkriterier om trykfald, effektivitet og produktionsduelighed. Veksleren er baseret på bundter af plastslanger, som i slag passerer luftstrømmen og dermed skaber modstrøm mellem luft og vand. Runde PE plastslanger anvendes. Plastrørene er almindeligt anvendt til vandbaserede gulvvarmesystemer. Mere aerodynamisk-formede rør kan have bedre varmeoverførsel og lavere luftmodstand, men runde rør kræver mindre omhyggelige produktionsprocedurer. Slangen bruges her fordi den er masseproduceret, billig og fleksibel. I udformningen, som præsenteres her, kræves dog en del koblinger.

I projektet blev adskillige designforslag modelleret og undersøgt for at bestemme den optimale løsning med hensyn til tryktab, varmeoverførsel og produktionsduelighed. Softwaremodeller blev udviklet til at simulere temperaturfordeling i rørbundtet.

Det endelige design består af to parallelle slangerør, som fastgøres i en 'radiator' med bukkebøjler og afstandsstykker. Radiatorerne stables i et forskudt gitter for at fremtvinge en mere bugtet luftstrøm, så så meget varme som muligt overføres.

Performance mht. tryktab og varmeoverførsel blev sammenlignet på en sektion med numeriske fluidberegninger og faglitteraturkilder. Målinger og beregninger er rimeligt vise rimeligt resultat.

Et fuldskalaeksperiment blev implementere i en del af bygning 118 ved DTU Byg. I bygningen forsyner systemet kontorer og to undervisningslokaler med frisk luft. Det gennemsnitlige specifikke elforbrug (SEL-værdi) er målt til ca. 240 $J/m^3$. SEL-værdien af hele systemet, herunder ventilatorer, pumpe og styring, er målt til at være ca. 600-700 $J/m^3$. Varmegenvindingseffektivitet for det samlede system er målt til 63%.

Natkøling er implementeret i CTS-systemet, hvilket betyder, at bygningen afkøles om natten i varme sommerperioder. Styringen sker på basis af temperaturføleren i et kritisk rum. Med det ekstremt lave strømforbrug til ventilatorer, er kølingen praktisk taget gratis.

# Table of Contents

# Chapter 1

# Introduction

The European building sector is responsible for about 40% of the total primary energy consumption. To promote cost-effective improvement of the overall energy performance of buildings, the European Union launched in 2002 the Energy Performance of Buildings Directive (EPBD 2002/91/EC) (EPBD, 2010). One of the key issues of the directive is to set a holistic approach on energy performance of buildings that covers the energy needs for space and hot water heating, cooling and lighting. Another key issue is the revision of requirements every five years. In the Danish context, the revisions are set to reduce the 2006 level in two steps with 25% in 2010 and 50% in 2015. Currently low-energy class 2020 has also been introduced, a 'near-zero' energy class. The magnitude of reduction is 25% of 2006 consumption (equal to 25 $\mathrm{kWh/m^2}$. Therefore, it is important to show feasible technical solutions that can comply with the requirements of 2020.

## 1.1 Background

Power consumption in new buildings due to ventilation and lighting constitutes a major part of the total energy consumption. Conventional mechanical ventilation solutions are usually based on costly plant installations, space-consuming duct penetrations and energy consuming fans. Generally, installations are not integrated in the building at an early stage in the design process, because historically it has been customary to divide the design of buildings in segregated activities each related to the construction side or the installation side. By considering the ventilation as an installation separated from the rest of the building the interaction with the building is ignored.

Natural ventilation solutions require a different approach to building design. The ventilation scheme makes active use of the building rooms to supply and extract air and in general the ventilation design and building design are not segregated activities. Rather the design of natural ventilation requires the gap between architecture and function to be bridged. However, supplying fresh air through openings in the facade close to the occupied zone causes draught and complaints especially during the winter season (Larsen et al., 2006).

Table 1.1 illustrates some current, typical properties of natural and mechanical ventilation schemes. Natural ventilation suffers from heat loss and comfort risks while mechanical ventilation excel in theses areas but at the price of high power consumption. The hybrid ventilation approach is to combine the advantages of both systems to achieve mechanical control, thermal comfort and heat recovery with low power consumption.

Most hybrid systems are two-mode or mixed-mode. Two-mode schemes require two fully autonomous installations of a natural and a mechanical system, and mixed-mode systems operate by natural stack ventilation and a helping fan. The former requires an inordinate investment and the operation is challenging during transitional seasons. The latter suffers from draught and/or

Table 1.1: Typical properties of different ventilation schemes.

| | Natural | Mechanical | Passive |
|---|---|---|---|
| Heat recovery | ☹ | ☺ | ☺ |
| Fan power | ☺ | ☹ | ☺ |
| Free cooling | ☺ | ☹ | ☺ |
| Airflow control | ☹ | ☺ | ☺ |
| Thermal comfort | ☹ | ☺ | ☺ |

lack of heat recovery.

## 1.2 Objective

The objective of the project is to develop heat recovery systems for natural ventilation with centralized intake and exhaust. Consequently natural ventilation with heat recovery may become a realistic alternative to conventional mechanical ventilation with large thermal and electrical energy savings and comfort improvements. Additionally the design of the system will improve the night cooling potential as running the fans at night is energy cost effective. This saves electrical energy for cooling. The project focuses on the development of heat recovery units with very low pressure loss, couplings and control strategies. During the project process, fans were also included in the system, thus the title of this report was changed to 'Stack and wind-assisted mechanical ventilation systems'.

## 1.3 Contents

The main body of this report is divided as follows. Chapter 2 describes the overall concept developed for natural ventilation with heat recovery. Chapter 3 deals with the development of a heat exchanger suitable for the task. Chapter 3 describes the performed tests on a preliminary section of the heat exchanger. Chapter 4 describes the results of the full scale tests. Chapter 5 concludes on the results and the project. Appendices holds details on the model framework and computer code.

# Chapter 2

# Stack and wind-assisted mechanical ventilation

The ventilation concept that is described in this chapter is a condensate of multiple feasible concepts. The criteria that lead to the presented solution are the possibility of heat recovery, low energy consumption, low risk of draught and low total costs.

The hybrid ventilation system that is presented here is a one-mode system of balanced mechanical system with extremely low pressure losses. We believe that the hybrid approach where only one mode exists has several advantages in temperate climatic conditions:

- One-mode systems do not require the implementation and inordinate investment of two separate ventilation systems in the same building
- One-mode systems require only one control system which makes it simpler to control
- Ducted systems distribute fresh supply air as intended because conventional dampers and balancing may be applied
- Ducted systems easily employ heat recovery and filtration
- Ducted systems with heat recovery do not suffer from draught risks in the occupied zone
- Frequency-controlled fans ensure steady and continuous performance by leveling out natural fluctuations while still allowing stack and wind to assist
- One-mode systems do not suffer from shifts in the neutral plane due to thermal stratification (Li et al., 1999)
- One-mode systems may exploit the stack from temperature drop in summer nights to provide night ventilation
- Conventional low-pressure mechanical systems suffer from uncontrollable stack. In the approach here the system is designed to actively exploit the stack effect

## 2.1 Concept

Figure 2.1 illustrates the building integrated ventilation concept. The concept is designed for maximum stack effect and for maximum responsive building integration. An embedded concrete

duct leads the fresh air through an electrostatic precipitator, through the first heat recovery coil and distributes it to the floors via separate ducts to each floor. On each floor supply ducts feeds the diffuse ceiling ventilation system, see (Hviid and Svendsen, 2012). The extract air flows from all floors via separate vertical ducts to the second heat recovery coil above the roof. Heat is transferred from the second coil in the exhaust to the first coil in the air intake. The recovery coils are linked with a pump-powered liquid loop. The properties of the employed coils are described in chapter chapter 3 and in even more detail by (Hviid and Svendsen, 2011).

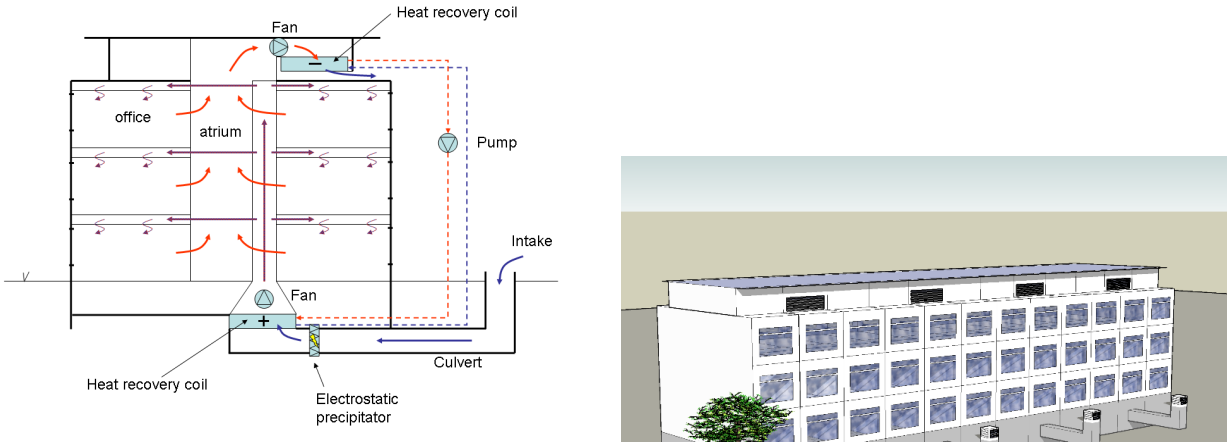


(a) Cross section (b) 3D rendering

Figure 2.1: Proposed building integrated ventilation concept.

The objective of the design is to achieve whole-year comfort ventilation at extremely low fan power consumption as well as total energy consumption and to provide sufficient night cooling through the same system purely by stack. A parallel objective is to use components with measured performances whether they are commercially available or are developed prototypes.

## 2.2 Air transport

Replacing the used air in a ventilated room with outdoor air requires transport of the air. Air flows from regions with high pressure to regions with low pressure. In mechanical ventilation fans create the pressure difference which transport the air molecules. In natural ventilation the pressure difference is induced by forces from wind and density. Wind creates positive pressure on the windward side and negative pressure on the leeward side. The density difference between two volumes of air causes the heavier to sink and the lighter to rise. In practice, density is proportional to temperature which is why hot fluids rise and colder fluids sink. Another commonly used term for the latter effect of rise and sink is *stack*.

### 2.2.1 Stack

In low-pressure ventilation systems the stack effect due to temperature differences between inside and outside is of significant magnitude. To illustrate the significance of the stack effect we present a small example: A building with a height difference between inlet and outlet of $h = 12\,\mathrm{m}$ and with a temperature difference of 15 °C between indoors and outdoors experiences a stack effect

$\Delta p$ of (equation 2.1):.

$$\begin{aligned} \Delta p &= (\rho_{out,5^\circ C} - \rho_{in,20^\circ C}) \cdot g \cdot h \\ &= (1.270 - 1.205)\text{kg/m}^3 \cdot 9.81\text{m/s}^2 \cdot 12\text{m} \\ &= 7.7\text{Pa} \end{aligned} \tag{2.1}$$

The concept presented here exploits the stack effect to induce airflow but it is not uniformly distributed across floors. The ground floor has a taller internal *column* of warm air than the third floor. This gives rise to differences in stack pressure between floors and consequently uneven air distribution. Equation 2.2 illustrates the different stack pressures between 1st floor and 3rd floor.

$$\begin{aligned} \Delta p_{1stfloor} &= (1.270 - 1.205)\,\text{kg/m}^3 \cdot 9.81\,\text{m/s}^2 \cdot 8\,\text{m} \\ &= 5.1\,\text{Pa} \\ \Delta p_{3rdfloor} &= (1.270 - 1.205)\,\text{kg/m}^3 \cdot 9.81\,\text{m/s}^2 \cdot 4\,\text{m} \\ &= 2.6\,\text{Pa} \end{aligned} \tag{2.2}$$

In section 2.2.1 it is shown that the pressure drop is related to the squared flow rate. Thus we see that even small changes in pressure have a large impact on the flow rate. This means that the scale of nonuniform air distribution between floors is even larger than the difference between 5.1 and 2.6 Pa first suggests.

Dampers are necessary to balance the airflow to each floor.

### 2.2.2 Wind

The wind induces different pressures on the building envelope. The windward side experiences higher pressure than the ambient conditions and the leeward side experiences negative pressure. The pressure distribution is depicted on Figure 2.2. The effect of the wind can be of significant magnitude. To illustrate the significance we use the previous example: A building with a height of $h = 12\,\text{m}$ and with an outdoor temperature 5 °C. The reference wind speed $v_{ref}$, also denoted meteorological wind speed and measured at 10 m, is set to the mean wind speed in the Danish Test Reference Year. Then the wind pressure $\Delta p$ of the windward facade is (equation 2.3):

$$\begin{aligned} \Delta p &= C_p \cdot \frac{1}{2} \cdot \rho_u \cdot v_{ref}^2 \\ &= 0.5 \cdot \frac{1}{2} \cdot 1.270\,\text{kg/m}^3 \cdot (4.4\,\text{m/s})^2 \\ &= 6.1\,\text{Pa} \end{aligned} \tag{2.3}$$

On a flat roof the wind pressure coefficient $C_p$ is negative (approx. -0.7) because the building shape forces the wind to speed up across the roof and this creates locally lower pressure conditions. Consequently, the roof negative pressure is of the order of -8.6 Pa. Thus, under favorable conditions the total wind induced driving pressure is $(6.1 + 8.6) \approx 15\,\text{Pa}$.

However, these wind pressures are calculated from mean wind speeds. If we look at the 95 % quantile (10.0 m/s), the resulting total wind pressure is 76 Pa. I.e. the wind pressure can sometimes be several orders of magnitude higher than the stack pressure and this must be taken into account

The prevailing wind conditions are illustrated on Figure 2.3 for different months. It is clear that, despite the location of Denmark in the Western Wind Belt, the direction of the wind is quite arbitrary. For this reason there is no obvious windward facade of any building in Denmark.

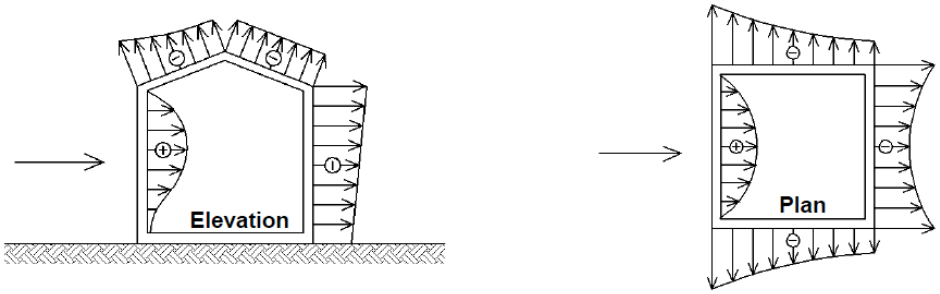


Figure 2.2: Wind pressure distribution on building envelope

Consequently, the position of the ventilation intake should be placed away from the nearest facade in order to minimize the negative (and positive) effects of a leeward position. The outlet, on the other hand, should always be placed on the roof, because, regardless of the wind direction, lower pressure always prevail here.

### 2.2.3 Dampening and balancing

Conventional mechanical ventilation systems are generally designed from a point of view where induced pressure losses dominates the system. There are multiple reasons for this practice but they all originate from the desire to maintain unconditional authority and hence control of the air flow paths.

Conventional blade dampers are only able to perform adequate airflow control in a narrow band of blade angles, e.g. from 30-60°. In this interval the gradient between blade angle and pressure drop is approx. linear. Below 30°the gradient is close to flat and above 60°very steep. Such gradients are difficult to evaluate accurately and to use for control of other things. It also means that blade dampers are never fully open even when no control is necessary. Conventional dampers require approx. 20-30 Pa pressure drop to operate.

Drop dampers are based on another principle with an aerodynamic ball or cone inside the duct. Figure 2.4 depicts a drop damper. These types yields a linear gradient from fully open to fully closed, i.e. the required pressure drop to operate is only 3-5 Pa.

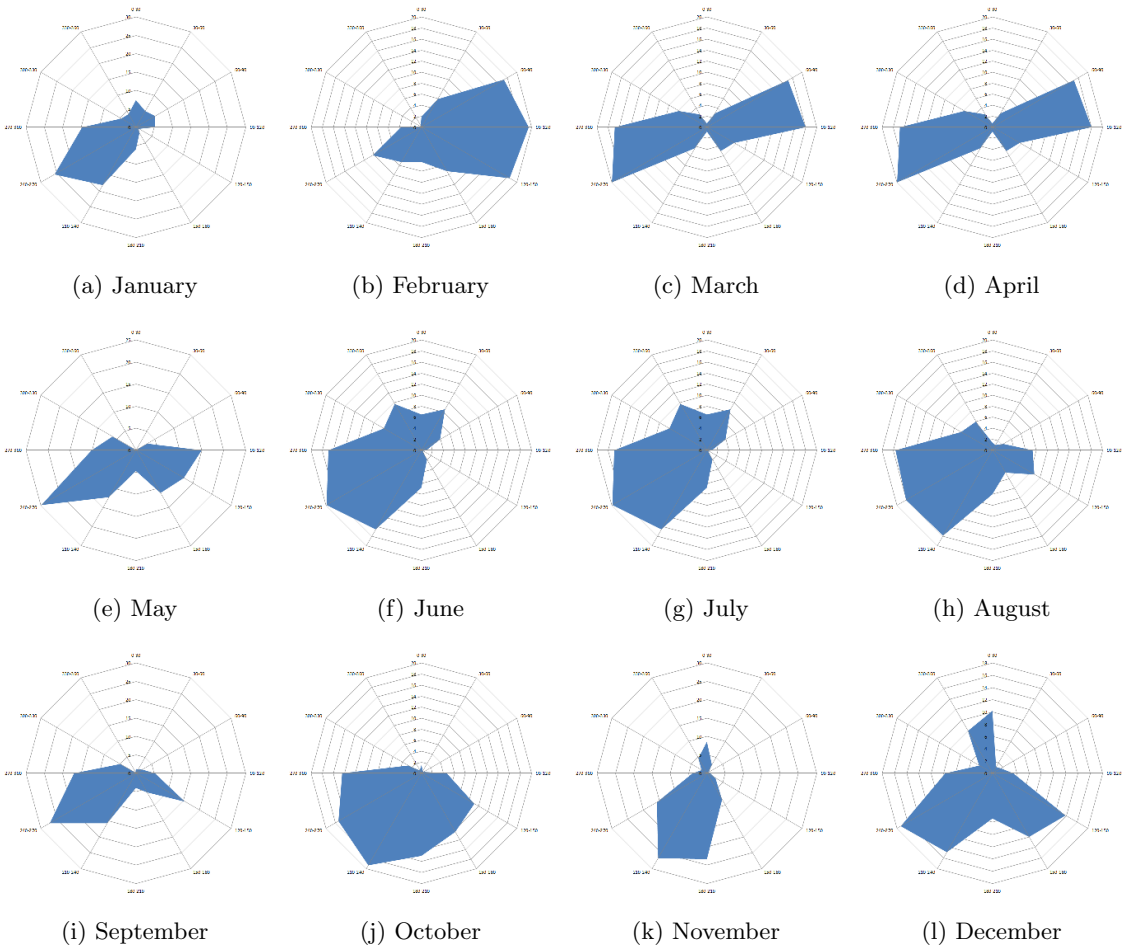

(a) January (b) February (c) March (d) April

(e) May (f) June (g) July (h) August

(i) September (j) October (k) November (l) December

Figure 2.3: Prevailing wind directions from Danish Test Reference Year. Source: Jensen (2003)

Figure 2.4: Aerodynamic drop damper. Source: www.LeanVent.dk

## 2.3 Heat recovery

The heat recovery concept is based on a well-known principle of two coupled air-to-liquid heat exchangers: one exchanger is placed in the inlet air and one in the outlet air, and they are inter-connected with a liquid loop powered by a pump. A schematic of the principle is depicted in Figure 2.5. Cold fresh air enters the heat exchanger in the inlet, heat is then transferred from the warm liquid to the colder air resulting in a temperature rise in the supply air. The now cooled liquid is pumped to the heat exchanger in the outlet where it is heated by the warm exhaust air leaving the building. The warm liquid returns to the inlet heat exchanger and the cycle is repeated continuously.

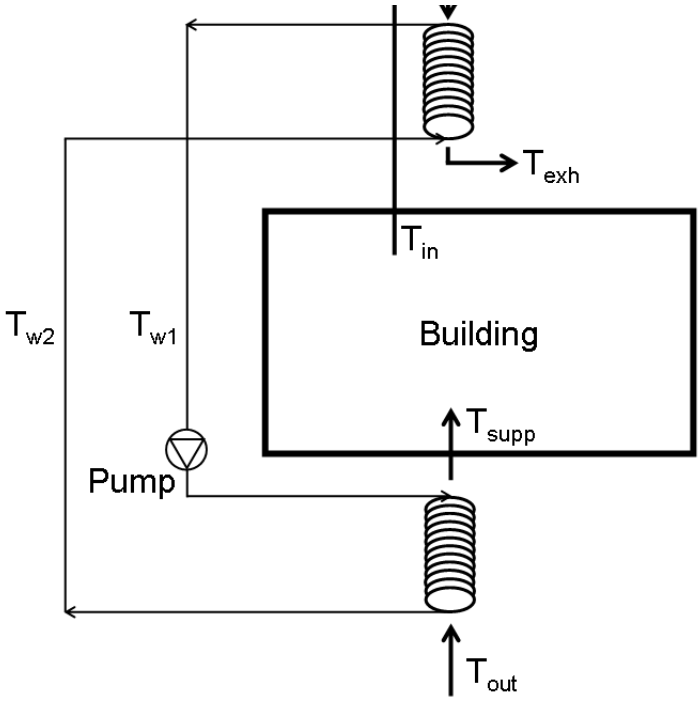


Figure 2.5: Schematic of heat recovery principle with two liquid-coupled heat exchangers.

The main advantage of the liquid-coupled heat exchanger principle is the flexible placement of inlet and outlet in the ventilation system because the airstreams are not required to meet. This flexibility is particularly advantageous for ventilation systems partly or purely driven by stack effect and wind pressures. The approach allows for optimum placement of the heat exchangers in the building to fully exploit fully the natural driving pressure differences.

## 2.4 Heating

Replacing the used air with outdoor air requires heating. Heating is required because the indoor warm air is discarded and the new outdoor air must be heated to match the comfort temperature. The temperature of the supply air to the ventilated rooms is crucial for the risk of draught. Ideally, the supply temperature is approx. 2-6 °C below room temperature (with a mixing ventilation scheme). When the outdoor temperature drops below 15 °C, the supply temperature drops below the desired threshold. By applying heat recovery in the ventilation system, heat is transferred from the warm exhaust air to the colder supply air. The higher the efficiency of the heat exchanger unit, the closer the supply temperature will be to the extract temperature.

In some cold periods, the transferred heat is insufficient for comfort and extra heat must be supplied via a heating coil and the central (water-based) heating system of the building.

In conventional ventilation systems, the heating coil induces a pressure loss. With liquid-coupled heat exchangers, the heating coil is integrated and extra heat can be supplied directly in the liquid loop and transferred to the airstream. In the future, if efficiencies of 85% is achievable, additional heat is even rendered obsolete, because the supply temperature will always follow the extract air temperature closely.

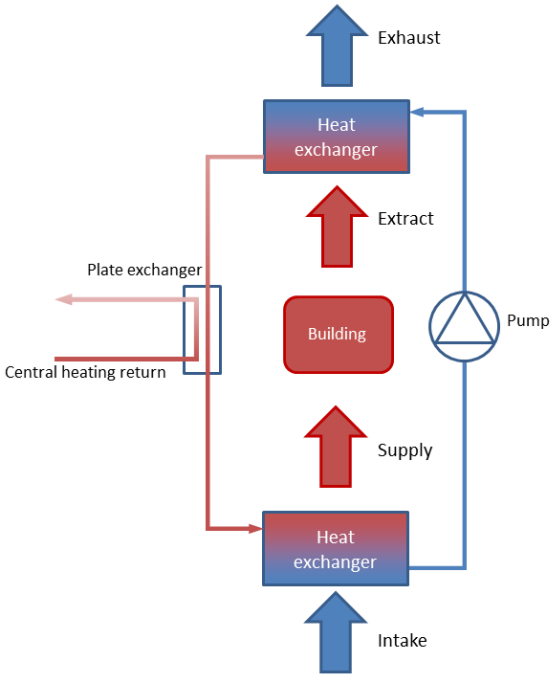


Figure 2.6: Schematic of the possibility of supplying extra heat to the liquid loop to raise the supply air temperature

## 2.5 Night cooling

Active cooling is required is buildings with high internal gains and/or insufficient protection from the sun. In high-performing office buildings with good indoor climate and near-zero carbon emissions, active cooling is, however, of less importance. I.e. excessive heat gains have been reduced and subsequently removed by other, passive means of cooling that do not consume energy.

Passive cooling includes night ventilation which removes excessive heat by airing the building with cool night air and creating a cooling buffer in the constructions of the building to be used for the next day. The most noticeable effect of night ventilation is reduction of peak temperatures, i.e. to give an example, instead of reaching daily temperatures of 28-30 °C, the temperature only reaches 26 °C. Ideally, mechanical cooling is rendered obsolete.

Night ventilation by fans is energy consuming, however, far from the level of a cooling compressor. Consequently, airing without fans is desired. The concept presented by Hviid (2010) (see Figure 2.7) showed simulation-wise that night ventilation is possible without fans in a concept similar to the one presented above. He showed that in a temperate climate fans were necessary to run the ventilation system during day time due to air quality requirements

and airflow regulation, however, during night time, the stack effect of the system was enough to air the building sufficiently, even during summer nights.

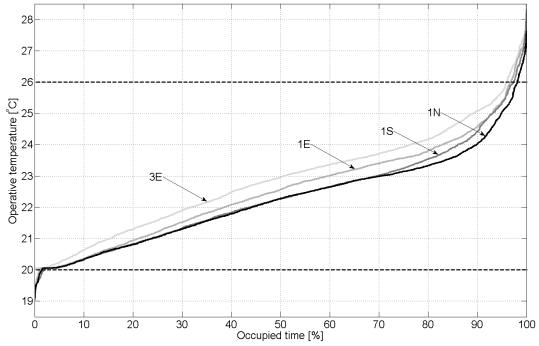


(a) Operative temperatures

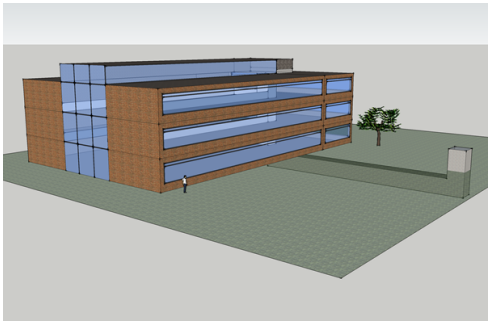

(b) Model

Figure 2.7: Simulated operative temperatures in an office building with different orientations. Cross section is similar to Figure 2.1. Cooling by night ventilation driven purely by stack and wind through ductsystem. Source: Hviid (2010)

Recently Bergsøe (2012) at SBi has published a critical review of underground ventilation intakes. One of the best performing was a concrete duct system which was open and manageable for inspection.

## 2.6 Filtering

Filtration has two objectives: to filter outdoor pollutants, primarily pollen and traffic soot, and to protect the inlet heat exchanger and the duct system from soiling. Filtering is conventionally implemented in mechanical ventilation systems by bag filters. During normal ventilation operation the filters are soiled with dust and particles with subsequent negative impact on the perceived indoor air quality (Bekö et al., 2008, 2009). In this concept we employ two types of filtration, passive settlement of particulate matter in an embedded culvert and active filtration by an electrostatic precipitator. The former type is documented in one study of a 15 m long culvert where the decrease of $>0.3\,\mu$m particles is 85% and 95% for larger particles (Schild, 2001). This emphasizes the need for the duct to be passable for manual cleaning.

The latter type is an electrostatic precipitator which is an active efficient filtration devices that minimally impede the airflow through the device and easily removes fine particulate matter such as dust and smoke from the airstream. An electrostatic precipitator charges passing particles and aerosols and remove them with an electrical field and like bag filters they must be cleaned regularly to avoid depletion of the efficiency. The pressure drop of an electrostatic precipitator is a fraction of a conventional bag filter and therefore is used in some hybrid ventilation projects (Schild, 2001). The filter induces 2 Pa pressure drop at the design flow speed (Terkildsen, 2009). On the down-side electrostatic precipitators are costly to buy and run, because they are power consuming. The power consumption depends on the amount of ionized particles and the ionization level of each particle. Therefore, it is difficult to accurately quantify the power consumption of an electrostatic precipitator, especially in a relatively particle free environment after a long culvert. Only vague sources are available stating a power consumption of 75 W for a flow rate of 1700 $m^3$/h (Terkildsen, 2009). An in-depth investigation of the aspects of filtration efficiency,

Figure 2.8: Fine filter combined with active carbon for filtration of traffic gases. Removes 50% of the ultra-fine particles. Source: www.CamFilFarr.dk

pressure drop, fan power and filter power is beyond the scope of this project.

Figure 2.9: Electrostatic filter. Removes 95-99% of the ultra-fine particles. Reported power consumption 9-16 W. Source: www.automatikprodukter.se

# Chapter 3

# Heat exchanger

This chapter describes the development of a heat exchanger suitable for a natural ventilation like the one described in the previous chapter. This chapter includes multiple sections on different development aspects:

- overall exchanger layout considerations and modeling of air/water heat transfer
- different cross-sectional tube layouts and coupling of tubes to the manifold
- design of exchanger box
- anti-freeze measures and condensation risks

The investigations are performed with analytical and computerized models, calculations by hand, CFD models (CFD: computational fluid dynamics). The development of the analytical framework and the results of pre-testing a limited scale exchanger are described in detail in Hviid and Svendsen (2011). The results have been used to investigate the validity of the models used in the final design.

## 3.1 Overall exchanger layout considerations

A number of optimum performance objectives govern the design. The following explains the design objectives.

**Low frictional loss on the air side** is critical for the heat recovery concept to be applicable in wind and stack-assisted ventilation systems. Equation 2.1 calculated the maximum natural driving pressure due to stack for typical winter operating conditions to be 7.7 Pa. Because other components also induce pressure losses in the system, a desired design criterion for the total pressure loss due to heat recovery was set to approx. 1 Pa.

**The frictional loss on the water side** is also important because it determines the size and energy consumption of the pump. To avoid excessive energy consumption by a secondary component in the ventilation system, we set the design criterion that a domestic circulation pump must be sufficient.

**The heat transfer** is governed by various factors, e.g. the velocity of the passing air, the resistance between the passing airstream and the tube fluid and the total heat transfer surface. We set an overall design criterion for the total heat recovery efficiency of 65%. This value was selected as a compromise between the heat recovery requirement in low-energy office buildings and the size of the exchanger.

**Production costs and lifetime expectancy** are important for the sake of robustness and penetration in a competitive global market. Production costs are typically proportional to material costs, and the number of fittings tends to be decisive for lifetime expectancy. Production costs and lifetime are essential for the exchanger to be competitive with existing heat recovery concepts and consequently cannot be disregarded for any practical implementation.

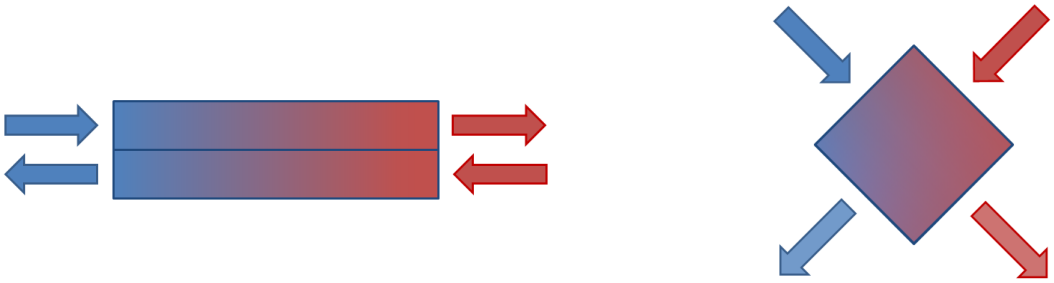

(a) Counterflow (b) Cross-flow

Figure 3.1: Principles of counterflow and cross flow heat exchangers

The heat exchanger is of an approximated counter-flow type. These types have the highest efficiency potential. The counter-flow principle is based on a heat exchange process where a hot and a cold fluid enter the heat exchanger from opposite ends; the cold fluid is warmed and the hot fluid is cooled. Because the hot input is at its maximum temperature, it can warm the exiting hot fluid to near its own temperature. In parallel the cold input can cool the exiting cold fluid to near its own (low) temperature; in other words, the temperatures 'swap' from one fluid to the other. In Figure 3.1 the principles of counterflow and cross flow are depicted. The lower efficiency of the cross flow exchanger is due to the 'smearing' of the temperatures.

If both exchangers employ counterflow then the total system is equivalent to a counterflow exchanger. However due to the extra resistance introduced by the liquid-coupling the required heat transfer area becomes somewhat larger than for a direct exchanger.

To keep the exchanger simple and with low material costs, round PE plastic tubing is used. The tubing is commonly used for water-based floor-heating systems. Oval or even wing shaped tubes have better heat transfer and lower drag coefficient (Horvat et al., 2006), but round tubes require less meticulous production procedures. The tubing used here is mass-produced, cheap, flexible and is produced in a continuous cycle and shipped on large cable drums. Fittings are used to connect the tubing to the manifold.

On Figure 3.2 the relation between total length of plastic tubing, thus material use, and efficiency and pressure loss on the air side is illustrated. The tube bank arrangement used in this figure corresponds to a uniformly staggered grid where $S_T = S_L = 16\,\text{mm}$. The final design was based on the a slightly non-uniform tube arrangement which is shown in Figure 3.7.

The pressure loss in the final design is slightly higher due to the non-uniformly staggered grid but not critical. Hviid and Svendsen (2011) showed that the analytical pressure loss model for tube banks overestimates the pressure drop in comparison to CFD-models. This is discussed in more detail in section 3.10. On the figure it is clear that moving from 80 to 90 % efficiency does not justify the relative increase in used material. Also the size (front area) increases from

$1.5\,\mathrm{m}^2$ to $3.7\,\mathrm{m}^2$.

Parallel exchangers are investigated in section 3.7, yet due to the complexity and limitations on the size of the heat exchanger a final efficiency of approx. 65% was settled on as design parameter.

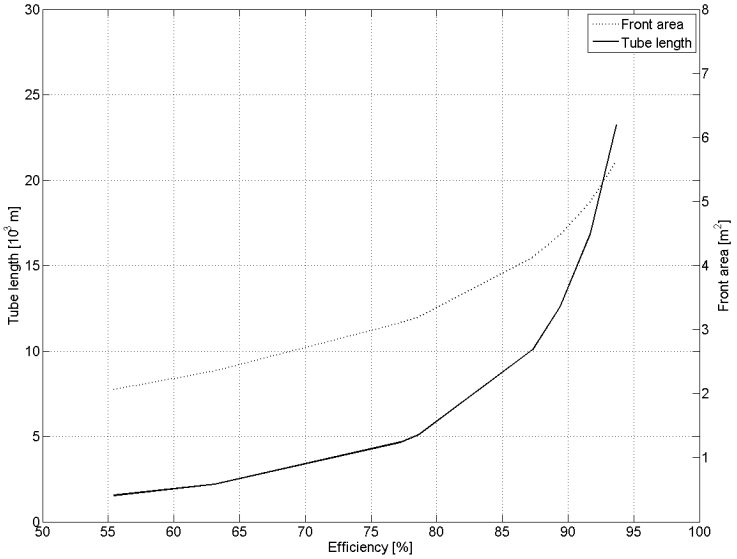


Figure 3.2: Heat exchange efficiency related to material consumption and necessary size of front area at a pressure drop of 0.6 Pa.

## 3.2 Tube banks in general

The plastic tubing is assembled in tube banks. Tube banks are well-known in the literature and have been investigated extensively, however less so for laminar or transitional flows. Figure 3.3 illustrates a tube bank in cross flow, i.e. one fluid (air) flows perpendicularly across the tubing. For each tube heat is transferred from one fluid to the other through the tube material by a combination of convective and conductive heat transfer.

Flow around the first tube in a tube bank corresponds to flow around a single cylinder in cross flow. Therefore, convective heat transfer may be calculated as if the tube was isolated from the others. However, in tube banks, subsequent rows are strongly affected by the tube arrangement because they lie in the turbulent wakes of upstream rows. Generally the turbulence intensity, and consequently the convective heat transfer, increases until the fifth row after which there is little change in turbulence.

Figure 3.4 depicts aligned or staggered arrays of tubes. For aligned arrangements the preferred flow path is in the lanes between the tubes and much of the fluid is not in contact with the tube surface.

> *For the staggered array, however, the path of the main flow is more tortuous and a greater portion of the surface area of downstream tubes remains in this path. In general, heat transfer enhancement is favored by the more tortuous flow of a staggered arrangement, particularly for small Reynolds number ($Re_D < 100$) (Incropera and DeWitt, 2002)*

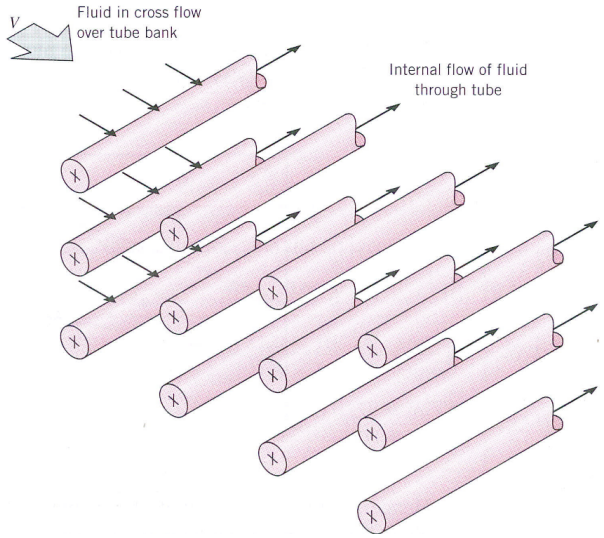


Figure 3.3: Schematic of a tube bank in cross flow. Source: Incropera and DeWitt (2002)

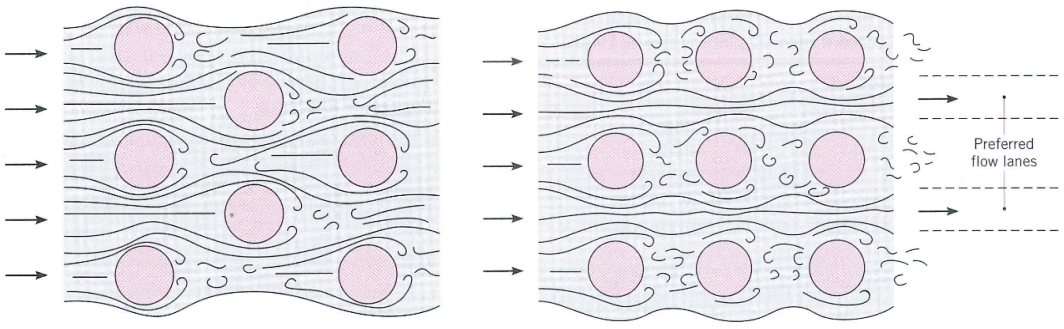


(a) Staggered (b) Aligned

Figure 3.4: Schematic of flow pattern for staggered and aligned tube arrangement. Source: Incropera and DeWitt (2002)

## 3.3 Tube bank arrangement

The spacing of tubes influences both the pressure drop across the bank, the overall heat transfer and the amount of material. The final tube bank spacing is a compromise between cross-sectional grid arrangement (section 3.3), considerations on manifold coupling (section 3.4) and on production feasibility.

The subsequent paragraphs are based on the analytical framework developed and published by Hviid and Svendsen (2011). Figure 3.5 shows the dimensional parameters of a tube bank.

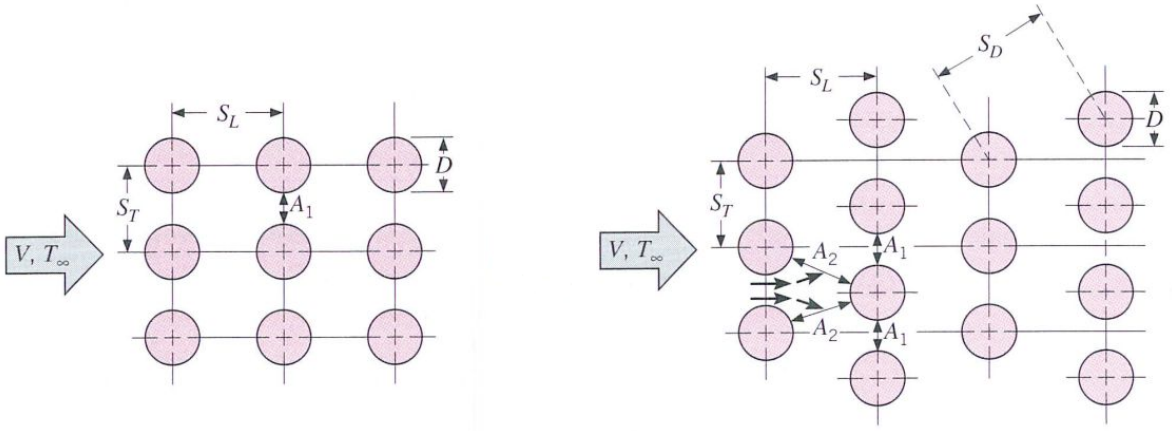


(a) Tube bank in aligned array

(b) Tube bank in staggered array

Figure 3.5: Grid arrangements in a tube bank. Source: Incropera and DeWitt (2002)

For the aligned arrangement, $U_{\max}$ occurs at the transverse plane $A_1$ of Figure 3.5a. It is determined by equation 3.1, where index *app* denotes approaching, i.e. face velocity.

$$\text{Aligned}: \quad U_{\max} = \frac{S_T}{S_T - D} U_{\text{app}} \tag{3.1}$$

For the staggered configuration on Figure 3.5b, the maximum velocity may occur at either the transverse plane $A_1$ or diagonal plane $A_2$ (equation 3.2).

$$\text{Staggered}: \quad U_{\max} = \frac{S_T}{2(S_D - D)} U_{\text{app}} \tag{3.2}$$

The maximum velocity will occur at $A_2$ if the tubes are spaced such that:

$$2(S_D - D) < (S_T - D) \tag{3.3}$$

Figure 3.6 shows pressure drop and heat exchanger efficiency versus the longitudinal tube distance. A constant transversal tube distance of 2 (dimensionless, i.e. distance divided by tube diameter) has been used. It is evident that the longitudinal distance has a minimum around 1.8. This is due to the path of the main flow being less tortuous which in turn affects the turbulence and thus the heat transfer.

With the optimal spacing in mind – that the longitudinal distance between tube layers should be a bit smaller than the transversal distance – the following aligned and staggered arrays has been proposed, (see Figure 3.7).

The different tube arrays were simulated in the computational fluid dynamics tool, Comsol. The velocity fields are depicted on Figure 3.8 and the temperature fields on Figure 3.9 (together

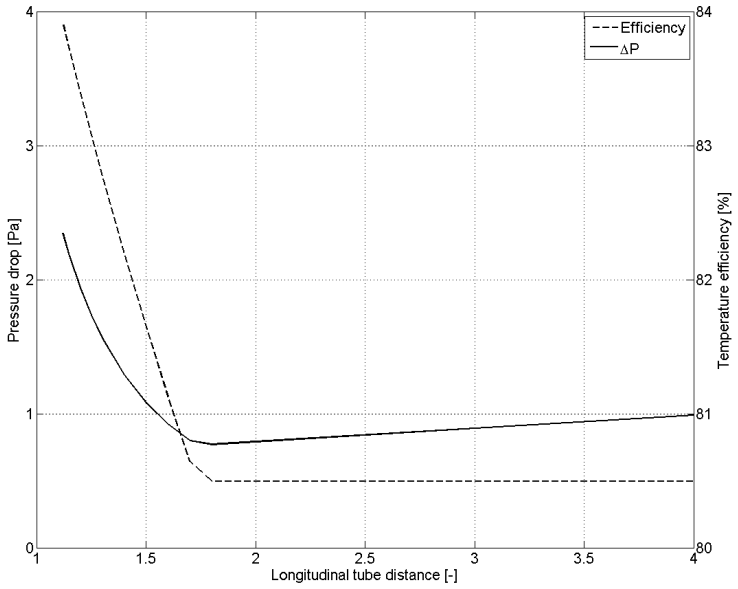


Figure 3.6: Dependency of heat transfer and pressure drop to longitudinal tube grid sizes (dimensionless). Perfect cross flow and staggered grid. Constant transversal grid size of 2 (dimensionless)

Table 3.1: Data for the tube bank temperature simulations in Figure 3.9

| | a | b | c | d | e | f |
|---|---|---|---|---|---|---|
| | Aligned | Aligned | Aligned | Staggered | Staggered | Staggered |
| Tube layers | 20 | 20 | 26 | 20 | 20 | 24 |
| Inlet temperature | 5 | 5 | 5 | 5 | 5 | 5 |
| Exit temperature | 12.8 | 11.5 | 13.6 | 15.0 | 14.4 | 14.9 |
| Face velocity | - | x1.5 | - | - | x1.5 | - |

with Table 3.1). It is evident, that the realized tube grid distances could induce a more effective tortuous flow path, but due to production constraints and manifold couplings, a compromise was settled on.

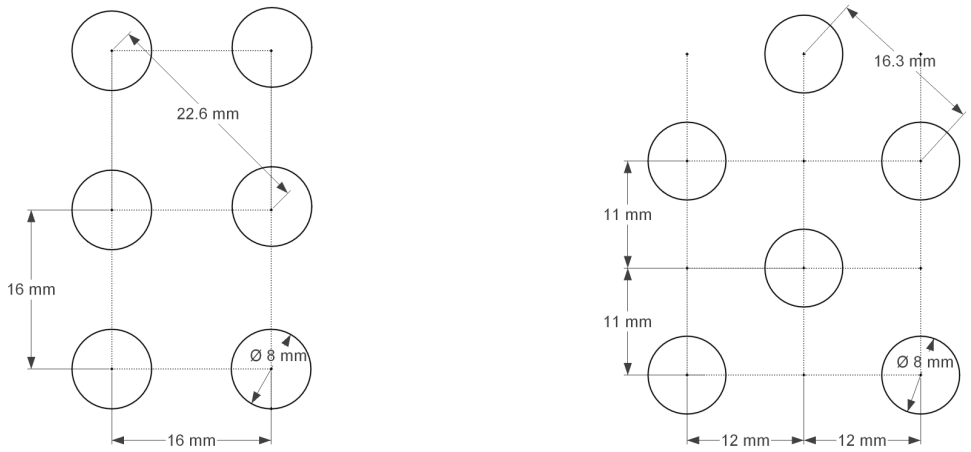


(a) Aligned (b) Staggered, realized

Figure 3.7: Cross section illustrating the spacing of tubes used in Figure 3.8

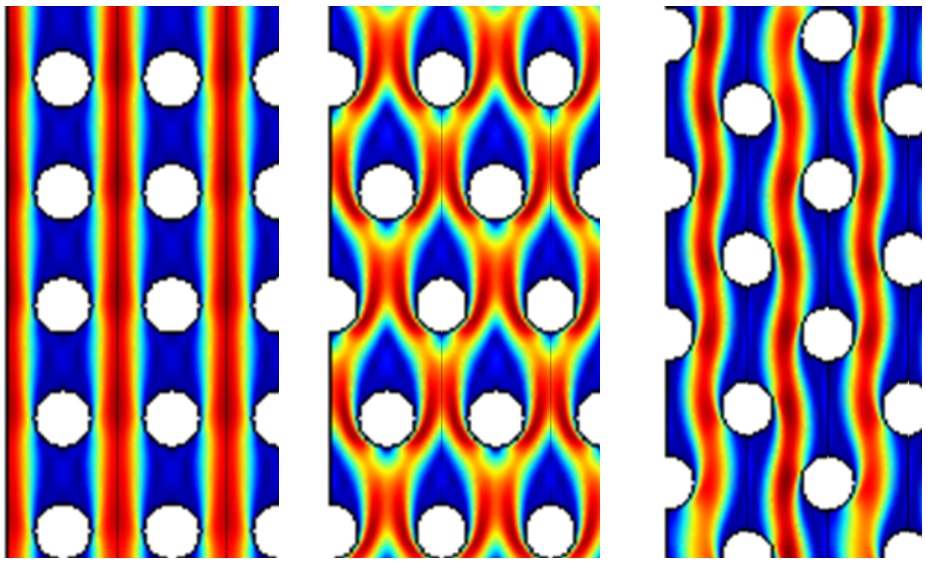

(a) Aligned, $S_T = S_L = 16$ mm (b) Staggered, $S_T = S_L = 16$ mm (c) Realized, $S_T = 24$ mm, $S_L = 11$ mm

Figure 3.8: Velocity field. Laminar flow. Color range 0–0.3 m/s

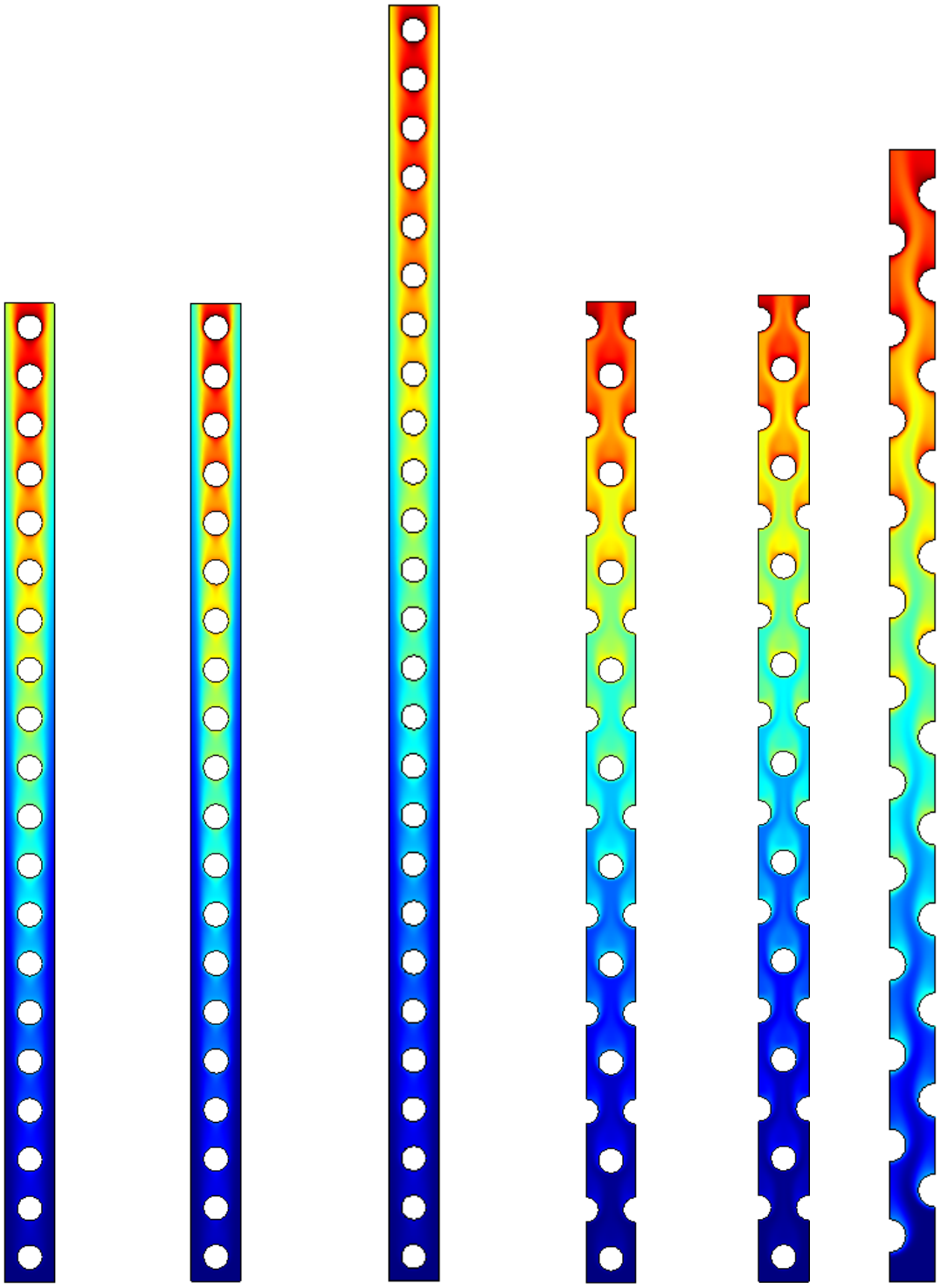


Figure 3.9: Temperature fields of different tube arrays. Laminar flow. Inlet temperature 5 °C. Color range 5–17.0 °C. More data in Table 3.1

## 3.4 Manifold couplings

Figure 3.12 depicts two parallel tubes cris-crossing the airflow. The choice of two parallel tubes was governed by the possible bend radius of a single tube, where two neighboring single bends would overlap at both ends. With two parallel tubes there is space for both tube bends at both ends, see Figure 3.13. This is a compromise between the concept of counterflow and practical implementation. When the tubes are locked into the brackets, a radiator is formed, and multiple radiators can be stacked with an inter-longitudinal offset between adjacent radiators, effectively creating a staggered array. Thus, the exchanger is fully scalable. Figure 3.10 and Figure 3.11 depicts earlier proposals for tube bending and for fixating.

The adjacent radiator is offset 11 mm to create a staggered array. Because there is no space for manifold couplings for every radiator (one coupling every 12 mm, see Figure 3.7), the adjacent radiator is mirrored and the inlet tubes *enter from opposite side*.

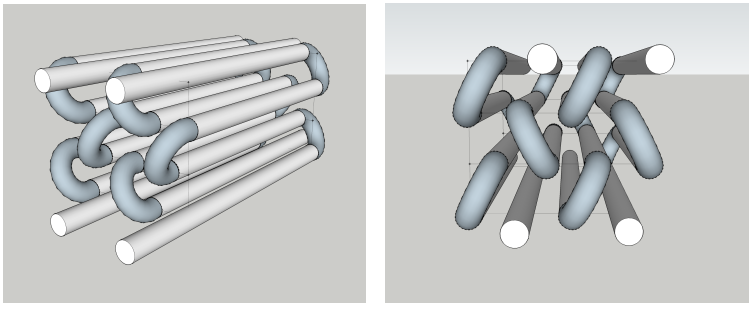

(a) Bends (b) Staggered tube connections

Figure 3.10: Early proposals for tube bends/manifold coupling/tube fixation

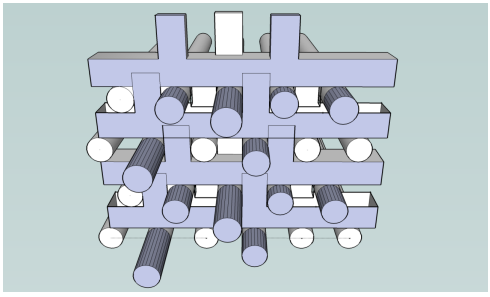

Figure 3.11: Load-bearing 'tube-combs'

The result is 4 inlet manifolds in each side and 4 outlet manifolds in each side, in total 16 manifolds with every other radiator mirrored. The manifolds are then assembled and connected to the main pipe via bigger manifolds with valves, see Figure 3.14 and Figure 3.15.

The tube exits a layer and enters a new layer with an alternating small and large bend radius. For each tube to be exactly the same length the number of tube layers in one radiator has to be a multiple of 4 plus 2. In terms of production this means that two radiator types are needed.

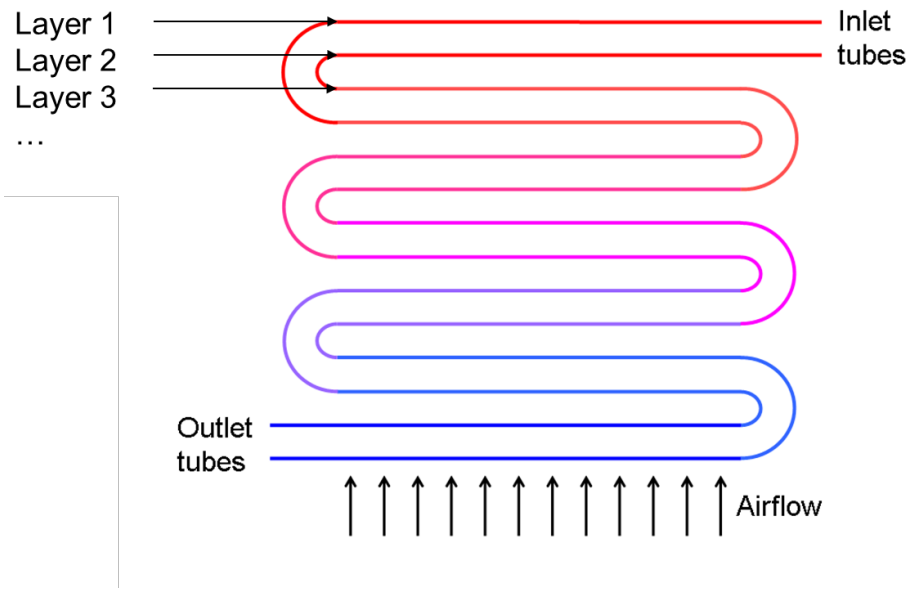


Figure 3.12: Schematic of radiator with two parallel inlet tubes. The tubes enter from alternating sides in adjacent radiators

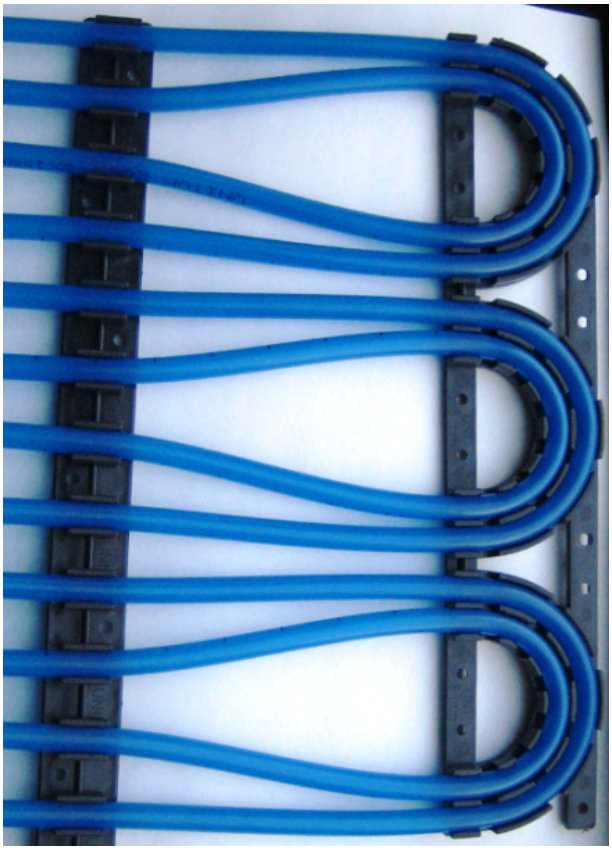

Figure 3.13: Photo of bending brackets and tube spacers

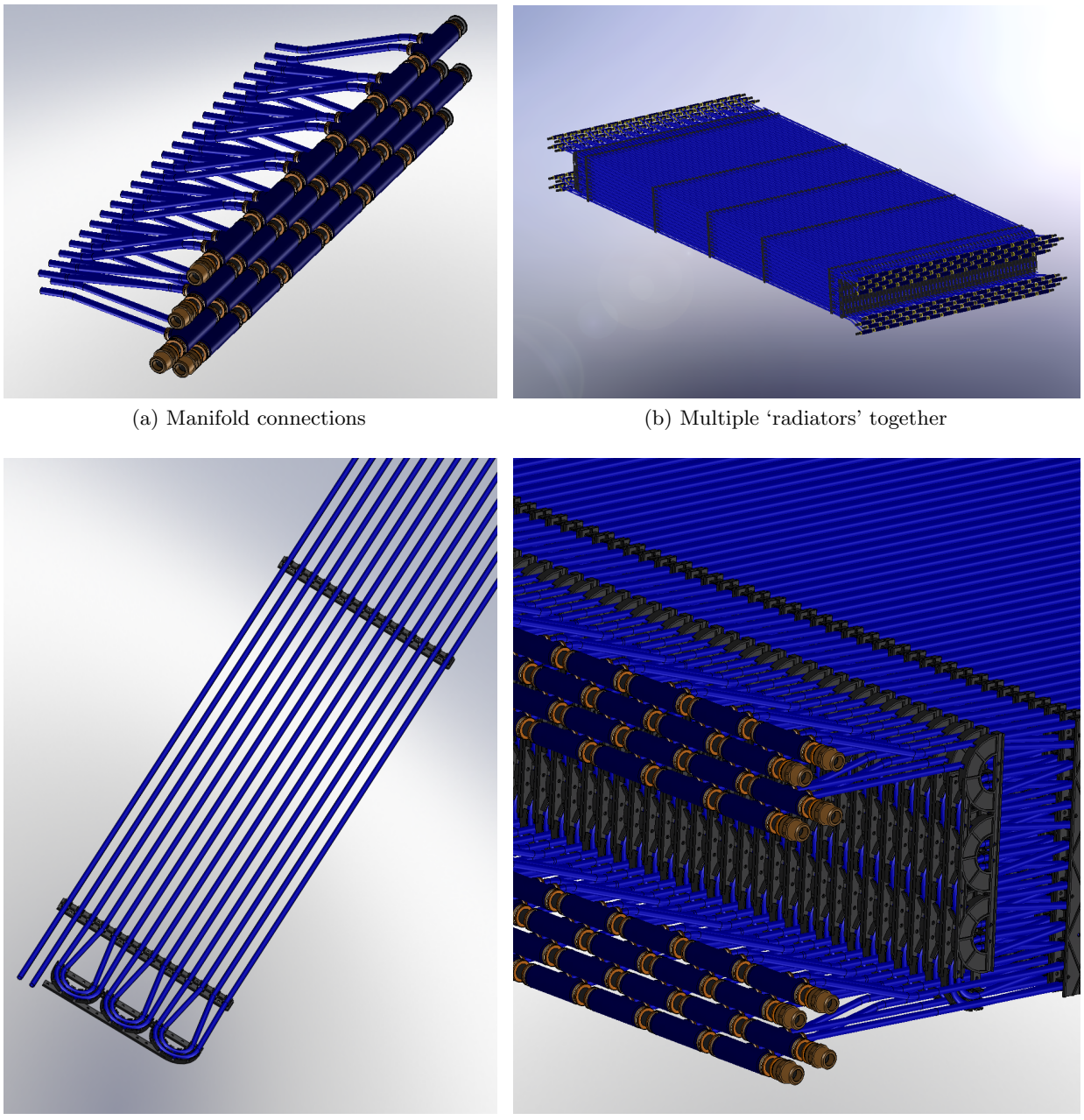

(a) Manifold connections

(b) Multiple ‘radiators’ together

(c) One ‘radiator’

(d) Assembly

Figure 3.14: Heat exchanger details

(a) Spring assembly

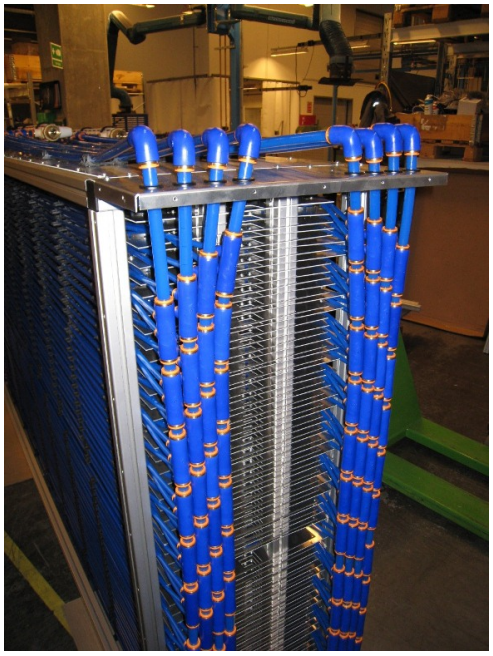

(b) Manifold fittings

(c) Manifold fittings

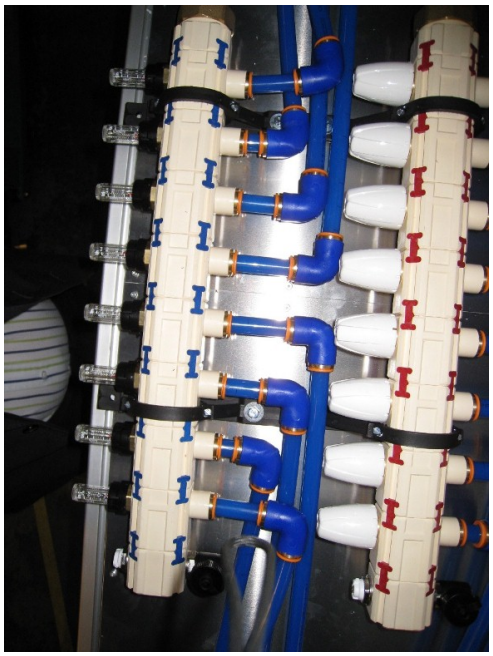

(d) Main manifold with valves (white cones) and flow meters (small glass cylinders)

Figure 3.15: Photos from heat exchanger production. Exchangers are viewed vertically

## 3.5 Modeling of heat transfer

This section describes the modeling of heat transfer on micro-scale, i.e. on sub-millimeter scale. Section 3.6 describes the modeling of temperature distribution on macro-scale, i.e. on meter scale.

The properties on the air side are modeled with Comsol as explained in the previous sections. However, to design the entire exchanger including number of tube layers, system efficiency, tube lengths, pressure losses etc., it is necessary to develop an analytical framework. In the following paragraphs the ultra-short version is presented of the of the framework which is otherwise developed and published in detail by Hviid and Svendsen (2011). The heat transfer coefficients (resistances), which are the main properties of the tube bank, are derived. The resistances are subsequently used to dynamically model the temperature distribution of the fluids of the entire exchanger, see section 3.6. The resistances are schematically presented in Figure 3.16.

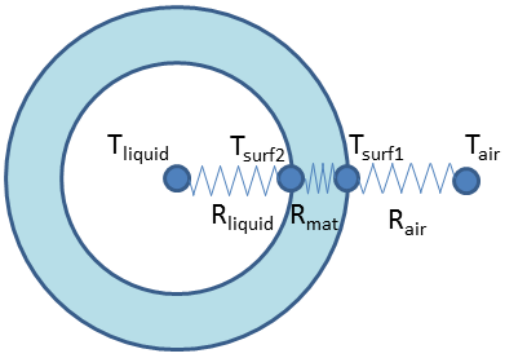


Figure 3.16: Schematic of the tube with temperatures and surface and material resistances

### 3.5.1 Air side

The heat transfer coefficient on the air side is governed by the Nusselt number ($Nu$), the heat conductivity of the fluid ($\lambda$), and (here) the external hydraulic diameter ($D$). The Nusselt number is an expression of the ratio of convective to conductive heat transfer across (normal to) the boundary. For air flowing across a single tube, the Nusselt number will then vary from front side to back side of the tube. However, this level of detail is beyond the scope and only the average value is used.

$$\overline{h}_{\mathrm{a}} = \frac{Nu \cdot \lambda_{\mathrm{a}}}{D_{\mathrm{o}}} \tag{3.4}$$

The Nusselt number has been extensively investigated by numerous authors (**?**). However, most studies address problems with highly turbulent flows. Reynolds number ($Re$) determines whether the flow is turbulent, laminar ($\ll 10^5$)) or transitional and is based on fluid density ($\rho$), maximum velocity ($U$) and the Prandtl number (see Table 4.3). Here the design objective is keep the pressure loss of the tube bank below 1 Pa. This gives very low Re value of $< 100$, thus laminar.

$$Re_{\mathrm{D_o}} = \frac{\rho_{\mathrm{a}} U_{\max} D_{\mathrm{o}}}{\mu_{\mathrm{a}}} \tag{3.5}$$

One applicable study of the Nusselt number by Beale (1997) is based on numerical studies and shows quite good agreement with the experimental data:

$$Nu = 1.309 Re_{\mathrm{D_o}}^{0.36} Pr_{\mathrm{a}}^{0.34} \tag{3.6}$$

### 3.5.2 Water side

The corresponding mean heat transfer coefficient on the water side of the tubing is determined in similar manner. The diameter ($D$) is the internal tube diameter:

$$\overline{h}_{\mathrm{w}} = \frac{Nu \cdot \lambda_{\mathrm{w}}}{D_{\mathrm{i}}} \tag{3.7}$$

The Reynolds number for the water flow is laminar ($\ll 2300$) and the Nusselt number is then fixated to 4.36 (Incropera and DeWitt, 2002). This fixation of the Nusselt number on the water side is quite significant, because it means that theoretically, the heat transfer between air and water is largely independent of the water flow.

$$Re_{\mathrm{D_i}} = \frac{\rho_{\mathrm{w}} U_{\mathrm{w}} D_{\mathrm{i}}}{\mu_{\mathrm{w}}} \tag{3.8}$$

With the heat transfer coefficients established on both sides of the tubes, the total heat transfer for one meter of tube length in cross-flow $\Phi$ can be established. Given that the thermal conductivity of the plastic tubing $\lambda_{\mathrm{tube}}$ is 0.35 W/m K and L a unit length of tube, $\Phi$ is calculated (Incropera and DeWitt, 2002):

$$\begin{aligned} \Phi &= \frac{\overline{\Delta T_{\mathrm{w-a}}}}{R_a + R_{tube} + R_w} \cdot L \\ &= \frac{\overline{\Delta T_{\mathrm{w-a}}}}{\frac{1}{\pi D_{\mathrm{o}} \overline{h}_{\mathrm{a}}} + \frac{\ln(D_{\mathrm{o}}/D_{\mathrm{i}})}{2\pi\lambda_{\mathrm{tube}}} + \frac{1}{\pi D_{\mathrm{i}} \overline{h}_{\mathrm{w}}}} \cdot L \end{aligned} \tag{3.9}$$

In equation 3.9 the resistance of the wall material between the fluids is calculated from $\frac{\ln(D_{\mathrm{o}}/D_{\mathrm{i}})}{2\pi\lambda_{\mathrm{tube}}}$. Using the analytical framework from above, the resistance constitutes approx. 5% of the total resistance. Consequently it is negligible compared to the surface resistances (see Figure 3.16). The resistance on the air side constitutes 90%.

## 3.6 Temperature distribution

This section describes the simulation of temperature distribution throughout the tube bank. The analytical framework from the previous section is used to model the local heat transfer between fluids. As the fluids flow through the tube bank, temperatures change dynamically and consequently the heat transfer changes. The model allows us to view the temperatures at any given point along a tube length as well as the water temperature development through the tube.

Figure 3.17 depicts schematically the sectioning of the tube bank into $n$ tube pieces each with the length of $dx$. Both water and air domain is divided into a number of discrete points. In each point heat transfer is a function of flow, speed and materials. Heat transfer affects temperature of both air and water in a point. The points are interconnected in the air domain and the water domain respectively. Iteratively the temperatures are updated with the temperature upstream. After a number of iterations, the temperatures have propagates throughout the calculation domain and steady state is achieved.

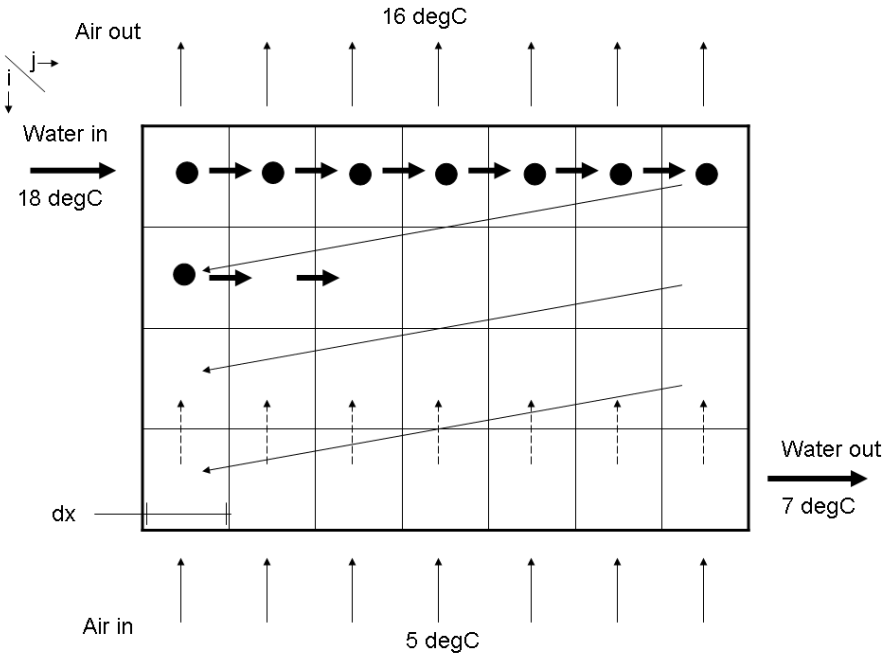


Figure 3.17: Schematic of model for local air and water temperature calculation. The thin diagonal arrows connecting row $i$ with $i-1$ are changed to match the actual tube connections

Figure 3.17 illustrates a simple counterflow principle where the water make several passes through the airstream and the temperature development through the sections is straightforward. However, more complicated situations where the inlet tubes are parallel and placed in a staggered grid (see Figure 3.12) are also possible to represent, simply by connecting the correct tube ends to each other. The software code for different solutions are included in Appendix A. The code is written in Matlab script. The effect of radiation from tube layer to tube layer is included in the model.

The results of the model is depicted on Figure 3.19. The figure is related to radiators with two parallel inlet tubes, see Figure 3.12, placed in staggered array and with alternating entry sides. As a result layer 1 is connected to layer 3, and further on to layer 5, layer 2 is connected to layer 4 etc. Layer 1 and layer 3 have the same inlet temperature and almost the same exit temperature (they are both connected to the manifold), the exit temperature of layer 3 is then the inlet temperature to layer 5 etc. The arrows indicate the flow direction of the water.

It is evident that despite the locally imperfect counterflow which is the result of parallel inlet tubes entering from alternating sides, the temperatures do 'swap' from one fluid to the other. Table 3.2 constitutes a parameter variation of the number of tube layers, staggered/aligned tubing and different flow rates as well as comparison of the simulation model with the computational fluid dynamics model of Comsol. $\delta T_a$ is the air temperature rise through the tube bank and $\delta P_a$ is the pressure drop. Two things are worth mentioning: 1) the analytical modeling of the pressure drop is insufficient when compared to Comsol and 2) the temperature rise is much more alike between models for staggered arrays than for aligned arrays.

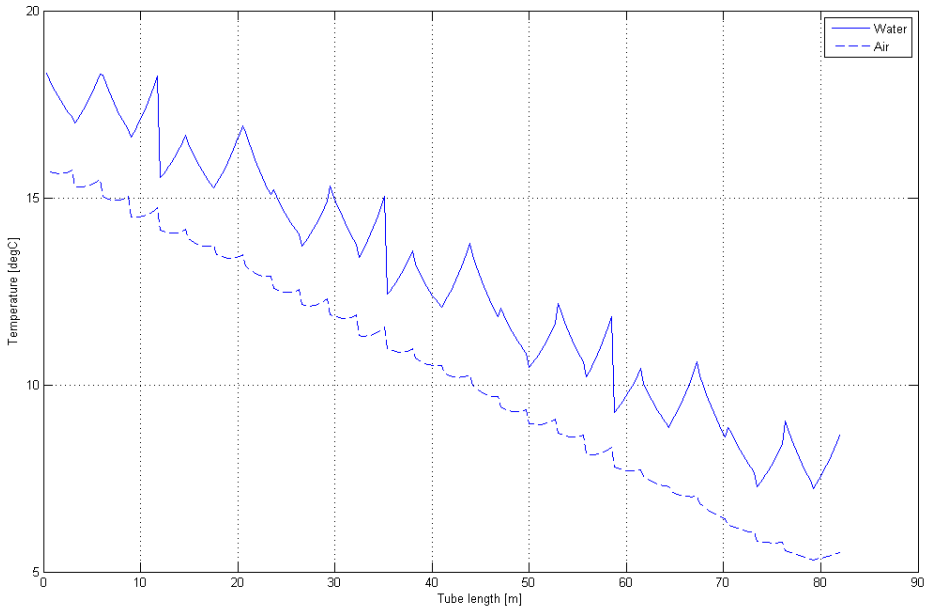


(a) Local temperatures of air and water

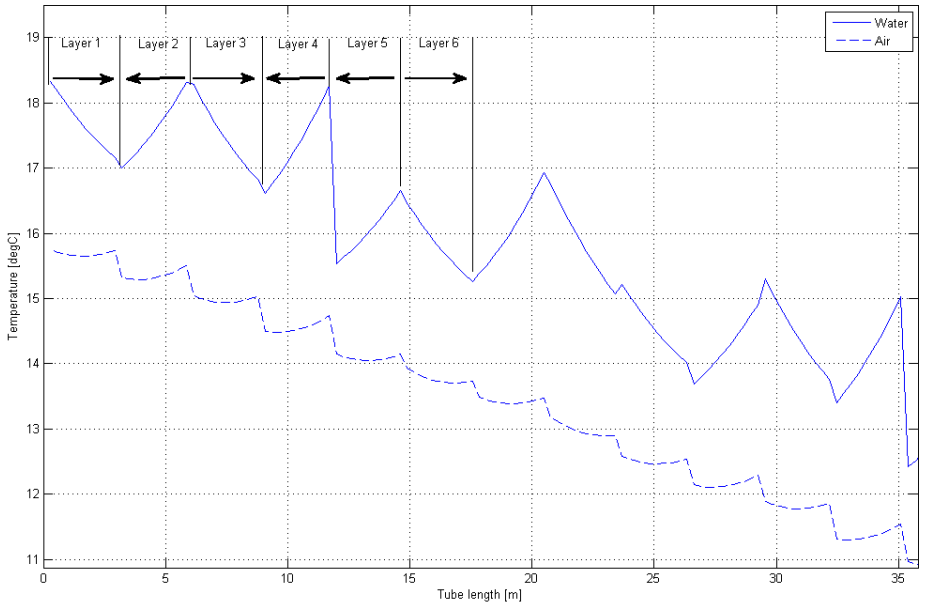


(b) Close up

Figure 3.18: The zig-zag curves are due the different tube layers starting in alternating sides of the exchanger

Table 3.2: Parameter variations. Tube temperatures in the Comsol simulation is adjusted to correspond with those calculated with the Matlab script.

| | $U_{app}$ [m/s] | Tube layers | Capacity flow air:water | Temperature efficiency [%] | $\Delta T_a$ Model | $\Delta T_a$ Comsol | $\Delta P_a$ Model | $\Delta P_a$ Comsol |
|---|---|---|---|---|---|---|---|---|
| Aligned | 0.125 | 30 | 1:1 | 85 | 11.44 | 9.95 | 0.66 | 0.32 |
| | 0.250 | 30 | 1:1 | 78 | 10.48 | 8.22 | 1.87 | 0.77 |
| | 0.125 | 20 | 1:1 | 78 | 10.58 | 8.77 | 0.44 | 0.23 |
| | 0.250 | 20 | 1:1 | 69 | 9.37 | 6.88 | 1.25 | 0.58 |
| | 0.250 | 30 | 2:1 | 49 | 6.63 | - | 1.87 | 0.77 |
| Staggered | 0.125 | 24 | 1:1 | 78 | 10.58 | 10.11 | 2.00 | 0.49 |
| | 0.250 | 24 | 1:1 | 69 | 9.32 | 9.17 | 7.21 | 1.86 |
| | 0.125 | 36 | 1:1 | 85 | 11.43 | 11.17 | 2.99 | 0.72 |
| | 0.250 | 36 | 1:1 | 77 | 10.43 | 10.56 | 10.81 | 3.44 |
| | 0.250 | 36 | 2:1 | 49 | 6.63 | - | 10.81 | 3.44 |

## 3.7 Alternative heat exchanger layouts

The described heat exchanger is constructed on the basis of stacking of radiators. Each radiator is coupled to a manifold and each tube length is a multiple of the number of tube layers and the length of one pass through the airstream.

Alternative heat exchanger layouts are briefly presented here. They are all characterized by tubes spiralling a core. In Appendix A software codes are available for the modeling of heat exchangers with spiralling tubing, e.g. round exchangers, elongated rectangular exchangers or even 8-shaped exchangers. Table 3.3 investigates the differences where in particular the face area, tubing length and water pressure drop are of major interest. The size of the face area can be reduced if two operating exchangers are stacked, like the two depicted on Figure 3.20.

The most important reason for discarding spiral exchangers is that not all tube lengths are equal; the outer tubes are quite a lot longer than the inner tubes. This was attempted remedied by the 8-shaped exchanger depicted on Figure 3.19b, but it also was discarded due to unsurpassable practical production challenges.

Rectangular

| | 2 parallel exchangers | 1 exchanger |
|---|---|---|
| Length | 2.3 m | 3.3 m |
| Width | 1.14 m | 1.6 m |
| Core length | 1.30 m | 1.40 m |
| Core width | 0.116 m | 0.116 m |
| Face area | 2.47 $m^2$ | 3.12 |
| Tube layers | 20 | 20 |
| Pressure drop air | 0.68 Pa | 0.61 Pa |
| Pressure drop water | 7 kPa | 13 kPa |
| Water through pump | 0.61 $m^3/h$ | 0.61 $m^3/h$ |
| Total tube length | 3093 m | 6559 m |

8-shape

| | 2 parallel exchangers | 1 exchanger |
|---|---|---|
| Length | 2.56 m | 3.5 m |
| Width | 1.41 m | 2 m |
| Small radius | 0.1 m | 0.1 m |
| Big radius | 0.7 m | 1 m |
| Face area | 2.93 $m^2$ | 5.78 $m^2$ |
| Tube layers | 20 | 20 |
| Pressure drop air | 0.64 Pa | 0.67 Pa |
| Pressure drop water | 4.5 kPa | 8 kPa |
| Water through pump | 0.61 $m^3/h$ | 0.61 $m^3/h$ |
| Total tube length | 4122 m | 8240 m |

Table 3.3: Some investigations on single and parallel exchangers of rectangular and 8-shape type

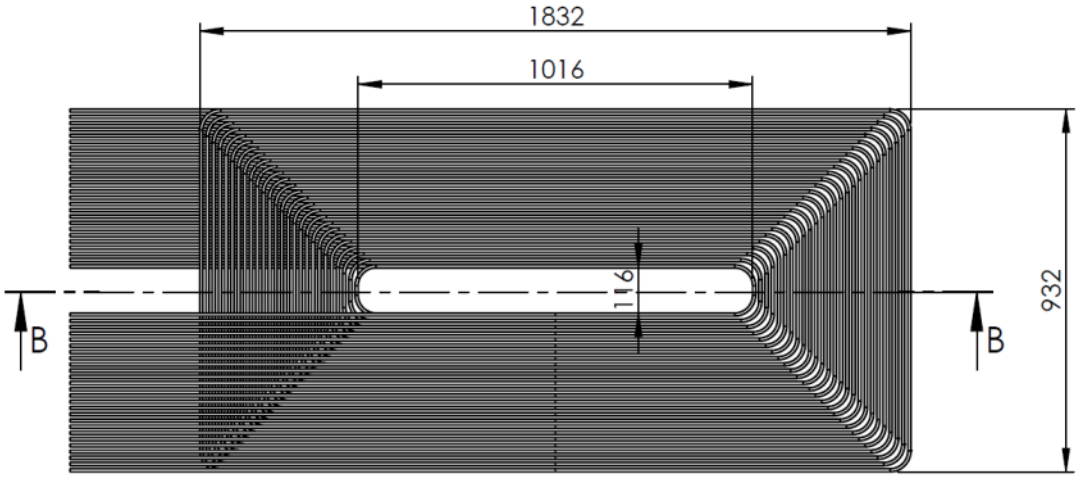


(a) Rectangular exchanger. Spiralling tubing of unequal length

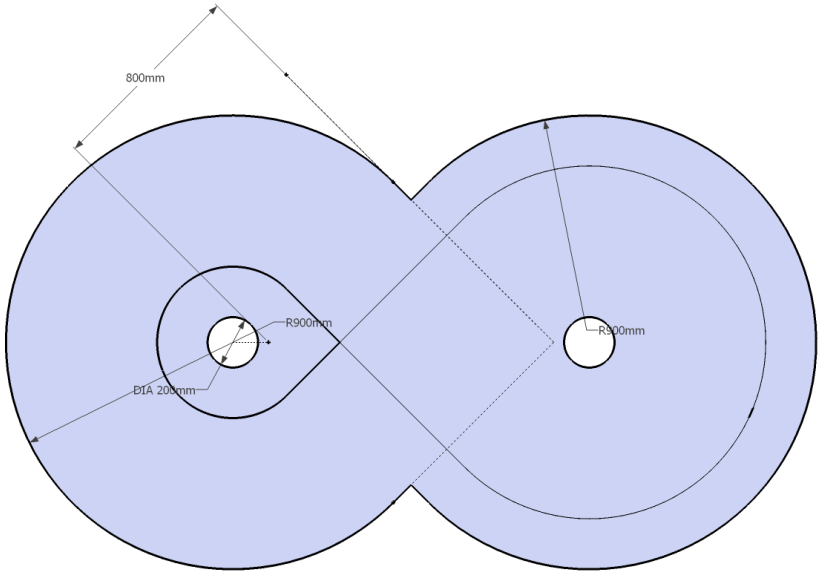


(b) Eight-shaped exchanger. Spiralling tubing of equal length

Figure 3.19: Schematics of early exchanger design proposals

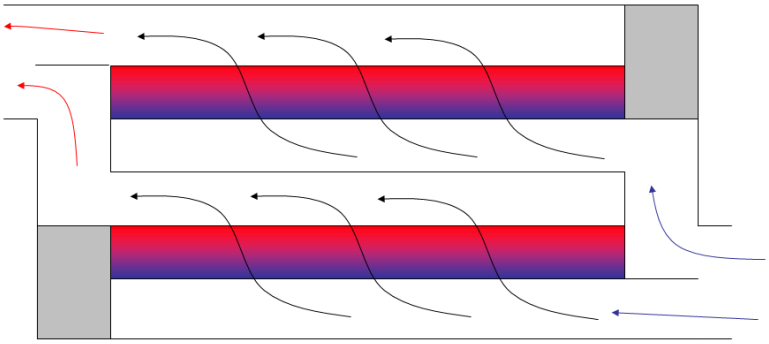

Figure 3.20: Two stacked exchangers operating in parallel

## 3.8 Exchanger box design

This section describes briefly the design of the exchanger box. It comprises general considerations and specific CFD simulations.

The number of tubes and tube layers is determined from the assumption that the air velocity through the exchanger is uniformly distributed so the entire tube surface area contributes equally to the heat transfer. If the velocity profile is non-uniform some individual tubes will suffer from a decrease in heat transfer resulting in overall heat exchange deficiency. The objective for a proper exchanger box is to ensure a velocity profile in the approaching air so it passes the tubes uniformly and perpendicularly to the tubes. A number of investigations on a narrow 3D slice of the box with tubes were carried out in the CFD program Fluent and in Comsol. Figure 3.21 illustrates the simulated specimen. Appendix **??** lists the program specific input.

It is important that the air enters the intake chamber at minimum velocity. When air enters the box, the dynamic pressure of the flow is converted to static pressure at the back wall. The static pressure must not be too great compared to the pressure drop across the tube bank or it will cause non-uniform cross flow perhaps with stagnant zones at the front wall of the box. On Figure 3.22 the streamlines are depicted showing quite uniformly distributed flow conditions. A further check is depicted on Figure 3.23 showing a slice of the velocity distribution, hence mass flow distribution, within the tube bank.

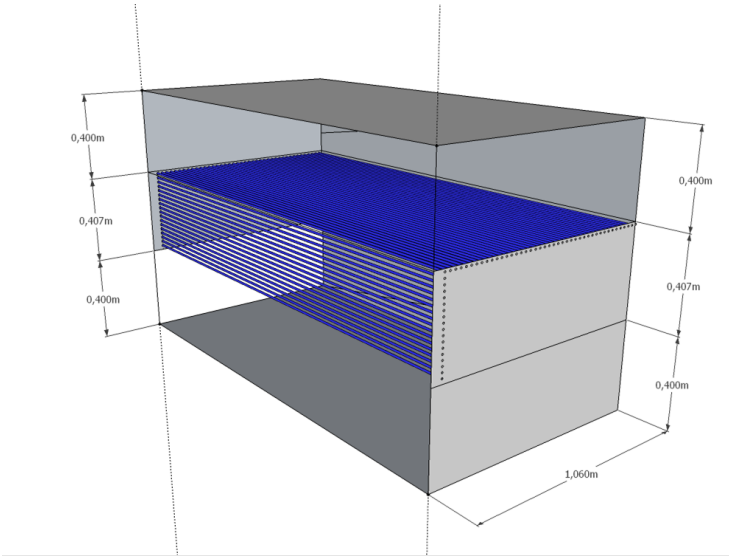


Figure 3.21: Sketch of exchanger box with inlet pressure chamber below and outlet chamber above

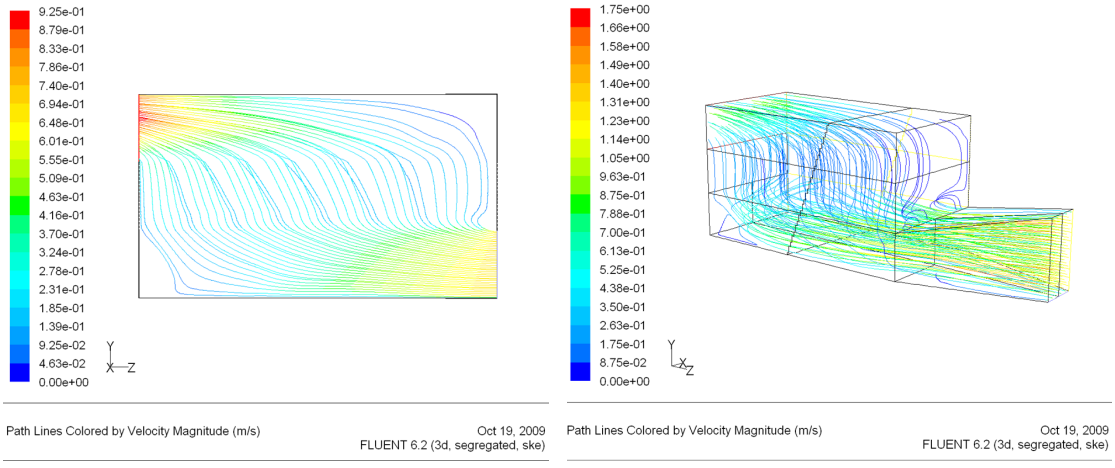


(a) 2D (b) 3D

Figure 3.22: Streamlines from inlet to outlet through exchanger tubes

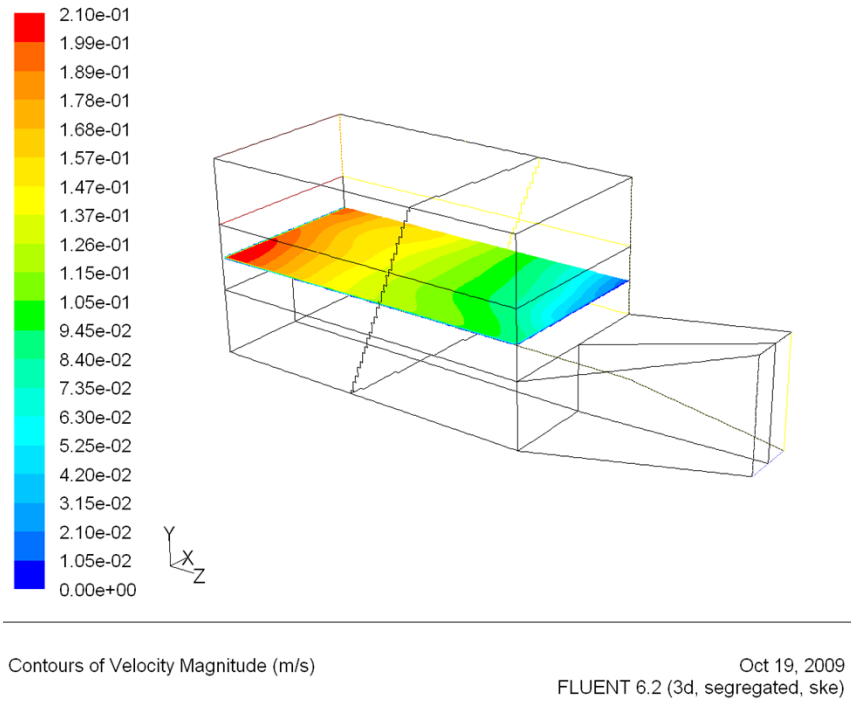


Figure 3.23: Velocity (mass flow) differences across exchanger tubes

## 3.9 Anti-freeze measures

In highly efficient heat exchangers the risk of ice forming is present. The phenomenon arises when the outdoor temperature is below zero and moist indoor air meets the cold fluid from the outside. It is important to notice that in liquid-coupled heat exchangers the circulating liquid has to have a freezing point below zero before ice can form on the outer surface of the tube.

Ice formation will never occur in the intake exchanger as air is heated up which increases the possible water content, making the risk of condensation smaller. However the exhaust air is moist and when it passes the outlet exchanger it may be cooled below the dew point. If the circulating liquid is below zero, e.g. at the first tube passes, ice will form on those tubes. Also condensed free water may drip down onto tube layers that subsequently will freeze it. If no action is taken, the exchanger may be clogged with ice quite quickly.

Even though the flexible plastic tubes are less vulnerable as opposed to exchangers of metal the formation of ice poses a risk. However, three solutions are feasible:

1. create a ventilation air bypass around the exchanger at times of risk
2. create imbalance between the capacity flows of air and water with the fan/pump
3. add heat to the water circuit e.g. with an electrical heater or a plate heat exchanger connected to the district heating (see Figure 2.6).

All solutions reduces the efficiency thus lowering the ice-forming temperature. The simplest solution is to create imbalance with the pump because it only requires a bit of CTS programming. Reduction of the pump speed will only increase the problem with sub-zero liquid temperature, because the water circuit will exit the exchangers with temperature values very close to the indoor or outdoor temperature, respectively. Water exiting the intake exchanger will then transfer

Table 3.4: Properties of glycols, alcohols and chlorides in aqueous solutions. Table is adapted from ASHRAE (2005)

| Property | Ethylene glycol | Propylene glycol | Methyl alcohol | Ethyl alcohol | Calcium chloride | Sodium chloride |
|---|---|---|---|---|---|---|
| Mass-% at −15 °C | 31 | 33 | 20 | 25 | 19 | 18 |
| Heat capacity[a] [J/kg K] | 3700 | 3860 | 4100 | 4300 | 3130 | 3450 |
| Viscosity[b] [$\cdot 10^{-5}$ m$^2$/s] | 0.29 | 0.50 | 0.23 | 0.37 | 0.20 | 0.16 |
| Level of toxicity | high | low | high | low | none | none |
| Flammability | low | low | high | high | none | none |

[a] Values found for mass fraction at −15 °C
[b] Dynamic.

sub-zero liquid to the outlet exchanger. By increasing the pump speed (infinitely) the water circuit eventually attains the mean value of indoor and outdoor temperature. In this case sub-zero temperatures are formed when the outdoor temperature drops below -20 °C.

### 3.9.1 The effect of anti-freeze on efficiency

Freezing of the water in the tubes would be more problematic than ice-forming on the outside of the tubes but not disastrous due to the flexibility of the plastic tubes. However, for the liquid to sustain sub-zero outdoor temperatures, an aqueous solution of propylene glycol is used. The properties of different anti-freeze agents are listed in Table 3.4 following a desired freezing point of −15 °C.

From the table we conclude that approximately 30% of propylene glycol is preferable. At this concentration the process of freezing will form an expanding slush. Therefore, expansion volume must be included in the system. Propylene is preferable over ethylene glycol simply because it is less toxic. Small amounts are used even in cosmetics. However more antifreeze is needed of propylene glycol to obtain the same freezing point. Consequently the viscosity is higher causing larger pump pressure in the circuit. On the other hand the solution can carry more heat than ethylene glycol, so less liquid must be circulated to transfer the same amount of energy; this reduces the pump volume.

The pump pressure to transfer the required heat through one exchanger actually implemented in building 118, DTU (see Chapter 4), is 0.7 kPa for pure water and 2.7 kPa for 30 vol-% for propylene glycol. Details on this calculation are published by Hviid and Svendsen (2011). Pump pressure and pump power are linearly proportional and therefore the propylene solution consumes 3.8 times more pump energy.

## 3.10 Discussion

The present design is not optimal in the sense that it is less efficient and has greater air pressure drop than the initial design proposal. However, it has the great advantage of being fully scalable and it fits into an industrial production. Furthermore, the design compromises has had a smaller impact on the performance than initially expected. The compromises affects the performance in terms of heat transfer, material consumption and pressure drop and they are represented by tube/manifold coupling (radiator layout), cross sectional tube arrangement and the exchanger box.

The present tube/manifold coupling with two parallel inlet tubes from alternating sides actually

causes the passing air to be cooled at some tube layers resulting in local heating *and* cooling within the same exchanger. With optimal tube coupling and a uniformly staggered grid where $S_T = S_L = 2$ (-) only heating or cooling will occur within the tube bank. Simulations shows that this will result in an temperature efficiency increase from 83 % to 88 % (per exchanger). The pressure drop is then reduced from 3.3 to 1.4 Pa (58 % decrease). However, studies by Hviid and Svendsen (2011) showed that the analytical pressure loss model was somewhat inadequate when it is compared to CFD-models. As discussed previously these values carries some uncertainty, but the relative change is expected to be the same. If the efficiency is held constant at 83 %, the pressure loss may be reduced to 0.9 Pa.

Another issue is the material used for plastic tubes. The exchanger contains very large quantities of tube material and material savings have a direct impact on the production costs of the exchanger. Figure 3.2 illustrates the costs of increasing the efficiency beyond reasonable values, but improving the exchanger design to optimal cross flow and tube grid would also reduce the material used. From present case to best case the material use could be halved while still maintaining both pressure drop and heat transfer performance.

The exchanger box design may be improved in several ways. It is important that the air enters the intake chamber at minimum velocity so the dynamic pressure of the fluid does not surpass the pressure drop of the tubes which in turn will cause non-uniform cross flow. This may be achieved by different means: a pressure drop plate, turning vanes, a long duct section upstream that changes the duct face area to the face area of the intake chamber or other. Possible changes are not investigated in detail as each investigation requires demanding CFD-simulations in 3D to assess the performance properly. Because the present box design is imperfect in terms of uniform cross flow an imbalance of local mass flows is tested with the analytical expressions from section 3.5. An imbalance of ±66 % is chosen, meaning that the smallest mass flow is only 66 % of the greatest. The effect, however, causes the efficiency, calculated with our own software code, to drop a mere 0.2 percentage-point.

# Chapter 4

# Full scale tests

The full hybrid concept was tested in a full scale setup in building 118 at the Technical University of Denmark. The building is mainly an office building with single offices but has some teaching facilities of class room size and some databars.

## 4.1 Building

The building is depicted on Figure 4.4. The length of the building is 100 m and width 12.6 m. The facades are facing due North and South. There are three levels above ground and one basement level. The floor height is 4 m. Access to the building is via the main stair case in the middle of the building and two secondary staircases at both ends. One corridor along the aisle of the building gives acces to rooms on both sides.

The structural system is concrete columns and beams with concrete slabs. Columns are placed in the facade and slightly over the middle of the building. The height of the beams is approx. 0.4 m. The corridor is without beams.

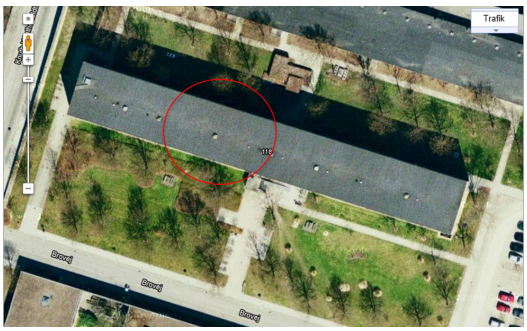


(a) Aerial photo with ventilated part encircled

(b) Facade

Figure 4.1: Building 118 at the Technical University of Denmark

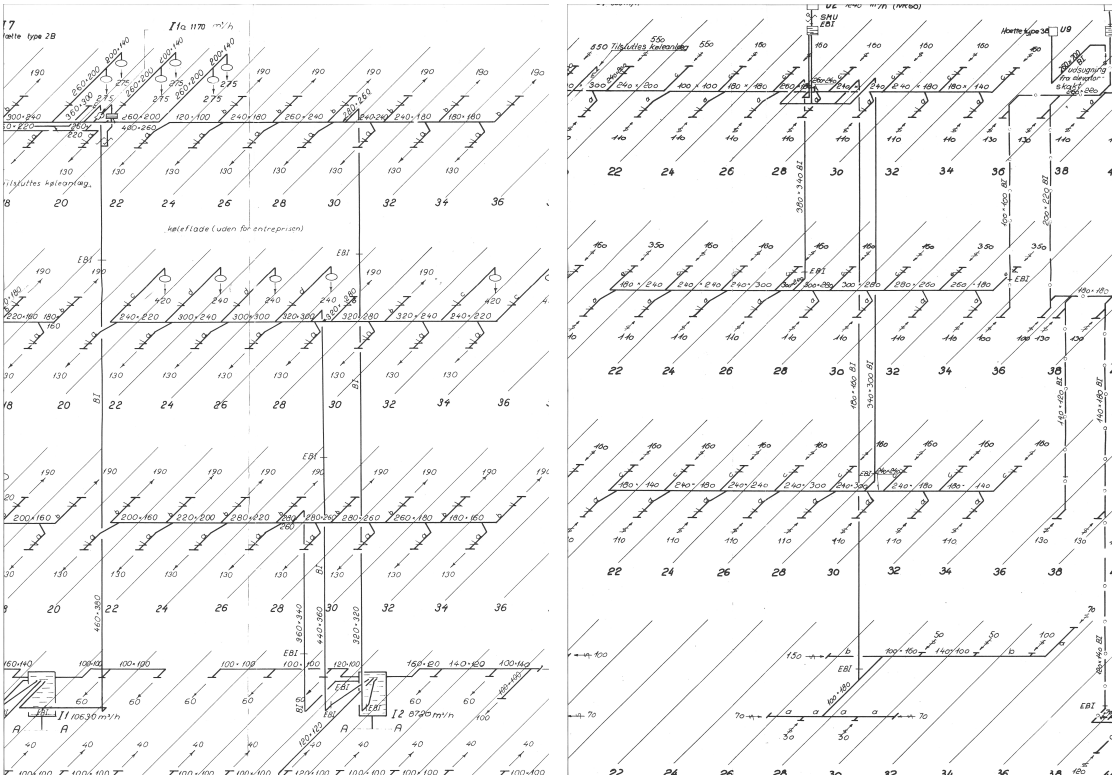

(a) Supply (b) Exhaust

Figure 4.2: Schematics of one of four identical original ventilation systems in building 118. Better resolution is found in Appendix E

## 4.2 Ventilation design

The passive ventilation system is implemented in one quarter of the building west of the main entrance. The building was designed in 1968 with four similar ventilation systems each ventilating one quarter of the building, see Figure 4.2. The original design was to heat the building by air at 4 airchanges per hour. All systems have intake at ground level, where the intake air passes a filter, a heating coil and a fan before being distributed to the floors via three main vertical ducts. Other three ducts collect the extracted room air below the roof, and exhausts it above the roof. In the full scale experiment, the installation room in the basement is retrofitted with one heat exchanger, filter, fans and dampers. On the roof, a fan and the other heat exchanger is placed and the two exchangers are linked by a water loop drilled through all the floors of the building.

Please note that the the full scale system differs from the ideal concept described in previous chapters on the following points:

- bagfilter replaces the electrostatic precipitator which raises the pressure loss from approx. 2 Pa to 16 Pa.
- fans are included because the pressure loss of system with dampers and bagfilter is too high
- the embedded culvert is only 1 m long

The ventilated building part comprises offices and the teaching rooms 119 and 225. The use of these rooms varies a lot from 0 persons to 40 persons. The intended strategy is a constant-air-volume system except for teaching room 225 (Figure 4.3) The air flow rate for the occupants in the ventilated quarter is determined by indoor climate category III of DS/EN 15251 (EN15251, 2007). Table 4.1 shows the airflow rate calculation.

Figure 4.3: Photos of teaching room 225.

In min flow rate mode, teaching room 225 is without ventilation. The total flow rate in min flow rate mode is 1764 $m^3/h$. Please note that the max flow rate in the teaching room of 182.7 l/s is in fact not enough to keep $CO_2$ level below the desired 1000 ppm. The expected $CO_2$ level is approx. 1400 ppm, but it still complies with the building code where 1500 ppm is allowed. When the room 225 sensors register no activity in the room the ventilation is shut down.

Table 4.1: Ventilation flow rates in max flow operation mode. †Numbers denote modes of operation: max/min flow rate

| | Orient. | W | D | H | Area | Vol. | No pers. | Occup. vent. | Build. vent. | Total | Air change |
|---|---|---|---|---|---|---|---|---|---|---|---|
| Level 00 | | m | m | m | $m^2$ | $m^3$ | | $4\,ls^{-1}pers.^{-1}$ | $0.3\,ls^{-1}m^{-2}$ | $ls^{-1}$ | $h^{-1}$ |
| Recept. | S | 3 | 4.5 | 3 | 13.5 | 41 | 1 | 4.0 | 4.1 | 8.1 | 0.7 |
| Depot | S | 3 | 4.5 | 3 | 13.5 | 41 | 0 | 0.0 | 4.1 | 4.1 | 0.4 |
| Office | S | 3 | 4.5 | 3 | 13.5 | 41 | 1 | 4.0 | 4.1 | 8.1 | 0.7 |
| Office | S | 6 | 4.5 | 3 | 27.0 | 81 | 2 | 8.0 | 8.1 | 16.1 | 0.7 |
| Office | S | 3 | 4.5 | 3 | 13.5 | 41 | 1 | 4.0 | 4.1 | 8.1 | 0.7 |
| Office | S | 3 | 4.5 | 3 | 13.5 | 41 | 1 | 4.0 | 4.1 | 8.1 | 0.7 |
| Office | S | 3 | 4.5 | 3 | 13.5 | 41 | 1 | 4.0 | 4.1 | 8.1 | 0.7 |
| Library | N | 3 | 6.3 | 3 | 18.9 | 57 | 1 | 4.0 | 5.7 | 9.7 | 0.6 |
| Library | N | 6 | 6.3 | 3 | 37.8 | 113 | 0 | 0.0 | 11.3 | 11.3 | 0.4 |
| Library | N | 3 | 6.3 | 3 | 18.9 | 57 | 0 | 0.0 | 5.7 | 5.7 | 0.4 |
| Copy | N | 6 | 6.3 | 3 | 37.8 | 113 | 0 | 0.0 | 11.3 | 11.3 | 0.4 |
| Copy | N | 3 | 6.3 | 3 | 18.9 | 57 | 0 | 0.0 | 5.7 | 5.7 | 0.4 |
| Postal | N | 3 | 6.3 | 3 | 18.9 | 57 | 0 | 0.0 | 5.7 | 5.7 | 0.4 |
| | 8 modules | | | | 259 | | | | | 110 l/s (395 $m^3$/h) | |
| Level 01 | | | | | | | | | | | |
| Depot | S | 3 | 4.5 | 3 | 13.5 | 41 | 0 | 0.0 | 4.1 | 4.1 | 0.4 |
| Office | S | 6 | 4.5 | 3 | 27.0 | 81 | 2 | 8.0 | 8.1 | 16.1 | 0.7 |
| Office | S | 3 | 4.5 | 3 | 13.5 | 41 | 1 | 4.0 | 4.1 | 8.1 | 0.7 |
| Office | S | 3 | 4.5 | 3 | 13.5 | 41 | 1 | 4.0 | 4.1 | 8.1 | 0.7 |
| Office | S | 3 | 4.5 | 3 | 13.5 | 41 | 1 | 4.0 | 4.1 | 8.1 | 0.7 |
| Office | S | 3 | 4.5 | 3 | 13.5 | 41 | 1 | 4.0 | 4.1 | 8.1 | 0.7 |
| Office | S | 3 | 4.5 | 3 | 13.5 | 41 | 1 | 4.0 | 4.1 | 8.1 | 0.7 |
| Office | N | 3 | 6.3 | 3 | 18.9 | 57 | 1 | 4.0 | 5.7 | 9.7 | 0.6 |
| Teach. 119 | N | 12 | 6.3 | 3 | 75.6 | 227 | 25 | 100.0 | 22.7 | 122.7 | 1.9 |
| Copy | N | 3 | 6.3 | 3 | 18.9 | 57 | 0 | 0.0 | 5.7 | 5.7 | 0.4 |
| Databar | N | 6 | 6.3 | 3 | 37.8 | 113 | 5 | 32.0 | 11.3 | 31.3 | 1.0 |
| | 8 modules | | | | 259 | | | | | 230 l/s (827 $m^3$/h) | |
| Level 02 | | | | | | | | | | | |
| Meeting | S | 6 | 4.5 | 3 | 27.0 | 81 | 7 | 40.0 | 8.1 | 36.1 | 1.6 |
| Databar | S | 6 | 4.5 | 3 | 27.0 | 81 | 8 | 32.0 | 8.1 | 40.1 | 1.8 |
| Office | S | 3 | 4.5 | 3 | 13.5 | 41 | 1 | 4.0 | 4.1 | 8.1 | 0.7 |
| Office | S | 6 | 4.5 | 3 | 27.0 | 81 | 2 | 8.0 | 8.1 | 16.1 | 0.7 |
| Office | N | 6 | 6.3 | 3 | 37.8 | 113 | 4 | 32.0 | 11.3 | 27.3 | 0.9 |
| Teach. 225 | N | 12 | 6.3 | 3 | 75.6 | 227 | 40/0† | 100.0/0† | 22.7 | 182.7/0† | 2.9/0† |
| | 6.5 modules | | | | 208 | | | 310 l/s (1117 $m^3$/h) or 150 l/s† (541 $m^3$/h)† | | | |
| | 22.5 (all) modules | | | | 726 | | | 650 l/s (2340 $m^3$/h) or 490 l/s† (1764 $m^3$/h)† | | | |

Table 4.2: Calculated selected pressure drops of the implemented system.

| | Pressure drop [Pa] | |
|---|---|---|
| | at max flow 2340 $m^3/h$ | at min flow 1764 $m^3/h$ |
| Exchangers | 2 x 0.9 | 2 x 0.7 |
| Bagfilter | 16.4 | 9.5 |
| Damper floor 1/2/3 | 54/18/0 | 7.6/0.2/0 |
| Inlet grilles | 1.5 | 1.5 |
| Ventilation ceiling | 4.4 | 2.7 |
| Ductwork | 50 | 4.9 |
| Total (not sum) | 74 | 20 |

Figure 4.4 to Figure 4.5 shows some of the components of the system. The entire system from intake to exhaust has approx. 74 Pa pressure drop at max flow rate. The corresponding pressure drop at min flow rate is 20 Pa. Table 4.2 lists some selected pressure drops among the components.

The model on Figure 4.6 was used to calculate the pressure drops and air distribution in the system. Three dampers were installed in the main vertical ducts to control the airflow to each floor. Two dampers and a new larger distribution duct were established to supply teaching room 225.

(a) Exchanger coil in the basement

(b) Exchanger coil on the roof

Figure 4.4: Photos of exchanger installation

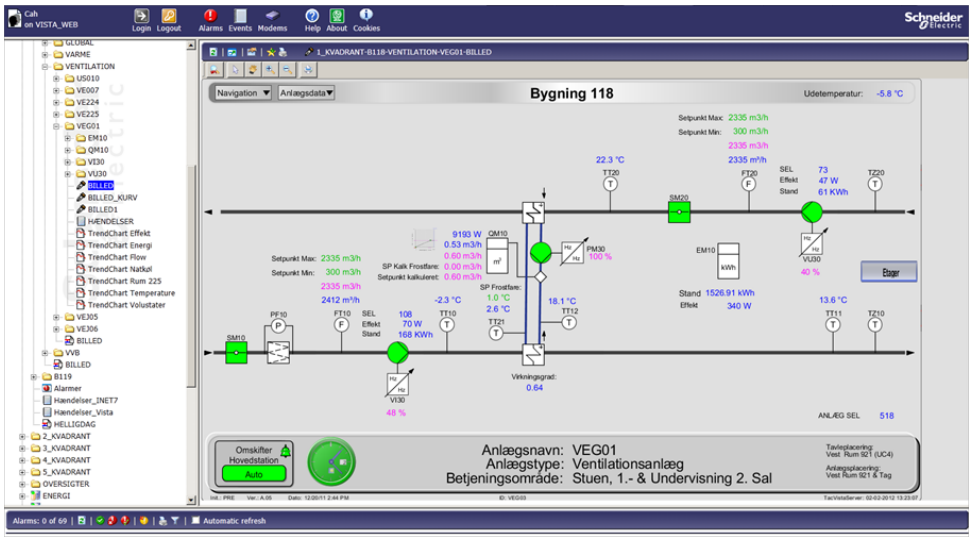


(a) Screen 1

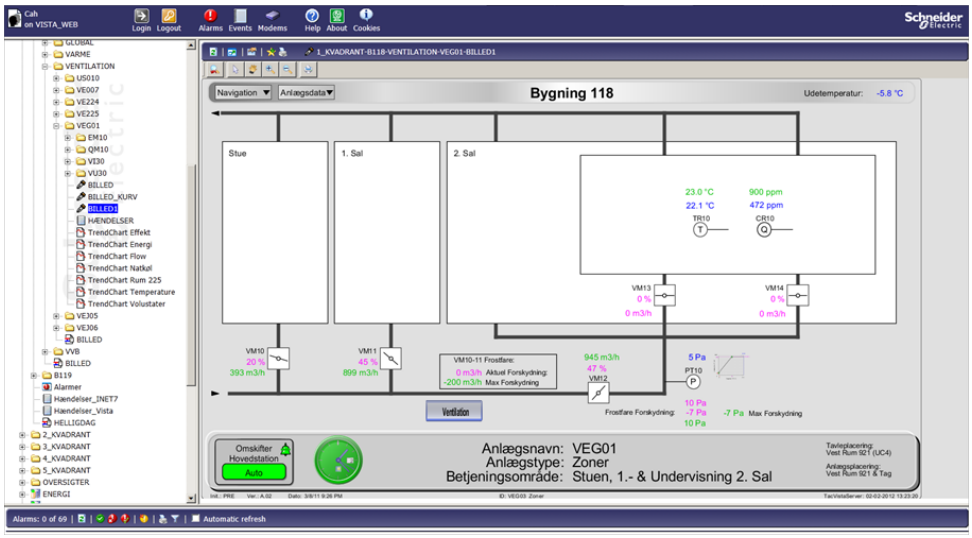


(b) Screen 2

Figure 4.5: Screen dumps from CTS system

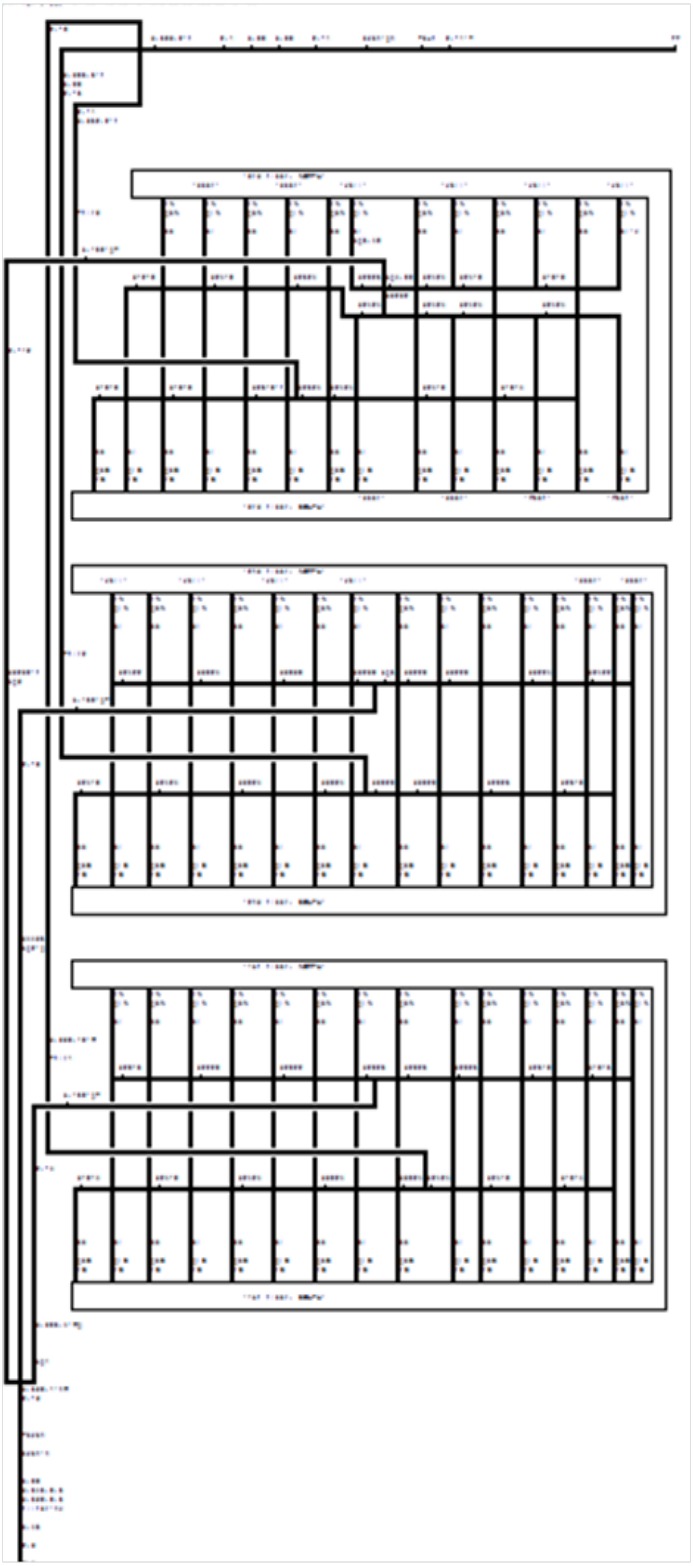

Figure 4.6: Calculation model of the implemented ventilation system

## 4.3 Capacity flows

The liquid-coupled heat recovery system is based on a counterflow regime. This requires equal capacity flow, i.e. mass flow and volumetric heat capacity multiplied. The equal capacity of the fluid flows causes the temperature change and the transferred power to be equal for the two fluid sides. There are two operations modes on the air side, max air flow and minimum air flow. The necessary volumetric water flow for minimum airflow ($1764\,\mathrm{m^3/h}$) is calculated from (Equation 4.1) with the fluid properties of Table 4.3.

$$\begin{aligned} \dot{V}_\mathrm{a} \cdot \rho_\mathrm{a} \cdot c_\mathrm{p,a} &= \dot{V}_\mathrm{w} \cdot \rho_\mathrm{w} \cdot c_\mathrm{p,w} \\ \dot{V}_\mathrm{w} &= \frac{\dot{V}_\mathrm{a} \cdot \rho_\mathrm{a} \cdot c_\mathrm{p,a}}{\rho_\mathrm{w} \cdot c_\mathrm{p,w}} \\ &= \frac{1764\,\mathrm{m^3/h} \cdot 1.249\,\mathrm{kg/m^3} \cdot 1007\,\mathrm{J/kg\,K}}{1033\,\mathrm{kg/m^3} \cdot 3820\,\mathrm{J/kg\,K}} \\ &\approx 562\,\mathrm{l/h} \end{aligned} \tag{4.1}$$

The corresponding water flow for operation mode maximum airflow ($2340\,\mathrm{m^3/h}$) is 746 l/h. However, due to much higher pressure drop than expected within the exchangers the liquid-loop and the employed pump are only capable of producing a flow of 560 l/h.

Table 4.3: Property values of air and water

| Properties at 10 °C | | Air | Water | 30 vol-pct. propylene glycol |
|---|---|---|---|---|
| Density | $\rho$ | $1.249\,\mathrm{kg/m^3}$ | $999.7\,\mathrm{kg/m^3}$ | $1033\,\mathrm{kg/m^3}$ |
| Thermal capacity | $c_\mathrm{p}$ | $1007\,\mathrm{J/kg\,K}$ | $4192\,\mathrm{J/kg\,K}$ | $3820\,\mathrm{J/kg\,K}$ |
| Thermal conductivity | $\lambda$ | $0.025\,\mathrm{W/m\,K}$ | $0.587\,\mathrm{W/m\,K}$ | $0.434\,\mathrm{W/m\,K}$ |
| Dynamic viscosity | $\mu$ | $1.77 \cdot 10^{-5}\,\mathrm{Pa\,s}$ | $1.30 \cdot 10^{-3}\,\mathrm{Pa\,s}$ | $4.52 \cdot 10^{-3}\,\mathrm{Pa\,s}$ |
| Prandtl number | $Pr$ | 0.71 | 9.28 | 39.78 |

## 4.4 Results

### 4.4.1 Heat recovery

The implemented exchangers have each a face area of $3.6\,\mathrm{m^2}$ and contains 5148 m of tubing. Each exchanger has 18 tube layers in each radiator, in effect creating a total of 36 tube layers seen from the approaching air. The analytical equations in section 3.5 can be used to model the heat transfer of the exchanger. An expected theoretical total efficiency of the heat recovery system is approx. 63% with min flow rate and 59% with max flow rate. However, for the max operation mode, the capacity flow of the pump is too small. However, the analytical framework states that the heat transfer on the water side is independent of the water flow, and we therefore expect quite small changes in the total efficiency.

Figure 4.7a depicts the measured heat recovery of the system. Due to the capacity of the pump, different water capacity flows are depicted. It is quite interesting to see that despite significant reductions in the water flow, the total heat recovery efficiency is approx. 63%. This shows that the system is robust to unequal capacity flows.

Figure 4.7b depicts on the same dates the airflow and water flows through the heat recovery system.

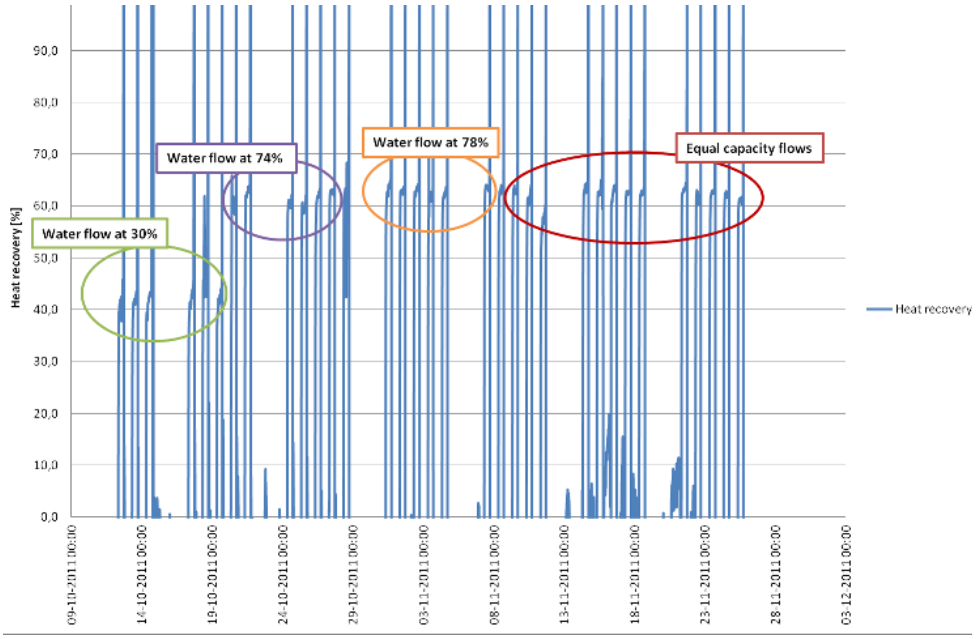


(a) Measured heat recovery


(b) Airflows through fans and water flow through pump

Figure 4.7: Heat recovery with air and water flows at the same time

### 4.4.2 Specific fan power

Figure 4.8 indicates the power consumption by the entire system, i.e. fans, pump and controls. The figure illustrates the specific fan power (SFP, in Danish: SEL-værdi), i.e. the power consumption for each transported $m^3$ of air in $J/m^3$ or $W/(m^3/s)$. On average the SFP is 600-700 $J/m^3$. The outdoor temperature is included in the figure because it affects the driving stack pressure of the building. In theory, the stack constitutes approx. 6-7 Pa of the 74 Pa pressure loss that the entire system has, i.e. it reduces power consumption of the fans by approx. 8%. The effect is not visible on Figure 4.8. Qualitatively, however, windy periods are visible in the CTS-system, because during those periods the wind induces too large airflow on the exhaust side of the ventilation system even though the extract fan is throttled to the absolutely minimum.

The SFP in min flow rate mode is approx. 600 $J/m^3$. I.e. it is not the fans which consume the largest part. In fact, the SFP can be split into the different contributing components. Table 4.4 shows how fans, pump and controls each roughly contribute. It is also a tool for further investigation because the pump and the controls in particular constitute much bigger percentages of the total SFP than initially expected.

With regard to the pump the pressure loss on the water side was measured in the final exchanger to be 4 times higher than expected. The reason is unclear but it must be due to the the manifolds, valves and small internal reductions of the cross sectional area at each tube fitting.

The controls constitute a rather large part because the other components use so little.

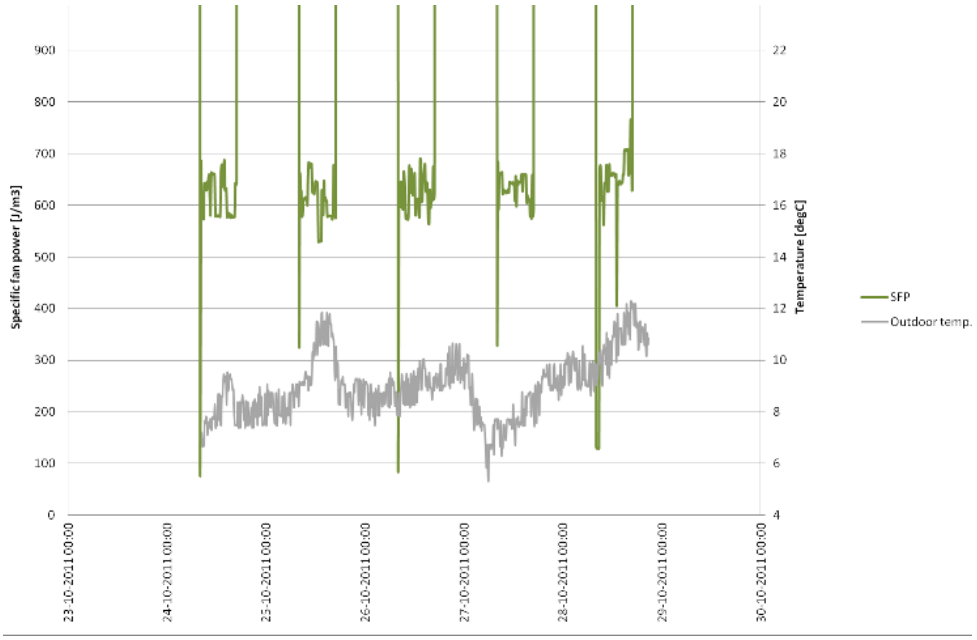


Figure 4.8: Specific fan power at max flow rate and outdoor temperature

### 4.4.3 $CO_2$ level and temperature

Figure 4.9 shows the temperature and $CO_2$ concentration of teaching room 225. The switch off of the heating system during weekends is visible and the expected $CO_2$ peak level of 1400 ppm during fully booked room is also visible. The system does not have the capacity to increase the airflow to room 225. The ducts are too leaky and the duct layout on the top floor causes room 225 to share the supplied air with the rest of the floor anyway. Consequently only a minor part

Table 4.4: Power consumption in Watt and in terms of transported air volume, i.e. as specific fan power at min/max flow rate

| | Power [W] min flow | SFP [J/m$^3$] min flow | Distribution % | Power [W] max flow | SFP [J/m$^3$] max flow | Distribution % |
|---|---|---|---|---|---|---|
| Fans | 90 | 185 | 27 | 180 | 245 | 40 |
| Pump | 140 | 285 | 41 | 140 | 215 | 35 |
| Controls | 110 | 225 | 32 | 110 | 155 | 25 |
| Sum | 340 | 695 | 100 | 430 | 615 | 100 |

of the increased air flow rate will end up in 225.

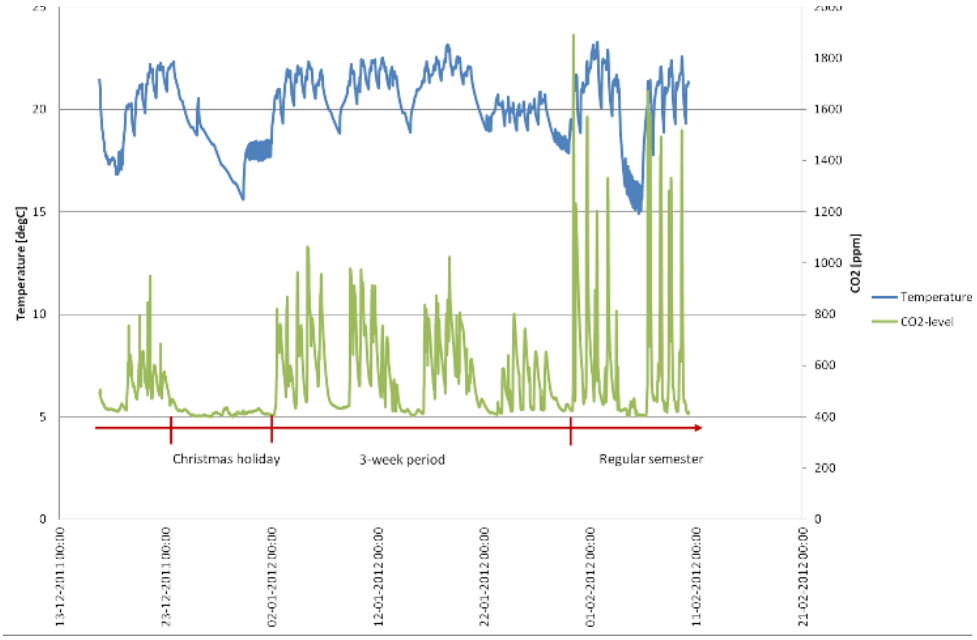


Figure 4.9: Temperature and $CO_2$ level in teaching room 225

### 4.4.4 Night cooling

Night cooling is implemented in the CTS-system, which means that the building is cooled at night in warm summer periods based on the temperature sensor in a critical room. With the extremely low fan power consumption, the cooling is practically free.

The sensor is placed in a north facing room because this room obtains the desired indoor air temperature first when the cooling program runs. If the sensor was placed in a south facing room, it would have caused all the north facing rooms to be cooled to temperatures below comfort temperature. Night cooling is activated when the indoor temperature is above 25 °C and the outdoor temperature is above 15 °C.

# Chapter 5

# Conclusion

The dual-sided issue of indoor environment and energy consumption have become increasingly important in building design. One possible solution is to ventilate by passive means, such as by stack effect and wind pressure, but this requires the development of new concepts and components. Here we have presented the outline of a heat recovery concept suitable for stack and wind-assisted mechanical ventilation systems with total system pressure losses of 74 Pa.

The heat recovery concept is based on two air-to-water exchangers connected by a liquid loop powered by a pump. The core element of the concept, a prototype of a heat exchanger, was developed based on design criteria about pressure drop, efficiency and production concerns. The performance was confirmed by comparing the pressure drop and heat transfer measured on a section with numerical fluid calculations and literature sources. The measurements and calculations agree reasonably well.

A full scale implementation was achieved in a part of building 118 at Dept. of Civil Eng., Tech. Univ. of Denmark. In this building the system supplies offices and two teaching rooms with fresh air. The mean specific fan power (SFP, in Danish: SEL-værdi) is measured to be approx. 240 $J/m^3$. The SFP of the entire system including fans, pump and controls is measured to be approx. 600-700 $J/m^3$.

The total heat recovery efficiency of the system, while subjected to realistic operation conditions in a building where fluctuating ventilation flow and parasitic heat losses may exist, was measured to be 63%. To compare with the efficiency of conventional heat recovery, the Danish Building Code requires a temperature efficiency of 65%, a value which is expected to increase to 70% in 2020.

The following points should be addressed in further investigations:

- the analytically calculated pressure drop is higher than measured. This can be exploited to include more tube layers and increase the heat transfer efficiency without compromising the initial design criterion of low pressure drop
- the pump power is much higher than expected. The pressure loss in one exchanger is 4 times higher than expected even though the theoretical calculation procedure including the use of anti-freeze is well documented. This is due to the fittings, manifolds, valves etc. which each induce a pressure loss
- power consumption for controls constitute 30% of the total power consumption in systems with ultra low fan power
- the system needs slow-rotating fans to level out fluctuating driving pressures and achieve proper airflow control. The drop dampers from LeanVent have proven that they are capable

of that in the present system. Thus the entire system including the heat exchangers should be designed and optimized with this knowledge in mind

## 5.1 10 good design advices

As the last concluding remarks ten advices are listed here for successful design of stack and wind-assisted mechanical ventilation.

1. Accept that the air quality may fluctuate or use variable speed fans to control the air change.
2. Exploit building spaces for ventilation air extraction: Use stairs, atriums, lightwells etc. instead of ducts. Regard fire safety precautions. Usually spaces used for transporting of air and humans is prohibited unless other measures are implemented
3. Place intake low and exhaust high: To maximize stack the vertical distance should be as high as possible. E.g. place service room on roof, use exhaust chimney, use natural landscape height differences.
4. Use liquid-coupled heat exchangers for heat recovery: The efficiency is lower than for conventional heat exchangers, but it is enough for 'near-zero' buildings
5. Place exhaust in negative pressure zones: As wind is deflected by the building, positive and negative pressure arises on opposing facades. Negative pressure also arises on horizontal roofs.
6. Place intake away from the facade: certain wind directions causes negative pressure in the intake which could result in reverse flow direction in the ventilation system
7. Design for low air speeds: Friction and losses in components are proportional with the airspeed squared
8. Design with extra-large components: Use a face speed of 1 m/s
9. Place heating and cooling coils horizontally: Reverse flow may occur with low-pressure components and local density differences. The liquid-coupled heat exchanger can be used for heating and cooling coil by an arrangement of on-off dampers.
10. Use fans to control ventilation rate: wind-induced ventilation systems experiences significant fluctuations. With variable fan speed the ventilation rate is controllable

# Bibliography


ASHRAE, 2005. ASHRAE Handbook of Fundamentals. American Society of Heating, Refrigerating and Air-Conditioning Engineers.

Beale, S.B., 1997. Tube banks, Single-phase heat transfer. International Encyclopedia of Heat and Mass Transfer. CRC Press Inc.

Bekö, G., Clausen, G., Weschler, C.J., 2008. Is the use of particle air filtration justified? Costs and benefits of filtration with regard to health effects, building cleaning and occupant productivity. Building and Environment 43 (10), 1647–1657.

Bekö, G., Fadeyi, M.O., Clausen, G., Weschler, C.J., 2009. Sensory pollution from bag-type fiberglass ventilation filters: Conventional filter compared with filters containing various amounts of activated carbon. Building and Environment 44 (10), 2114–2120.

Bergsøe, N.C., 2012. Udeluftindtag gennem kanaler i jord. Tech. rep., Statens Byggeforskningsinstitut, Hørsholm.

EN15251, 2007. Indoor environmental input parameters for design and assessment of energy performance of buildings addressing indoor air quality, thermal environment, lighting and acoustics. European StandardNot read.

EPBD, 2010. Energy Performance Building Directive 2010 (29-03-2010).

Horvat, A., Leskovar, M., Mavko, B., 2006. Comparison of heat transfer conditions in tube bundle cross-flow for different tube shapes. International Journal of Heat and Mass Transfer 49 (5-6), 1027–1038.

Hviid, C.A., 2010. Building integrated passive ventilation systems. Ph.d. thesis, Technical University of Denmark.

Hviid, C., Svendsen, S., 2011. Analytical and experimental analysis of a low-pressure heat exchanger suitable for passive ventilation. Energy and Buildings 43 (2–3), 275–284.

Hviid, C., Svendsen, S., 2012. Experimental analysis of perforated suspended ceilings as diffuse ventilation air inlets. Energy and Buildings, in press.

Incropera, F.P., DeWitt, D.P., 2002. Introduction to heat transfer. John Wiley & Sons, Inc., New York.

Jensen, H.T., 2003. Naturlig ventilation. Tech. rep., BYG.DTU U-058.

Larsen, T.S., Jensen, R.L., Kalyanova, O., Heiselberg, P., 2006. Indeklimaundersøgelser hos Københavns Energi. Tech. rep., Aalborg Universitet.

Li, Y., Delsante, A., Chen, L., 1999. Integrating thermal stratification in natural and hybrid ventilation analysis. In: anonymous (Ed.), HybVent Forum 99. IEA Annex 35.

Schild, P.G., 2001. An overview of Norwegian buildings with hybrid ventilation. In: anonymous (Ed.), HybVent Forum 01. IEA Annex 35.

Terkildsen, S., 2009. Udvikling af ventilationsanlæg med lavt elforbrug. Master thesis, Technical University of Denmark.

# Appendix A

# Exchanger model source codes

This appendix comprises the program source code for calculating local temperature variations and heat exchange efficiency. Models have been created for four very different exchanger layouts.

- Circling tubes around an elongated core, spiraling downward. Radiative exchange not included.
- Downward spiraling tubes, but circling in an 8-form. Radiative exchange not included.
- Tubes placed in separate radiators, then stacked grid to form an exchanger. Two parallel tubes in each radiator. Inlets from the same side. Radiative exchange included.
- Tubes placed in separate radiators, then stacked grid to form an exchanger. Two parallel tubes in each radiator. Inlets from *alternating* sides. Radiative exchange included.

The main differences are the interconnection of tubes and the inclusion of radiative exchange.

## A.1 Circling, spiraling tubes

This section comprises the Matlab source code to exch_simul_spiral.m

---

```
%Matlab script
%Calculates heat transfer efficiency for several parallel tubes circling
%an elongated core, spiraling down

%Methodology:
%Water and air domain is divided into a number of discrete
%points. In each point heat transfer is a function of flow, speed and
%materials. Heat transfer affects temperature of both air and water in a
%point. The points are interconnected in the air domain and the water
%domain respectively.
%After a number of iterations, where temperatures in each iteration are
%updated with the temperature upstream, steady state is achieved.
%Heat exchange efficiency = air_out-air_in / (water_in-air_in)

%Figure of tube interconnections:
```

```
%             air
%       ^ ^ ^ ^ ^ ^ ^ ^ ^
%       | | | | | | | | |
%
%------|-|-|-|-|-|-|-|-|------| i=1 layer=1
%                              |
%  |---------------------------|
%  |
%  |---|-|-|-|-|-|-|-|-|------| i=2 layer=2
%                              |
%  |---------------------------|
%  |
%  |---|-|-|-|-|-|-|-|-|--|---| i=3 layer=3
%    j= 1 2 3 4 5 6 7 8 9

%By Christian Anker Hviid, July 9 2009

%PROGRAM
clear

tube_layers = 20;
tubes = 32; %Number of parallel tubes
A = 2.3; %m, length of exchanger

D_o = 0.008; %m, outer tube diameter
D_i = 0.0072; %m, inner tube diameter
S_v = 2.0; %vertical tube distance, dimensionless
S_h = 2; %horizontal tube distance, dimensionless
S_d = (sqrt((2*D_o)^2+(2*D_o)^2))/D_o; %diagonal tube distance, dimensionless

lambda_a = 0.025; %W/mK, heat conduction, air
lambda_mat = 0.35; %W/mK, heat conduction, plastic
lambda_w = 0.591; %W/mK, heat conduction, water

core_width = 0.116; %m
B = 2*D_o*S_h*tubes+core_width; %m, width of exchanger
core_length = A-tubes*2*S_h*D_o; %m
area = A*B-core_width*core_length; %Front area 'seen' by air

airflow = .5*0.562; %m3/2, only one side of core is looked upon

%Properties of air @ 10 degC
rho_a = 1.247; %kg/m3
cp_a = 1007; %J/kgK
dynvisc_a = 1.79e-5;
Pr_a = 0.711; %Prandtl number
```

```
%Properties of water @ 10 degC
rho_w = 999.8; %kg/m3
cp_w = 4193; %J/kgK
dynvisc_w = 1.23e-3;
Pr_w = 8.81; %Prandtl number

T_indoor = 20; %degC
T_outdoor = 5; %degC
T_air_in = T_outdoor; %degC
efficiency_tot = 0.8; % Desired total heat exchange efficiency of system

% AIR SIDE
T_inlet = T_outdoor + efficiency_tot*(T_indoor-T_outdoor); %degC
T_mean_a_w = (T_indoor-T_inlet)/2; %degC
power = airflow*rho_a*cp_a*(T_inlet-T_outdoor); %W
U_a_app = airflow/area;
U_a_max = max(S_h/(S_h-1)*U_a_app,S_h/(S_d-1)*U_a_app);
Re_a = rho_a*U_a_max*D_o/dynvisc_a;
if Re_a > 50000
    warn('Reynolds number on air side indicates turbulent flow.')
end
Nu_a_B = 1.309*Re_a^0.36*Pr_a^0.34; %Nusselt number acc. to Beale
C = 0.61*S_h^0.091*S_v^0.053/(1-2*exp(-1.09*S_v));
Nu_K = C*Re_a^0.5*Pr_a^(1/3); %Nusselt number acc. to Khan
h_o = min(Nu_a_B,Nu_K)*lambda_a/D_o; %Worst-case Nusselt number is selected

%WATER SIDE
T_water_in = T_inlet + T_mean_a_w; %degC
waterflow = power/(rho_w*cp_w*(T_inlet-T_outdoor)); % total waterflow, m3/s
U_w = waterflow/(pi*(D_i/2)^2*tubes); %m/s
Re_w = rho_w*U_w*D_i/dynvisc_w;
if Re_w < 2000
    Nu_w_B = 4.36;
else
    warn('Reynolds number on water side indicates turbulent flow.')
end
h_i = Nu_w_B*lambda_w/D_i;

R_i = 1/(pi*D_i*h_i);
R_o = 1/(pi*D_o*h_o);
R_mat = log(D_o/D_i)/(2*pi*lambda_mat);%W/m2K

L(1) = 2*A+2*B; %m, LONGEST TUBE
L(3) = core_length*2+core_width*2; %m, SHORTEST TUBE
L(2) = (L(1)+L(3))/2; %m, MEAN LENGTH TUBE

% PRESSURE LOSS on air side
K_1 = 1.175*S_v/(S_h*Re_a^0.3124)+.5*Re_a^0.0807; %Correction factor
```

```
f = K_1*(378.6/(S_h^(13.1/S_h)))/(Re_a^(.68/(S_h^1.29))); %Friction factor
dP_a = tube_layers*f*0.5*rho_a*U_a_max^2 %Pa

% PRESSURE LOSS on water side
f = 64/Re_w; %Friction factor
dP_w_max = f*(rho_w*U_w^2)/(2*D_i)*L(1)*tube_layers %Worst-case pressure loss, Pa

nodx = 20; %m, no of dx elements per tube layer

vec_length=tube_layers*nodx;

%waterflow must be adjusted to length of tubing to fullfil equal capacity
wflow(1) = L(1)/L(2)*waterflow/tubes;
wflow(2) = L(2)/L(2)*waterflow/tubes;
wflow(3) = L(3)/L(2)*waterflow/tubes;

for m=1:3
    T_air = ones(tube_layers,nodx).*5;
    T_air_new = ones(tube_layers,nodx);
    T_air_old = ones(tube_layers,nodx).*5;
    T_water = ones(tube_layers,nodx).*18;
    T_water_new = ones(tube_layers,nodx);
    T_water_old = ones(tube_layers,nodx).*18;
    err_a = 1; err_w = 1;

    dx(m) = L(m)/nodx;
    k=0;
    waterflow = wflow(m); %For different waterflows
%    airflow = aflow(m); %For differentiated airflow in accordance with tube lengths

    %***************************** LOOP ***********************************
    %continue loop until residual is minimal
    while err_a > 1e-3 || err_w > 1e-3
        T_air_old = T_air_new;
        T_water_old = T_water_new;

        j1=1;
        for i=1:tube_layers
            for j=1:nodx
                T_air = T_air_new;
                T_water = T_water_new;

                if j==1
                    if j1==1 %Water inlet
                        T_water(i,j) = T_water_in;
                        j1=0;
                    else
                        T_water(i,j) = T_water(i-1,nodx);
```

```
                    end
                else

                    T_water(i,j) = T_water(i,j-1);
                end
                if i==tube_layers %Bottom of exchanger reached
                    T_air(i,j) = T_air_in;
                else
                    T_air(i,j) = T_air(i+1,j);
                end
                %phi is positive for heat transfer from water to air
                phi{m}(i,j) = ((T_water(i,j)-T_air(i,j))./(R_i+R_mat+R_o))*dx(m);

                T_air_new(i,j) = T_air(i,j) + phi{m}(i,j)/...
                    ((airflow/area)*D_o*S_h*dx(m)*rho_a*cp_a);
                T_water_new(i,j) = T_water(i,j) - phi{m}(i,j)/...
                    (waterflow*rho_w*cp_w);
            end
        end

        k=k+1;
        err_a = abs(sum(sum(T_air_old,2)) - sum(sum(T_air_new,2)));
        err_w = abs(sum(sum(T_water_old,2)) - sum(sum(T_water_new,2)));
    end
    %%%%%%%%%%%%%%%%%%%%%%%%%% LOOP END ****************************
    T_air = T_air_new;
    T_water = T_water_new;

    T_at{m} = T_air;
    T_wt{m} = T_water;

    T_a{m} = reshape(T_air',1,vec_length);
    T_w{m} = reshape(T_water',1,vec_length);

    T_a_o = mean(T_a{m}(1:nodx));
    T_a_i = mean(T_a{m}((tube_layers*nodx-nodx):(tube_layers*nodx)));
%    T_w_i = mean(T_w{m}(1:nodx));
%    T_w_o = mean(T_w{m}((tube_layers*nodx-nodx):(tube_layers*nodx)));

    efficiency_exch = (T_a_o-T_outdoor)/(T_water_in-T_outdoor)
end

figure

dx1 = 100*(1:vec_length)*dx(1)/(vec_length*dx(1));
dx2 = 100*(1:vec_length)*dx(2)/(vec_length*dx(2));
dx3 = 100*(1:vec_length)*dx(3)/(vec_length*dx(3));
```

```
plot(dx1,T_a{1},'-b',dx2,T_a{2},'-g',dx3,T_a{3},'-r',...
    dx1,T_w{1},'--b',dx2,T_w{2},'--g',dx3,T_w{3},'--r') %tubelength in percentage
xlabel('Tube length [m]'); ylabel('Temperature [degC]')
title('Air/water temperature development, spiralling')
legend('Air, longest','Air, mean','Air, shortest','Water, longest','Water, mean','Water, s
grid('on');

L(2)*tube_layers*tubes; %Total length of mean tube
```

---

## A.2 8-form exchanger

This section comprises the Matlab source code to exch_simul_eight.m

---

```
%Matlab script
%Calculates heat transfer efficiency for several parallel tubes circling
%in an eight number, spiraling down and crossing each other in the middle
%of the 8. The crossings in the middle are not included in effective
%heat transfer area.

%Methodology:
%Water and air domain is divided into a number of discrete
%points. In each point heat transfer is a function of flow, speed and
%materials. Heat transfer affects temperature of both air and water in a
%point. The points are interconnected in the air domain and the water
%domain respectively.
%After a number of iterations, where temperatures in each iteration are
%updated with the temperature upstream, steady state is achieved.
%Heat exchange efficiency = air_out-air_in / (water_in-air_in)

%Figure of tube interconnections:

%             air
%       ^ ^ ^ ^ ^ ^ ^ ^ ^
%       | | | | | | | | |
%
%------|-|-|-|-|-|-|-|-|------| i=1 layer=1
%                              |
%  |---------------------------|
%  |
%  |---|-|-|-|-|-|-|-|-|------| i=2 layer=2
%                              |
%  |---------------------------|
%  |
%  |---|-|-|-|-|-|-|-|-|--|---| i=3 layer=3
%    j= 1 2 3 4 5 6 7 8 9

%By Christian Anker Hviid, July 9 2009

%PROGRAM
clear

tube_layers = 20;
tubes = 38; %Parallel

D_o = 0.008; %m, outer tube diameter
D_i = 0.0072; %m, inner tube diameter
```

```
S_v = 2; %vertical tube distance, dimensionless
S_h = 2; %horizontal tube distance, dimensionless
S_d = (sqrt((2*D_o)^2+(2*D_o)^2))/D_o; %diagonal tube distance, dimensionless

lambda_a = 0.025; %W/mK, heat conduction, air
lambda_mat = 0.35; %W/mK, heat conduction, material
lambda_w = 0.591; %W/mK, heat conduction, water

r = 0.1; %m, small radius in 8-form
R = r+D_o*S_v*tubes; %large radius in 8-form
d = 2*r; %small diameter
D = 2*R; %large diameter
d_mark = ((D*pi+d*pi)/2)/pi; %d' is the diameter that corresponds to the mean circumferenc
tube_width = R-r;

A = 2*R+2*sqrt(2)*r+sqrt(2)*tube_width %m, length of 8-form
B = D %m, width of 8-form
area = 2*(3/4*pi*R^2-3/4*pi*r^2)+4*r*tube_width+tube_width^2;
area_eff = area-(tube_width^2);

airflow = .5*0.562; %m3/2, only one side is looked upon

%Properties of air @ 10 degC
rho_a = 1.247; %kg/m3
cp_a = 1007; %J/kgK
dynvisc_a = 1.79e-5;
Pr_a = 0.711; %Prandtl number

%Properties of water @ 10 degC
rho_w = 999.8; %kg/m3
cp_w = 4193; %J/kgK
dynvisc_w = 1.23e-3;
Pr_w = 8.81; %Prandtl number

T_indoor = 20; %degC
T_outdoor = 5; %degC
T_air_in = T_outdoor; %degC
efficiency_tot = 0.8; %Desired total heat exchange efficiency of system

% AIR SIDE
T_inlet = T_outdoor + efficiency_tot*(T_indoor-T_outdoor); %degC
T_mean_a_w = (T_indoor-T_inlet)/2; %degC
power = airflow*rho_a*cp_a*(T_inlet-T_outdoor); %W
U_a_app = airflow/area_eff;
U_a_max = max(S_h/(S_h-1)*U_a_app,S_h/(S_d-1)*U_a_app);
Re_a = rho_a*U_a_max*D_o/dynvisc_a;
if Re_a > 50000
    warn('Reynolds number on air side indicates turbulent flow.')
```

```
end
Nu_a_B = 1.309*Re_a^0.36*Pr_a^0.34; %Nusselt number acc. to Beale
C = 0.61*S_h^0.091*S_v^0.053/(1-2*exp(-1.09*S_v));
Nu_K = C*Re_a^0.5*Pr_a^(1/3); %Nusselt number acc. to Khan
h_o = min(Nu_a_B,Nu_K)*lambda_a/D_o; %Worst-case Nusselt number is selected


%WATER SIDE
T_water_in = T_inlet + T_mean_a_w; %degC
waterflow = power/(rho_w*cp_w*(T_inlet-T_outdoor)); % total waterflow, m3/s
U_w = waterflow/(pi*(D_i/2)^2*tubes); %m/s
Re_w = rho_w*U_w*D_i/dynvisc_w;
if Re_w < 2000
    Nu_w_B = 4.36;
else
    warn('Reynolds number on water side indicates turbulent flow.')
end
h_i = Nu_w_B*lambda_w/D_i;

R_i = 1/(pi*D_i*h_i);
R_o = 1/(pi*D_o*h_o);
R_mat = log(D_o/D_i)/(2*pi*lambda_mat);%W/m2K

L{1}(1) = 3/4*D*pi; %LONGEST -> SHORTEST
L{1}(2) = r;
L{1}(3) = tube_width;
L{1}(4) = L{1}(2); %r
L{1}(5) = 3/4*d*pi;
L{1}(6) = L{1}(2); %r
L{1}(7) = L{1}(3); %tube_width
L{1}(8) = L{1}(2); %r

L{2}(1) = 3/4*d_mark*pi; %MEAN
L{2}(2) = r;
L{2}(3) = tube_width;
L{2}(4) = L{2}(2); %r
L{2}(5) = 3/4*d_mark*pi;
L{2}(6) = L{2}(2); %r
L{2}(7) = L{2}(3); %tube_width
L{2}(8) = L{2}(2); %r

L{3}(1) = 3/4*d*pi; %SHORTEST -> LONGEST
L{3}(2) = r;
L{3}(3) = tube_width;
L{3}(4) = L{3}(2); %r
L{3}(5) = 3/4*D*pi;
L{3}(6) = L{3}(2); %r
L{3}(7) = L{3}(3); %tube_width
```

```
L{3}(8) = L{3}(2); %r

L_layer(1) = L{1}(1)+L{1}(5)+2*L{1}(3)+4*L{1}(2); %m, LONG -> SHORTEST
L_layer(2) = 2*3/4*d_mark*pi+2*L{2}(3)+4*L{2}(2); %m, MEAN
L_layer(3) = L{3}(1)+L{3}(5)+2*L{3}(3)+4*L{3}(2); %m, SHORTEST -> LONGEST

L_eff(1) = L{1}(1)+L{1}(5)+4*L{1}(2); %m, LONGEST -> SHORTEST
L_eff(2) = 2*3/4*d_mark*pi+4*L{2}(2); %m, MEAN
L_eff(3) = L{3}(1)+L{3}(5)+4*L{3}(2); %m, SHORTEST -> LONGEST

% PRESSURE LOSS on air side
K_1 = 1.175*S_v/(S_h*Re_a^0.3124)+.5*Re_a^0.0807; %Correction factor
f = K_1*(378.6/(S_h^(13.1/S_h)))/(Re_a^(.68/(S_h^1.29))); %Friction factor
dP_a = tube_layers*f*0.5*rho_a*U_a_max^2 %Pa

% PRESSURE LOSS on water side
f = 64/Re_w; %Friction factor
dP_w = f*(rho_w*U_w^2)/(2*D_i)*L_layer(2)*tube_layers %Pa

nodx = 1; %no of dx elements

eff(1:nodx) = 1;
eff(nodx+1:2*nodx) = 1;
eff(2*nodx+1:3*nodx) = 0; %Not effective area
eff(3*nodx+1:4*nodx) = 1;
eff(4*nodx+1:5*nodx) = 1;
eff(5*nodx+1:6*nodx) = 1;
eff(6*nodx+1:7*nodx) = 0; %Not effective area
eff(7*nodx+1:8*nodx) = 1;

%waterflow must be adjusted to length of tubing to fullfil equal capacity
%wflow(1) = L(1)/L(2)*(8.42e-5)/tubes;
%wflow(2) = L(2)/L(2)*(8.42e-5)/tubes;
%wflow(3) = L(3)/L(2)*(8.42e-5)/tubes;

for m=1:1
     % no of elements on first circle length
    dx{m}(1:nodx) = L{m}(1)/nodx;
     % no of elements on entry to tube crossing
    dx{m}((nodx+1):(2*nodx)) = L{m}(2)/nodx;
     % no of elements across tube crossing
    dx{m}((2*nodx+1):(3*nodx)) = L{m}(3)/nodx;
     % no of elements exit from tube crossing
    dx{m}((3*nodx+1):(4*nodx)) = L{m}(4)/nodx;
     % no of elements on last circle length
    dx{m}((4*nodx+1):(5*nodx)) = L{m}(5)/nodx;
     % no of elements on entry to tube crossing
    dx{m}((5*nodx+1):(6*nodx)) = L{m}(6)/nodx;
```

```
     % no of elements across tube crossing
    dx{m}((6*nodx+1):(7*nodx)) = L{m}(7)/nodx;
     % no of elements exit from tube crossing
    dx{m}((7*nodx+1):(8*nodx)) = L{m}(8)/nodx;

    dxl(m) = length(dx{m});
    %eff = ones(1,dxl); %eff is a check for the ...
        unusable/uneffective tube crossing in the middle
    phi{m} = zeros(tube_layers,dxl(m));

    T_air = ones(tube_layers,dxl(m)).*5;
    T_air_new = ones(tube_layers,dxl(m));
    T_air_old = ones(tube_layers,dxl(m)).*5;
    T_water = ones(tube_layers,dxl(m)).*18;
    T_water_new = ones(tube_layers,dxl(m));
    T_water_old = ones(tube_layers,dxl(m)).*18;
    err_a = 1; err_w = 1;
    k=0;
%    waterflow = wflow(m); %For different waterflows

    %***************************** LOOP ***********************************
    %continue loop until residual is minimal
    while err_a > 1e-3 || err_w > 1e-3
        T_air_old = T_air_new;
        T_water_old = T_water_new;

        j1=1;
        for i=1:tube_layers
            for j=1:dxl(m)
                T_air = T_air_new;
                T_water = T_water_new;

                if j==1
                    if j1==1 %Water inlet
                        T_water(i,j) = T_water_in;
                        j1=0;
                    else
                        T_water(i,j) = T_water(i-1,dxl(m));
                    end
                else
                    T_water(i,j) = T_water(i,j-1);
                end
                if i==tube_layers %Bottom of exchanger reached
                    T_air(i,j) = T_air_in;
                else
                    T_air(i,j) = T_air(i+1,j);
                end
                %phi is positive for heat transfer from water to air
```

```
                phi{m}(i,j) = eff(j)*((T_water(i,j)-T_air(i,j))./...
                    (R_i+R_mat+R_o))*dx{m}(j);
                T_air_new(i,j) = T_air(i,j) + phi{m}(i,j)/...
                    ((airflow/area_eff)*D_o*S_h*dx{m}(j)*rho_a*cp_a);
                T_water_new(i,j) = T_water(i,j) - ...
                    phi{m}(i,j)/(waterflow/tubes*rho_w*cp_w);
            end
        end
        k=k+1;
        err_a = abs(sum(sum(T_air_old,2)) - sum(sum(T_air_new,2)));
        err_w = abs(sum(sum(T_water_old,2)) - sum(sum(T_water_new,2)));
    end
    %%%%%%%%%%%%%%%%%%%%%%%%%% LOOP END ****************************
    T_air = T_air_new;
    T_water = T_water_new;

    T_at{m} = T_air;
    T_wt{m} = T_water;

    T_a{m} = reshape(T_air',1,tube_layers*dxl(m));
    T_w{m} = reshape(T_water',1,tube_layers*dxl(m));
end

dx0{1} = (dx{1}'*ones(1,tube_layers))';
%dx0{2} = (dx{2}'*ones(1,tube_layers))';
%dx0{3} = (dx{3}'*ones(1,tube_layers))';
dx1{1} = reshape(dx0{1}',1,dxl(1).*tube_layers);
%dx1{2} = reshape(dx0{2}',1,dxl(2).*tube_layers);
%dx1{3} = reshape(dx0{3}',1,dxl(3).*tube_layers);

dx2{1}(1) = dx1{1}(1);
%dx2{2}(1) = dx1{2}(1);
%dx2{3}(1) = dx1{3}(1);
for q=2:dxl(1).*tube_layers
    dx2{1}(q) = dx2{1}(q-1)+dx1{1}(q);
end
%for q=2:dxl(2).*tube_layers
%    dx2{2}(q) = dx2{2}(q-1)+dx1{2}(q);
%end
%for q=2:dxl(3).*tube_layers
%    dx2{3}(q) = dx2{3}(q-1)+dx1{3}(q);
%end

figure

dx3{1} = 100*dx2{1}./(sum(dx{1})*tube_layers);
%dx3{2} = 100*dx2{2}./(sum(dx{2})*tube_layers);
%dx3{3} = 100*dx2{3}./(sum(dx{3})*tube_layers);
```

```
%plot(dx3,T_a{1},'-b',dx3,T_a{2},'-g',dx3,T_a{3},'-r',...
%    dx3,T_w{1},'--b',dx3,T_w{2},'--g',dx3,T_w{3},'--r')
plot(dx2{1},T_a{1},'-b',...
    dx2{1},T_w{1},'--b')
%plot(dx2{1},T_a{1},'-b',dx2{2},T_a{2},'-g',dx2{3},T_a{3},'-r',...
%    dx2{1},T_w{1},'--b',dx2{2},T_w{2},'--g',dx2{3},T_w{3},'--r')
%plot((1:vec_length),T_a{1},'-b',(1:vec_length),T_a{2},'-g',...
    (1:vec_length),T_a{3},'-r',...
%    (1:vec_length),T_w{1},'--b',(1:vec_length),T_w{2},'--g',...
    (1:vec_length),T_w{3},'--r')
xlabel('Tube length [m]'); ylabel('Temperature [degC]')
title('Air/water temperature development, eight-number, spiralling')
legend('Air','Water')
%legend('Air, long->short','Air, mean','Air, short->long','Water, ...
    long->short','Water, mean','Water, short->long')
grid('on');

%T_a{1}(1)
%T_w{1}(1)
%T_a{1}(length(dx1{1}))
%T_w{1}(length(dx1{1}))
efficiency_exch = (T_a{1}(1)-T_outdoor)/(T_w{1}(1)-T_outdoor)
```

---

## A.3 Square form exchanger: 2 parallel inlets

This section comprises the Matlab source code to exch_simul_radiator_2_parallel_inlets.m

---

```
%Matlab script
%Calculates heat transfer efficiency for two parallel tubes with flowing
%water crossing an airstream

%Two neighbouring radiators are placed, so the tubes form a staggered grid
%2 parallelle inlet tubes in each radiator.
%2 radiators in a staggered grid is treated as one radiator with x2 tubes,
%which means that air meets water from left and right alternately

%Methodology:
%Water and air domain is divided into a number of discrete
%points. In each point heat transfer is a function of flow, speed and
%materials. Heat transfer affects temperature of both air and water in a
%point. The points are interconnected in the air domain and the water
%domain respectively.
%After a number of iterations, where temperatures in each iteration are
%updated with the temperature upstream, steady state is achieved.
%Heat exchange efficiency = air_out-air_in / (water_in-air_in)

%Figure of tube interconnections:

%             air
%       ^ ^ ^ ^ ^ ^ ^ ^ ^
%       | | | | | | | | |
%
%------|-|-|-|-|-|-|-|-|----| i=1 layer=1 layer_type=1
%------|-|-|-|-|-|-|-|-|--| | i=2 layer=2 layer_type=2
%                           | |
% |----|-|-|-|-|-|-|-|-|--| | i=3 layer=3 layer_type=3
% | |--|-|-|-|-|-|-|-|-|----| i=4 layer=4 layer_type=0
% | |
% | |--|-|-|-|-|-|-|-etc.       i=5 layer=5 layer_type=1
% |----|-|-|-|-|-|-|-etc.       i=6 layer=6 layer_type=2
%    j= 1 2 3 4 5 6 7 8 9

%By Christian Anker Hviid, July 9 2009

%PROGRAM
clear

tube_layers = 20;
B = 2.12;
A = 2.12; %Manifold side
```

```
gratio = 0.3; %glycol ratio, mass fraction!!
%Mass fraction = volume fraction*density_glycol /
%       (volumefrac*density_glycol + (1-volfrac)*density_wtr)
%Vol fraction = mass fraction*density_water((1-massfrac)*density_glycol +
%       massfrac*density_wtr)
T_b = 10; %brine temperature, degC

isStag = 1; %ctrl variable for in-line or staggered layout
radIsOn = 1; %ctrl variable for radiative heat exchange

D_o = 0.008; %m, outer tube diameter
D_i = 0.0058; %m, inner tube diameter
S_v = 0.022/D_o; %vertical tube distance, dimensionless
S_h = 0.024/D_o; %horizontal tube distance, dimensionless

% If the tube layout is staggered, diagonal distance is adjusted
if isStag ==1
    S_d = (sqrt((S_h/2)^2+(S_v)^2)); %diagonal tube distance, dimensionless
else
    S_d = (sqrt((S_h)^2+(S_v)^2)); %diagonal tube distance, dimensionless
end

lambda_a = 0.025; %W/mK, heat conduction, air
lambda_mat = 0.35; %W/mK, heat conduction, plastic

radiators = A/(D_o*S_h); %Number of parallel radiators
area = A*B; %front area 'seen' by air


%**************************************************************************
%Calculation of formfactors between neighbouring tubes, Danvak, A.03.07 for
%radiation calculation
r1=D_o/2;
r2=D_o/2;
s_v = S_v/2*D_o;
s_h = S_h/2*D_o;
s_d = S_d*D_o-D_o;
A_v = r2/r1; A_h = r2/r1; A_d = r2/r1;
B_v = s_v/r1; B_h = s_h/r1; B_d = s_d/r1;
C_v = 1+A_v+B_v; C_h = 1+A_h+B_h; C_d = 1+A_d+B_d;

formfactor_d = abs(1/(2*pi)*(pi + (C_d^2-(A_d+1)^2)^0.5 - ...
    (C_d^2-(A_d-1)^2)^0.5 + (A_d-1)*acos(A_d/C_d-1/C_d) - ...
    (A_d+1)*acos(A_d/C_d-1/C_d))); %formfactor dia
formfactor_v = abs(1/(2*pi)*(pi + (C_v^2-(A_v+1)^2)^0.5 - ...
    (C_v^2-(A_v-1)^2)^0.5 + (A_v-1)*acos(A_v/C_v-1/C_v) - ...
    (A_v+1)*acos(A_v/C_v-1/C_v))); %formfactor vertically
```

```
formfactor_h = abs(1/(2*pi)*(pi + (C_h^2-(A_h+1)^2)^0.5 - ...
    (C_h^2-(A_h-1)^2)^0.5 + (A_h-1)*acos(A_h/C_h-1/C_h) - ...
    (A_h+1)*acos(A_h/C_h-1/C_h))); %formfactor horiz
%**************************************************************************

airflow = 1.0*0.562; %m3/s

% Properties of air @ 10degC
rho_a = 1.24246; %kg/m3
cp_a = 1006.5; %J/kgK
dynvisc_a = 1.79202e-5;
Pr_a = 0.712; %Prandtl number

if gratio == 0
    % Properties of T_w = 10degC
    rho_w = 999.509; %kg/m3
    cp_w = 4194.74; %J/kgK
    dynvisc_w = 1.18667e-3;
    Pr_w = 8.641; %Prandtl number
    lambda_w = 0.58328; %W/mK, varmeledningsevne, water
else % Must be updated according to
    % Properties of water @ 10degC
    %pg: propylene glycol
    rho_pg = [508.411 -182.408 965.765 280.291 -472.225];
    cp_pg = [4.476 .609 -.715 -1.939 .479];
    dynvisc_pg = [-1.028 -10.033 -19.935 14.658 14.621];
    Pr_pg = [6.661 -6.994 -18.551 12.046 14.477];
    lambda_pg = [.838 -1.376 -0.076 1.077 -0.202];

    rho_w = rho_pg(1) + rho_pg(2)*gratio + ...
        rho_pg(3)*273.15/(273.15+T_b) + ...
        rho_pg(4)*gratio*273.15/(273.15+T_b) + ...
        rho_pg(5)*(273.15/(273.15+T_b))^2; %kg/m3
    cp_w = (cp_pg(1) + cp_pg(2)*gratio + ...
        cp_pg(3)*273.15/(273.15+T_b) + ...
        cp_pg(4)*gratio*273.15/(273.15+T_b) + ...
        cp_pg(5)*(273.15/(273.15+T_b))^2)*1000; %J/kgK
    dynvisc_w = 3e-3; %aflæst for ratio .3
    Pr_w = 38; %aflæst for ratio .3
    lambda_w = lambda_pg(1) + lambda_pg(2)*gratio + ...
        lambda_pg(3)*273.15/(273.15+T_b) + ...
        lambda_pg(4)*gratio*273.15/(273.15+T_b) + ...
        lambda_pg(5)*(273.15/(273.15+T_b))^2; %W/mK, heat conduction, water
end


T_indoor = 20; %indoor temp, degC
T_outdoor = 5; %outdoor temp, degC
```

```
T_air_in = T_outdoor; %degC
efficiency_tot = 0.80; %Desired total heat exchange efficiency of system

% AIR SIDE
T_inlet = T_outdoor + efficiency_tot*(T_indoor-T_outdoor); %degC
T_mean_a_w = (T_indoor-T_inlet)/2; %degC
power = airflow*rho_a*cp_a*(T_inlet-T_outdoor); %necessary heat transfer, W
U_a_app = airflow/area;

if isStag
    U_a_max = max(S_h/(S_h-1)*U_a_app,S_h/(S_d-1)*U_a_app);
else
    U_a_max = S_h/(S_h-1)*U_a_app;
end
Re_a = rho_a*U_a_max*D_o/dynvisc_a;
if Re_a > 50000
    disp('Reynolds number on air side indicates turbulent flow.')
end
Nu_a_B = 1.309*Re_a^0.36*Pr_a^0.34; %Nusselt number acc. to Beale
C = 0.61*S_h^0.091*S_v^0.053/(1-2*exp(-1.09*S_v));
Nu_K = C*Re_a^0.5*Pr_a^(1/3); %Nusselt number acc. to Khan
h_o = min(Nu_a_B,Nu_K)*lambda_a/D_o; %Worst case Nusselt number is selected

%WATER SIDE
T_water_in = T_inlet + T_mean_a_w; %degC
waterflow = power/(rho_w*cp_w*(T_inlet-T_outdoor)); % total waterflow, m3/s
U_w = waterflow/(pi/4*D_i^2*radiators*2); %m/s x2 because a radiator has two inlets
Re_w = rho_w*U_w*D_i/dynvisc_w;
if Re_w < 2000
    Nu_w_B = 4.36;
else
    Nu_w_B = 4.36;
    disp('Reynolds number on water side indicates turbulent flow.')
end
h_i = Nu_w_B*lambda_w/D_i;

R_i = 1/(pi*D_i*h_i);
R_o = 1/(pi*D_o*h_o);
R_mat = log(D_o/D_i)/(2*pi*lambda_mat);%W/m2K

L = B*tube_layers/2; %m, length of one tube in one radiator

% PRESSURE LOSS on air side
if isStag
    K_1 = 1.175*S_v/(S_h*Re_a^0.3124)+.5*Re_a^0.0807; %Correction factor
    f = K_1*(378.6/(S_h^(13.1/S_h)))/(Re_a^(.68/(S_h^1.29))); %Friction factor
else
    K_1 = 1.009*(((S_h-1)/(S_v-1))^(1.09/(U_a_max^0.0553))); %Correction factor
```

```
    f = K_1*(0.233+45.78/((S_h-1)^1.1*Re_a)); %Friction factor
end
dP_a = tube_layers*f*0.5*rho_a*U_a_max^2 %Pressure loss on air side, Pa

% PRESSURE LOSS on water side
f = 64/Re_w; %Friction factor
dP_w_max = f*(rho_w*U_w^2)/(2*D_i)*L %Pressure loss on water side, Pa

nodx = 10; %m, no of dx elements per tube layer

vec_length=tube_layers*nodx; %plot parameter

%Waterflow in one tube in one radiator, NB! two inlets in each radiator
wflow = waterflow/(2*radiators);

layer_type = mod(1:tube_layers,4);

for m=1:1
    T_air = ones(tube_layers,nodx).*5;
    T_air_new = ones(tube_layers,nodx);
    T_air_old = ones(tube_layers,nodx).*5;
    T_water = ones(tube_layers,nodx).*18;
    T_water_new = ones(tube_layers,nodx);
    T_water_old = ones(tube_layers,nodx).*18;
    T_surf = ones(tube_layers,nodx);
    rad = ones(tube_layers,nodx);
    err_a = 1; err_w = 1;
    phi{m} = zeros(tube_layers,nodx);

    dx(m) = B/nodx;
    k=0;
    %***************************** LOOP ***********************************
    %continue loop until residual is minimal
    while err_a > 1e-3 || err_w > 1e-3
        T_air_old = T_air_new;
        T_water_old = T_water_new;

        j1=1; %Ctrl variables
        j2=1; %Ctrl variables
        for i=1:tube_layers
            for j=1:nodx
                T_air = T_air_new;
                T_water = T_water_new;

                if j==1 %Water inlet side
                    if j1==1 %Water inlet #1
                        T_water(i,j) = T_water_in;
                        j1=0;
```

```
    elseif j2==1 %Water inlet #2
        T_water(i,j) = T_water_in;
        j2=0;
    elseif layer_type(i)==3
        T_water(i,j) = T_water(i,j+1);
    elseif layer_type(i)==0
        T_water(i,j) = T_water(i,j+1);
    elseif layer_type(i)==1
        T_water(i,j) = T_water(i-1,j);
    elseif layer_type(i)==2
        T_water(i,j) = T_water(i-3,j);
    else
        disp('error in j=1')
    end
elseif j==nodx %Opposite water inlet side
    if layer_type(i)==1
        T_water(i,j) = T_water(i,j-1);
    elseif layer_type(i)==2
        T_water(i,j) = T_water(i,j-1);
    elseif layer_type(i)==3
        T_water(i,j) = T_water(i-1,j);
    elseif layer_type(i)==0
        T_water(i,j) = T_water(i-3,j);
    else
        disp('error in j=nodx')
    end
else
    if layer_type(i)==1 || layer_type(i)==2
        T_water(i,j) = T_water(i,j-1);
    elseif layer_type(i)==3 || layer_type(i)==0
        T_water(i,j) = T_water(i,j+1);
    else
        disp('error in j=x')
    end
end
%rad_v: radiation to and from vertical tube neighbours
%rad_d: radiation to and from diagonally placed tube neighbours
%Each tube sees one tube up and one tube down and 2 diagonally
%up and two diagonally down. Extra contributions are
%ignored.
if i==1
    rad_v_down = formfactor_h * 5.6697E-08 * D_o*dx(m) * ...
        ((273.15+T_surf(i,j))^4 - (273.15+T_surf(i+1,j))^4);
    rad_d_down = 2* formfactor_d * 5.6697E-08 * D_o*dx(m) * ...
        ((273.15+T_surf(i,j))^4 - (273.15+T_surf(i+1,j))^4);
    rad_v_up = 0;
    rad_d_up = 0;
    rad(i,j) = rad_v_up + rad_v_down + rad_d_up + rad_d_down;
```

```
                T_air(i,j) = T_air(i+1,j);
            elseif i==tube_layers %Bottom of exchanger reached
                rad_v_down = 0;
                rad_d_down = 0;
                rad_v_up = formfactor_h * 5.6697E-08 * D_o*dx(m) * ...
                    ((273.15+T_surf(i,j))^4 - (273.15+T_surf(i-1,j))^4);
                    %positive from present tube
                rad_d_up = 2* formfactor_d * 5.6697E-08 * D_o*dx(m) * ...
                    ((273.15+T_surf(i,j))^4 - (273.15+T_surf(i-1,j))^4);
                    %positive from present tube
                rad(i,j) = rad_v_up + rad_v_down + rad_d_up + rad_d_down;
                T_air(i,j) = T_air_in;
            else
                rad_v_up = formfactor_h * 5.6697E-08 * D_o*dx(m) * ...
                    ((273.15+T_surf(i,j))^4 - (273.15+T_surf(i-1,j))^4);
                    %positive from present tube
                rad_v_down = formfactor_h * 5.6697E-08 * D_o*dx(m) * ...
                    ((273.15+T_surf(i,j))^4 - (273.15+T_surf(i+1,j))^4);
                rad_d_up = 2* formfactor_d * 5.6697E-08 * D_o*dx(m) * ...
                    ((273.15+T_surf(i,j))^4 - (273.15+T_surf(i-1,j))^4);
                    %positive from present tube
                rad_d_down = 2* formfactor_d * 5.6697E-08 * D_o*dx(m) * ...
                    ((273.15+T_surf(i,j))^4 - (273.15+T_surf(i+1,j))^4);
                rad(i,j) = rad_v_up + rad_v_down + rad_d_up + rad_d_down;

                T_air(i,j) = T_air(i+1,j);

            end
            phi{m}(i,j) = ((T_water(i,j)-T_air(i,j))./(R_i+R_mat+R_o))*dx(m);
            %phi is positive for heat transfer from water to air

            T_air_new(i,j) = T_air(i,j) + phi{m}(i,j)/...
                ((airflow/area)*D_o*S_h*dx(m)*rho_a*cp_a);
            if radIsOn == 1
                T_water_new(i,j) = T_water(i,j) - ...
                    (phi{m}(i,j)+rad(i,j))/(wflow*rho_w*cp_w);
            else
                T_water_new(i,j) = T_water(i,j) - ...
                    phi{m}(i,j)/(wflow*rho_w*cp_w);
            end
            T_surf(i,j) = T_water_new(i,j)-(T_water_new(i,j)-T_air_new(i,j))*...
                (R_i+R_mat)/(R_i+R_mat+R_o);
        end
    end
    k=k+1;
    err_a = abs(sum(sum(T_air_old,2)) - sum(sum(T_air_new,2)));
    err_w = abs(sum(sum(T_water_old,2)) - sum(sum(T_water_new,2)));
end
```

```
    %%%%%%%%%%%%%%%%%%%%%%%%%% LOOP END ****************************

    T_air = T_air_new;
    T_water = T_water_new;

    T_at{m} = T_air;
    T_wt{m} = T_water;

    T_a{m} = reshape(T_air',1,vec_length);
    T_w{m} = reshape(T_water',1,vec_length);

    T_a_o = mean(T_a{m}(1:nodx));
%    T_a_i = mean(T_a{m}((tube_layers*nodx-nodx):(tube_layers*nodx)));

    efficiency_exch = (T_a_o-T_outdoor)/(T_water_in-T_outdoor)
end

%PLOT
figure

dx1 = 100*(1:vec_length)*dx(1)/(vec_length*dx(1));

plot((1:vec_length)*dx(1),T_w{1},'-b',(1:vec_length)*dx(1),T_a{1},'--b')
xlabel('Tube length [m]'); ylabel('Temperature [degC]')
title('Air/water temperature development, radiator, two parallel inlet ...
tubes to each radiator')
legend('Water','Air')
grid('on');
```

## A.4 Square form exchanger: 4 parallel inlet tubes

This section comprises the Matlab source code to exch_simul_radiator_4_parallel_inlets.m

---

```
%Matlab script
%Calculates heat transfer efficiency for two parallel tubes with flowing
%water crossing an airstream

%Two neighbouring radiators are placed, so the tubes form a staggered grid.
%2 radiators in a staggered grid is treated as one radiator with x2 tube
%layers because the air 'sees' x2 tube layers. This means that air meets
%water from left and right alternately, see the sketch.
%If the tubes are aligned, the number of tube layers is off course x1

%Methodology:
%Water and air domain is divided into a number of discrete
%points. In each point heat transfer is a function of flow, speed and
%materials. Heat transfer affects temperature of both air and water in a
%point. The points are interconnected in the air domain and the water
%domain respectively.
%After a number of iterations, where temperatures in each iteration are
%updated with the temperature upstream, steady state is achieved.
%Heat exchange efficiency = air_out-air_in / (water_in-air_in)

%Figure of tube interconnections:

%                   air
%            ^ ^ ^ ^ ^ ^ ^ ^ ^
%            | | | | | | | | |
%
%>---------|-|-|-|-|-|-|-|-|-|-----|       i=1 layer=1 layer_type=1
%    |-----|-|-|-|-|-|-|-|-|-|-----}----<  i=2 layer=2 layer_type=2
%>---{-----|-|-|-|-|-|-|-|-|-|--|  |       i=3 layer=1 layer_type=3
%    |  |--|-|-|-|-|-|-|-|-|-|--}--}----<  i=4 layer=2 layer_type=4
%<---{--{--|-|-|-|-|-|-|-|-|-|--|  |       i=5 layer=1 layer_type=5
%    |  |--|-|-|-|-|-|-|-|-|-|-----}---->  i=6 layer=1 layer_type=6
%<---{-----|-|-|-|-|-|-|-|-|-|-----|       i=7 layer=1 layer_type=7
%    |-----|-|-|-|-|-|-|-|-|-|---------->  i=8 layer=1 layer_type=8
%        j= 1 2 3 4 5 6 7 8 9

%By Christian Anker Hviid, July 9 2009


%PROGRAM
clear

tube_layers = 28; %Multiple of 4+2
```

```
B = 2.12;
A = 2.12; %Manifold side

gratio = 0.3; %glycol ratio, mass fraction!!
%Mass fraction = volume fraction*density_glycol /
%       (volumefrac*density_glycol + (1-volfrac)*density_wtr)
%Vol fraction = mass fraction*density_water((1-massfrac)*density_glycol +
%       massfrac*density_wtr)
T_b = 10; %brine temperature, degC

isStag = 1; %ctrl variable for in-line or staggered layout
radIsOn = 1; %ctrl variable for radiative heat exchange

D_o = 0.008; %m, outer tube diameter
D_i = 0.0058; %m, inner tube diameter
S_v = 0.011/D_o; %vertical tube distance c-c, dimensionless
S_h = 0.022/D_o; %horizontal tube distance c-c, dimensionless

% If the tube layout is staggered, diagonal distance is adjusted
if isStag ==1
    S_d = (sqrt((S_h/2)^2+(S_v)^2)); %diagonal tube distance, dimensionless
else
    S_d = (sqrt((S_h)^2+(S_v)^2)); %diagonal tube distance, dimensionless
end

lambda_a = 0.025; %W/mK, heat conduction, air
lambda_mat = 0.35; %W/mK, heat conduction, plastic

radiators = A/(D_o*S_h/2); %Number of parallel radiators
area = A*B; %front area 'seen' by air

%**************************************************************************
%Calculation of formfactors between neighbouring tubes, Danvak, A.03.07 for
%radiation calculation
r1=D_o/2;
r2=D_o/2;
s_v = 3/2*S_v*D_o;
s_h = S_h/2*D_o;
s_d = S_d*D_o-D_o;
A_v = r2/r1; A_h = r2/r1; A_d = r2/r1;
B_v = s_v/r1; B_h = s_h/r1; B_d = s_d/r1;
C_v = 1+A_v+B_v; C_h = 1+A_h+B_h; C_d = 1+A_d+B_d;

formfactor_d = abs(1/(2*pi)*(pi + (C_d^2-(A_d+1)^2)^0.5 - ...
    (C_d^2-(A_d-1)^2)^0.5 + (A_d-1)*acos(A_d/C_d-1/C_d) - ...
    (A_d+1)*acos(A_d/C_d-1/C_d))); %formfactor dia
formfactor_v = abs(1/(2*pi)*(pi + (C_v^2-(A_v+1)^2)^0.5 - ...
    (C_v^2-(A_v-1)^2)^0.5 + (A_v-1)*acos(A_v/C_v-1/C_v) - ...
```

```
    (A_v+1)*acos(A_v/C_v-1/C_v))); %formfactor vertically
formfactor_h = abs(1/(2*pi)*(pi + (C_h^2-(A_h+1)^2)^0.5 - ...
    (C_h^2-(A_h-1)^2)^0.5 + (A_h-1)*acos(A_h/C_h-1/C_h) - ...
    (A_h+1)*acos(A_h/C_h-1/C_h))); %formfactor horiz
%************************************************************************

airflow = 1.0*0.562; %m3/s

% Properties of air @ 10degC
rho_a = 1.24246; %density, kg/m3
cp_a = 1006.5; %heat capacity, J/kgK
dynvisc_a = 1.79202e-5; %dynamic viscosity, Pa*s
Pr_a = 0.712; %Prandtl number

if gratio == 0
    % Properties of water @ 10degC
    rho_w = 999.509; %density, kg/m3
    cp_w = 4194.74; %heat capacity, J/kgK
    dynvisc_w = 1.18667e-3; %dynamic viscosity, Pa*s
    Pr_w = 8.641; %Prandtl number
    lambda_w = 0.58328; %heat conduction, W/mK
else % Must be updated according to
    % Properties of T_w = 10degC
    %pg: propylene glycol
%Factors from http://www.mrc-eng.com/Downloads/Brine%20Properties.pdf
    rho_pg = [508.411 -182.408 965.765 280.291 -472.225];
    cp_pg = [4.476 .609 -.715 -1.939 .479];
    dynvisc_pg = [-1.028 -10.033 -19.935 14.658 14.621];
    Pr_pg = [6.661 -6.994 -18.551 12.046 14.477];
    lambda_pg = [.838 -1.376 -0.076 1.077 -0.202];

    rho_w = rho_pg(1) + rho_pg(2)*gratio + rho_pg(3)*273.15/(273.15+T_b) + ...
        rho_pg(4)*gratio*273.15/(273.15+T_b) + ...
        rho_pg(5)*(273.15/(273.15+T_b))^2; %kg/m3
    cp_w = (cp_pg(1) + cp_pg(2)*gratio + cp_pg(3)*273.15/(273.15+T_b) + ...
        cp_pg(4)*gratio*273.15/(273.15+T_b) + ...
        cp_pg(5)*(273.15/(273.15+T_b))^2)*1000; %J/kgK
    dynvisc_w = exp(dynvisc_pg(1) + dynvisc_pg(2)*gratio + ...
        dynvisc_pg(3)*273.15/(273.15+T_b) + ...
        dynvisc_pg(4)*gratio*273.15/(273.15+T_b) + ...
        dynvisc_pg(5)*(273.15/(273.15+T_b))^2);
    Pr_w = exp(Pr_pg(1) + Pr_pg(2)*gratio + Pr_pg(3)*273.15/(273.15+T_b) + ...
        Pr_pg(4)*gratio*273.15/(273.15+T_b) + ...
        Pr_pg(5)*(273.15/(273.15+T_b))^2); %Prandtl number
    lambda_w = lambda_pg(1) + lambda_pg(2)*gratio + ...
        lambda_pg(3)*273.15/(273.15+T_b) + ...
        lambda_pg(4)*gratio*273.15/(273.15+T_b) + ...
        lambda_pg(5)*(273.15/(273.15+T_b))^2; %W/mK, heat conduction, water
```

```
    %dynvisc_w = 3e-3; %aflæst for ratio .3 Danvak, A.00.10, obsolete
    %Pr_w = 38; %aflæst for ratio .3, obsolete
end

T_indoor = 20; %indoor temp, degC
T_outdoor = 5; %outdoor temp, degC
T_air_in = T_outdoor; %degC
efficiency_tot = 0.80; % Desired total heat exchange efficiency of system

% AIR SIDE
T_inlet = T_outdoor + efficiency_tot*(T_indoor-T_outdoor); %degC
T_mean_a_w = (T_indoor-T_inlet)/2; %degC
power = airflow*rho_a*cp_a*(T_inlet-T_outdoor); %necessary heat transfer, W
U_a_app = airflow/area;

if isStag
    U_a_max = max(S_h/(S_h-1)*U_a_app,S_h/(S_d-1)*U_a_app);
else
    U_a_max = S_h/(S_h-1)*U_a_app;
end
Re_a = rho_a*U_a_max*D_o/dynvisc_a;
if Re_a > 50000
    disp('Reynolds number on air side indicates turbulent flow.')
end
Nu_a_B = 1.309*Re_a^0.36*Pr_a^0.34; %Nusselt number acc. to Beale
C = 0.61*S_h^0.091*S_v^0.053/(1-2*exp(-1.09*S_v));
Nu_K = C*Re_a^0.5*Pr_a^(1/3); %Nusselt number acc. to Khan
h_o = min(Nu_a_B,Nu_K)*lambda_a/D_o; %Worst case Nusselt number is selected

%WATER SIDE
T_water_in = T_inlet + T_mean_a_w; %degC
waterflow = power/(rho_w*cp_w*(T_inlet-T_outdoor)); % total waterflow, m3/s
U_w = waterflow/(pi/4*D_i^2*radiators*2); %m/s x2 because a radiator has two inlets
Re_w = rho_w*U_w*D_i/dynvisc_w;
if Re_w < 2000
    Nu_w_B = 4.36;
else
    Nu_w_B = 4.36;
    disp('Reynolds number on water side indicates turbulent flow.')
end
h_i = Nu_w_B*lambda_w/D_i;

R_i = 1/(pi*D_i*h_i);
R_o = 1/(pi*D_o*h_o);
R_mat = log(D_o/D_i)/(2*pi*lambda_mat);%W/m2K

L = B*tube_layers/4; %m, length of one tube in one radiator
```

```
% PRESSURE LOSS on air side
if isStag
    K_1 = 1.175*S_v/(S_h*Re_a^0.3124)+.5*Re_a^0.0807; %Correction factor
    f = K_1*(378.6/(S_h^(13.1/S_h)))/(Re_a^(.68/(S_h^1.29))); %Friction factor
else
    K_1 = 1.009*(((S_h-1)/(S_v-1))^(1.09/(U_a_max^0.0553))); %Correction factor
    f = K_1*(0.233+45.78/((S_h-1)^1.1*Re_a)); %Friction factor
end
dP_a = tube_layers*f*0.5*rho_a*U_a_max^2 %Pressure loss on air side, Pa

% PRESSURE LOSS on water side
f = 64/Re_w; %Friction factor
dP_w_max = f*(rho_w*U_w^2)/(2*D_i)*L %Pressure loss on water side, Pa

nodx = 10; %m, no of dx elements per tube layer

vec_length=tube_layers*nodx; %plot parameter

%Waterflow in one tube in one radiator, NB! two inlets in each radiator
wflow = waterflow/(2*radiators);

layer_type = mod(1:tube_layers,8); %calculation parameter

for m=1:1
    T_air = ones(tube_layers,nodx).*5;
    T_air_new = ones(tube_layers,nodx);
    T_air_old = ones(tube_layers,nodx).*5;
    T_water = ones(tube_layers,nodx).*18;
    T_water_new = ones(tube_layers,nodx);
    T_water_old = ones(tube_layers,nodx).*18;
    T_surf = ones(tube_layers,nodx);
    rad = ones(tube_layers,nodx);
    err_a = 1; err_w = 1;
    phi{m} = zeros(tube_layers,nodx);

    dx(m) = B/nodx;
    k=0;
    %***************************** LOOP ***********************************
    %continue loop until residual is minimal
    while err_a > 1e-3 || err_w > 1e-3
        T_air_old = T_air_new;
        T_water_old = T_water_new;

        j1=1; %Ctrl variables
        j2=1; %Ctrl variables
        j3=1; %Ctrl variables
        j4=1; %Ctrl variables
        for i=1:tube_layers
```

```
for j=1:nodx
    T_air = T_air_new;
    T_water = T_water_new;

    if j==1 %Left side
        if j1==1 && layer_type(i)==1 %Water inlet #1
            T_water(i,j) = T_water_in;
            j1=0;
        elseif j3==1  && layer_type(i)==3 %Water inlet #3
            T_water(i,j) = T_water_in;
            j3=0;
        elseif layer_type(i)==1 || layer_type(i)==6
            T_water(i,j) = T_water(i-2,j);
        elseif layer_type(i)==2 || layer_type(i)==4 || layer_type(i)==5 ...
            || layer_type(i)==7
            T_water(i,j) = T_water(i,j+1);
        elseif layer_type(i)==3 || layer_type(i)==0
            T_water(i,j) = T_water(i-6,j);
        else
            disp('error in j=1')
        end
    elseif j==nodx %Right side
        if j2==1  && layer_type(i)==2 %Water inlet #2
            T_water(i,j) = T_water_in;
            j2=0;
        elseif j4==1  && layer_type(i)==4 %Water inlet #4
            T_water(i,j) = T_water_in;
            j4=0;
        elseif layer_type(i)==1 || layer_type(i)==3 || layer_type(i)==6 ...
        || layer_type(i)==0
            T_water(i,j) = T_water(i,j-1);
        elseif layer_type(i)==2 || layer_type(i)==5
            T_water(i,j) = T_water(i-2,j);
        elseif layer_type(i)==4 || layer_type(i)==7
            T_water(i,j) = T_water(i-6,j);
        else
            disp('error in j=nodx')
        end
    else
        if layer_type(i)==1 || layer_type(i)==3 || layer_type(i)==6 ...
            || layer_type(i)==0
            T_water(i,j) = T_water(i,j-1);
        elseif layer_type(i)==2 || layer_type(i)==4 || layer_type(i)==5 ...
            || layer_type(i)==7
            T_water(i,j) = T_water(i,j+1);
        else
            disp('error in j=x')
        end
```

```
end
%rad_v: radiation to and from vertical tube neighbours
%rad_d: radiation to and from diagonally placed tube neighbours
%Each tube sees one tube up and one tube down and 2 diagonally
%up and two diagonally down. Extra contributions are
%neglected.
if i==1
    rad_v_down = formfactor_h * 5.6697E-08 * D_o*dx(m) * ...
        ((273.15+T_surf(i,j))^4 - (273.15+T_surf(i+2,j))^4);
    rad_d_down = 2* formfactor_d * 5.6697E-08 * D_o*dx(m) * ...
        ((273.15+T_surf(i,j))^4 - (273.15+T_surf(i+1,j))^4);
    rad_v_up = 0;
    rad_d_up = 0;

    rad(i,j) = rad_v_up + rad_v_down + rad_d_up + rad_d_down;
    T_air(i,j) = T_air(i+1,j);
elseif i==2
    rad_v_down = formfactor_h * 5.6697E-08 * D_o*dx(m) * ...
        ((273.15+T_surf(i,j))^4 - (273.15+T_surf(i+2,j))^4);
    rad_d_down = 2* formfactor_d * 5.6697E-08 * D_o*dx(m) * ...
        ((273.15+T_surf(i,j))^4 - (273.15+T_surf(i+1,j))^4);
    rad_v_up = 0;
    rad_d_up = 2* formfactor_d * 5.6697E-08 * D_o*dx(m) * ...
        ((273.15+T_surf(i,j))^4 - (273.15+T_surf(i-1,j))^4);
        %positive from present tube

    rad(i,j) = rad_v_up + rad_v_down + rad_d_up + rad_d_down;
    T_air(i,j) = T_air(i+1,j);
elseif i==tube_layers-1 %Bottom of exchanger almost reached
    rad_v_down = 0;
    rad_d_down = 2* formfactor_d * 5.6697E-08 * D_o*dx(m) * ...
    ((273.15+T_surf(i,j))^4 - (273.15+T_surf(i+1,j))^4);
    rad_v_up = formfactor_h * 5.6697E-08 * D_o*dx(m) * ...
    ((273.15+T_surf(i,j))^4 - (273.15+T_surf(i-2,j))^4);
    %positive from present tube
    rad_d_up = 2* formfactor_d * 5.6697E-08 * D_o*dx(m) * ...
    ((273.15+T_surf(i,j))^4 - (273.15+T_surf(i-1,j))^4);
    %positive from present tube

    rad(i,j) = rad_v_up + rad_v_down + rad_d_up + rad_d_down;
    T_air(i,j) = T_air_in;
elseif i==tube_layers %Bottom of exchanger reached
    rad_v_down = 0;
    rad_d_down = 0;
    rad_v_up = formfactor_h * 5.6697E-08 * D_o*dx(m) * ...
    ((273.15+T_surf(i,j))^4 - (273.15+T_surf(i-2,j))^4);
    %positive from present tube
    rad_d_up = 2* formfactor_d * 5.6697E-08 * D_o*dx(m) * ...
```

```
                    ((273.15+T_surf(i,j))^4 - (273.15+T_surf(i-1,j))^4);
                    %positive from present tube

                    rad(i,j) = rad_v_up + rad_v_down + rad_d_up + rad_d_down;
                    T_air(i,j) = T_air_in;
                else
                    rad_v_up = formfactor_h * 5.6697E-08 * D_o*dx(m) * ...
                    ((273.15+T_surf(i,j))^4 - (273.15+T_surf(i-2,j))^4);
                    %positive from present tube
                    rad_v_down = formfactor_h * 5.6697E-08 * D_o*dx(m) * ...
                    ((273.15+T_surf(i,j))^4 - (273.15+T_surf(i+2,j))^4);
                    rad_d_up = 2* formfactor_d * 5.6697E-08 * D_o*dx(m) * ...
                    ((273.15+T_surf(i,j))^4 - (273.15+T_surf(i-1,j))^4);
                    %positive from present tube
                    rad_d_down = 2* formfactor_d * 5.6697E-08 * D_o*dx(m) * ...
                    ((273.15+T_surf(i,j))^4 - (273.15+T_surf(i+1,j))^4);

                    rad(i,j) = rad_v_up + rad_v_down + rad_d_up + rad_d_down;
                    T_air(i,j) = T_air(i+1,j);
                end
                phi{m}(i,j) = ((T_water(i,j)-T_air(i,j))./...
                (R_i+R_mat+R_o))*dx(m);
                %phi is positive for heat transfer from water to air

                T_air_new(i,j) = T_air(i,j) + phi{m}(i,j)/...
                ((airflow/area)*D_o*S_h*dx(m)*rho_a*cp_a);  %Yields same result as below
%                T_air_new(i,j) = T_air(i,j) + phi{m}(i,j)/...
%                (U_a_max*((D_o*S_h)-D_o)*dx(m)*rho_a*cp_a);
                if radIsOn == 1
                    T_water_new(i,j) = T_water(i,j) - ...
                    (phi{m}(i,j)+rad(i,j))/(wflow*rho_w*cp_w);
                else
                    T_water_new(i,j) = T_water(i,j) - ...
                    phi{m}(i,j)/(wflow*rho_w*cp_w);
                end
                T_surf(i,j) = T_water_new(i,j)-(T_water_new(i,j)-T_air_new(i,j))*...
                (R_i+R_mat)/(R_i+R_mat+R_o);
            end
        end
        k=k+1;
        err_a = abs(sum(sum(T_air_old,2)) - sum(sum(T_air_new,2)));
        err_w = abs(sum(sum(T_water_old,2)) - sum(sum(T_water_new,2)));
    end
    %%%%%%%%%%%%%%%%%%%%%%%%%% LOOP END ****************************

    T_air = T_air_new;
    T_water = T_water_new;
```

```
    T_at{m} = T_air;
    T_wt{m} = T_water;

    T_a{m} = reshape(T_air',1,vec_length);
    T_w{m} = reshape(T_water',1,vec_length);

    T_a_o = mean(T_a{m}(1:nodx));
%    T_a_i = mean(T_a{m}((tube_layers*nodx-nodx):(tube_layers*nodx)));

    efficiency_exch = (T_a_o-T_outdoor)/(T_water_in-T_outdoor)
end

%PLOT
figure

dx1 = 100*(1:vec_length)*dx(1)/(vec_length*dx(1));

plot((1:vec_length)*dx(1),T_w{1},'-b',(1:vec_length)*dx(1),T_a{1},'--b')
xlabel('Tube length [m]'); ylabel('Temperature [degC]')
title('Air/water temperature development, radiator, two parallel ...
inlet tubes to each radiator (4 inputs)')
legend('Water','Air')
grid('on');
```

# Appendix B

# CFD codes

This appendix lists the CFD codes and settings employed in the project. Two codes is used because they are both considered adequate for individual tasks.

## B.1 Comsol

- Solver type: stationary direct: PARDISO
- Relative tolerance: $10^{-6}$
- Turbulence model: none, laminar, Re ¡¡ 2500
- Number of degrees of freedom: approx. 40000

## B.2 Fluent

- Fluent 6.2.16
- Grid size: see figure **??**

  Among tubes approx. 2 mm

  Otherwise $10 \times 5 \times 2$ mm
- Discretization scheme pressure: Fluent standard
- Discretization scheme momentum and turbulence: First Order Upwind
- Pressure-velocity coupling: SIMPLE
- Turbulence model: k-$\epsilon$
- Convergence criteria

  Continuity $10^{-3}$

  Momentum $10^{-3}$

  k-$\epsilon$: $10^{-3}$

  Energy $10^{-6}$
- Iterations: 60

- Turbulent kinetic energy: $k_0 = 1.5(0.04 \cdot \text{inletvelocity})^2 \qquad [\text{m}^2/\text{s}^2]$
- Turbulent dissipation rate: $\epsilon_0 = k_0^1.5/l_0[\text{m}^2/\text{s}^3]$ where $l_0 = \text{inletheight}/10$

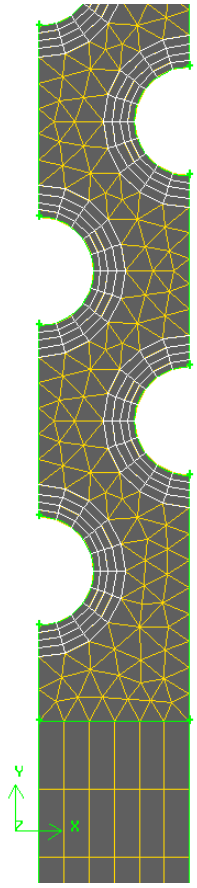


Figure B.1: Grid size in exchanger.

# Appendix C

# Properties of antifreeze fluids

The appendix comprises three figures that illustrates the properties of some antifreeze fluids. The glycols and chlorides are very common; alcohols are less common because of flammability but should be considered due to their superior performance. All fluids are applicable for a wide range of equipment if proper corrosion inhibition is applied.

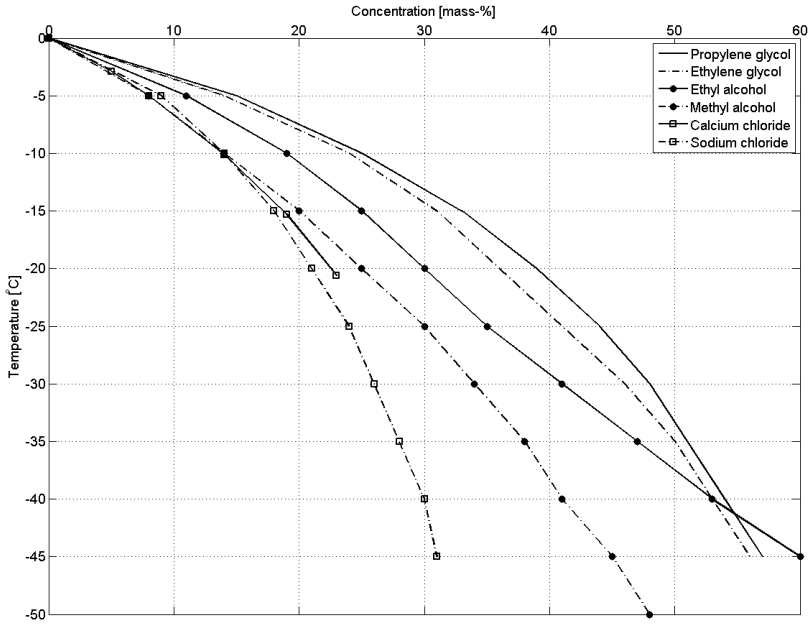


Figure C.1: Freezing points of different antifreeze fluids in aqueous solutions

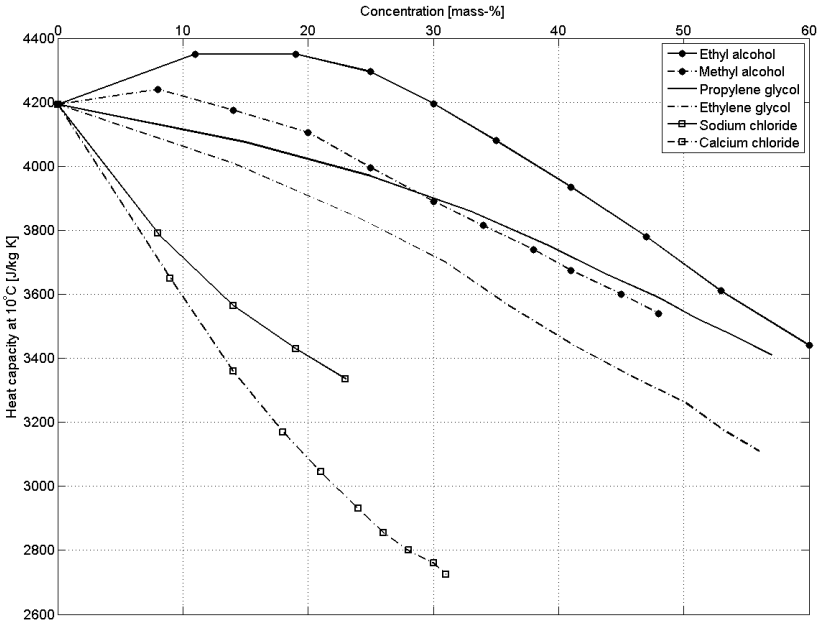


Figure C.2: Energy carrier efficiency of different antifreeze fluids in aqueous solutions

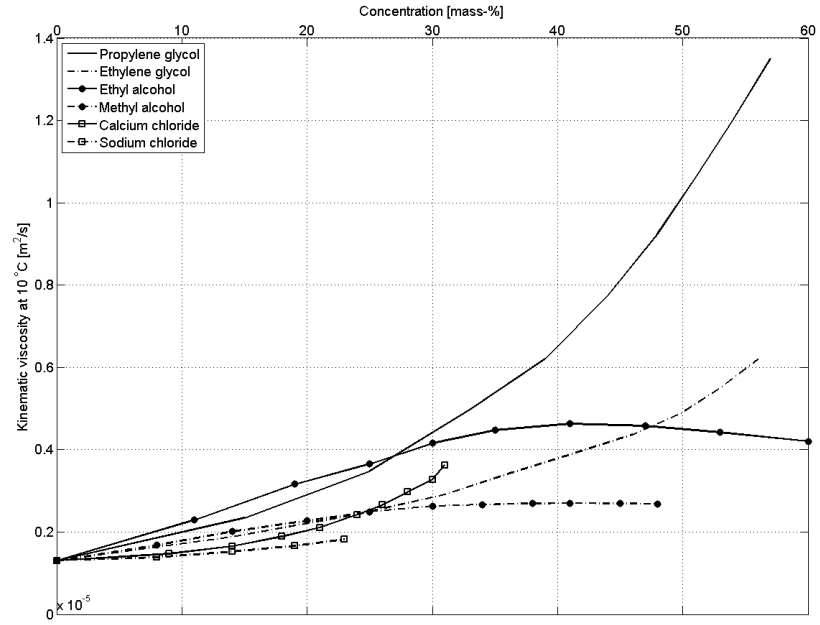


Figure C.3: Viscosity of different antifreeze fluids in aqueous solutions. The y-axis is erroneous – it should say $x10^{-2}$

# Appendix D

# Pressures and flows in building 118

This appendix comprises the pressure and flow models of the ventilation system in building 118. Simulations were carried to investigate multiple setups but only four are presented here:

1. wind and stack-assisted mechanical ventilation in *existing* ducts, heat recovery with liquid-coupled coils, pump on liquid circuit and electrostatic precipitator. No wind or stack effect.

2. like 1, but with control, so teaching rooms are ventilated better during occupancy. Stack effect.

3. like 2, but existing in- and outlet ducts to two teaching rooms are replaced with larger ducts due to the higher load of theses rooms. New ventilation ceilings in the teaching rooms act as diffuse ventilation inlets and distributes the air. $CO_2$-control and dampers ensure that rooms are optimally ventilated. Stack effect.

4. like 3, but without fans. Included because 1) it is fully optimized in terms of low pressure loss and 2) it is purely driven by stack. Therefore it acts as reference to the others.

5. Realized FINAL implementation. Existing ducts are used, but an extra large duct supplies teaching room 225. Diffuse ceiling in teaching room 225. $CO_2$-control and dampers ensure that rooms are optimally ventilated. Fans implemented but stack effect exploited with the outdoor temperature at 5 °C. Pressure loss for max/min flow rate: 74/20 Pa.

The principle of equivalent diameter is used to represent rectangular ducts due to PFS issues. For detailed information on the program PFS the reader is referred to Lars Jensen at www.hvac.lth.se

## D.1 Scenario 1

D:\MyDoc\PhD\PSO\System\building118_Dæ_Campus_scen1.pfs

```
com
begin
date                2009-07-30  10.24.51
flow l/s
pressure Pa
format  v 2  q 1 R 3
com 5C=denz1.27 0C=denz1.29 20C=denz1.2
control bend=1  duct=16 con=1 dim=1 denz=1.205 dencase=1 cp=1006
set ai=d,119,1.5
set ao=d,138,1.5
set bi=d,192,1.5
set bo=d,192,1.5
set ci=d,215,1.5
set co=d,132,1.5
set di=d,165,1.5
set do=d,253,1.5
set eo=d,209,1.5
set d1814=d,175,3
set d1816=d,187,3
set d1818=d,198,3
set d2418=d,228,3
set d2424=d,264,3
set d2624=d,275,3
set d2618=d,237,3
set d1210=d,121,3
set d2826=d,297,3
set d1010=d,110,3
set d2422=d,253,3
set d3024=d,295,3
set d3030=d,330,3
set d3230=d,341,3
set d3228=d,330,3
set d3224=d,305,3
set d3028=d,319,3
set d2016=d,197,3
set d2222=d,242,3
set d2220=d,231,3
set d2822=d,273,3
set d3232=d,352,12
set d4436=d,438,8
set exch=g,.7,500,.8,600
set filter=g,2,500,3,600
set Tin=T,20:<
set Tout=T,20
set Texch=T,20:<
set Tflr1=T,20:<
set Tflr2=T,20:<
set Tflr3=T,20:<
set qiN=s,-8:q
set qiS=s,8:q
set qoN=s,8:q
set qoS=s,-8:q
com set rN=g,.5,30,.6,50:h
com set rS=g,.5,30,.6,50:h
set rN=g,10,40,60,100:h
set rS=g,10,22,50,50:h
com set koll=h?-35.5
com set rN=e,50:h
com set rS=e,50:h
set TF=h?-562
set FF=h,0
com fan TF 25:155 21:200 12:300 1:400
com fan TF 11:400 10:562 9:700
com fan FF 11:400 10:562 9:700
set sp1=e,47
set sp2=e,13
set sp3=e,0.01
set sp4=e,0
set sp5=e,0
```

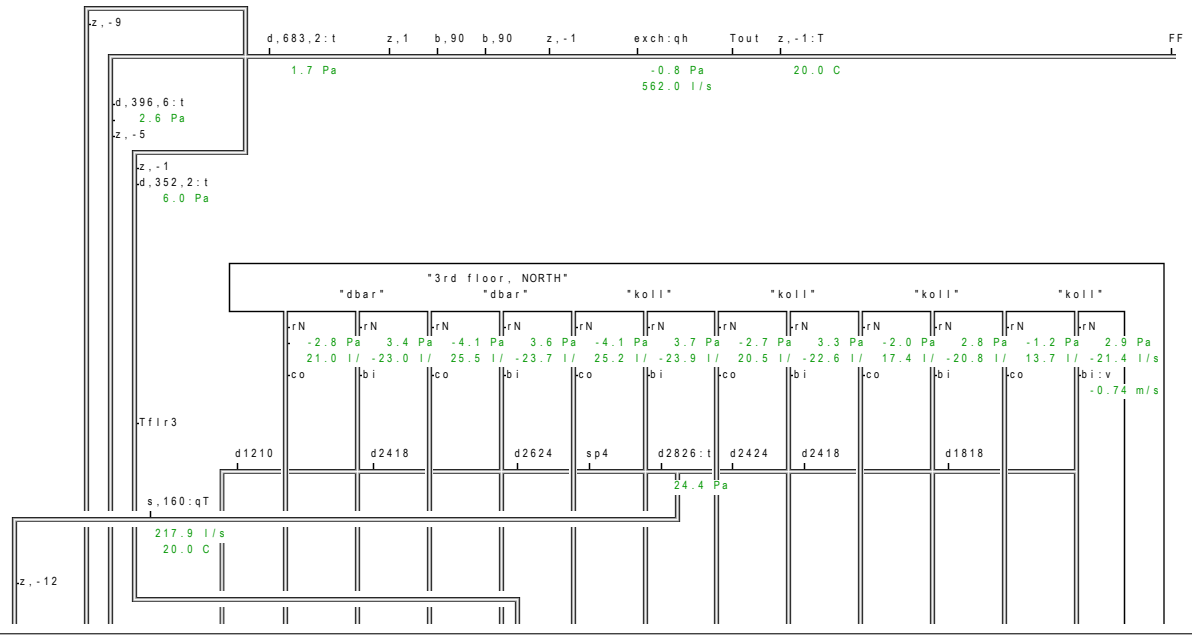

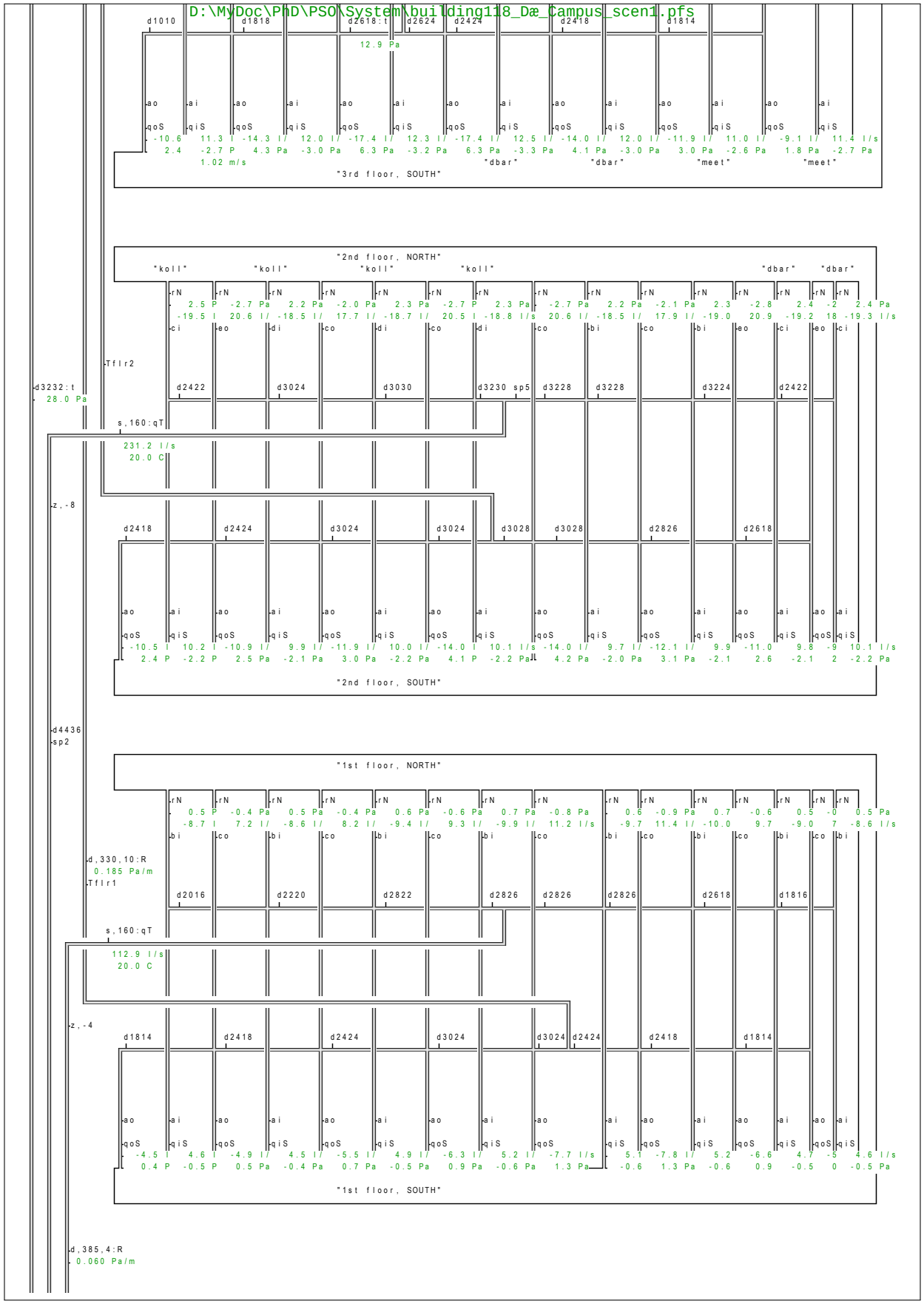
D:\MyDoc\PhD\PSO\System\building118_Dæ_Campus_scen1.pfs
d1010
d1818
d2618:t
12.9 Pa
d2624
d2424
d2418
d1814
"3rd floor, SOUTH"
"2nd floor, NORTH"
"koll"
"dbar"
d3232:t
28.0 Pa
Tflr2
d2422
d3024
d3030
d3230 sp5
d3228
d3224
s,160:qT
231.2 l/s
20.0 C
z,-8
d2826
d2618
"2nd floor, SOUTH"
d4436
sp2
"1st floor, NORTH"
d,330,10:R
0.185 Pa/m
Tflr1
d2016
d2220
d2822
d2826
d1816
112.9 l/s
z,-4
d1814
d2418
"1st floor, SOUTH"
d,385,4:R
0.060 Pa/m

D:\MyDoc\PhD\PSO\System\building118_Dæ_Campus_scen1.pfs

```
d,683,2:hR
   0.1 Pa
  0.058 Pa/m


Texch

exch:h
   0.8 Pa

b,90


filter:hv
   2.6 Pa
 -1.53 m/s

z,3

Tin

h?-562:tsdqh<
  -41.0 Pa
   41.0 Pa
   39.6 Pa
    1.4 Pa
  -41.0 Pa
 -562.0 l/s


end 1  1 system  560 elements  0 errors  75 observations  2009-07-30  10.24.55
```

## D.2 Scenario 2

D:\MyDoc\PhD\PSO\System\building118_Dæ_Campus_scen2.pfs

```
com
begin
date                2009-07-30  10.24.16
flow l/s
pressure Pa
format  v 2  q 1 R 3
com 5C=denz1.27 0C=denz1.29 20C=denz1.2
control bend=1  duct=16 con=1 dim=1 denz=1.27  dencase=1 cp=1006
set ai=d,119,1.5
set ao=d,138,1.5
set bi=d,192,1.5
set bo=d,192,1.5
set ci=d,215,1.5
set co=d,132,1.5
set di=d,165,1.5
set do=d,253,1.5
set eo=d,209,1.5
set d1814=d,175,3
set d1816=d,187,3
set d1818=d,198,3
set d2418=d,228,3
set d2424=d,264,3
set d2624=d,275,3
set d2618=d,237,3
set d1210=d,121,3
set d2826=d,297,3
set d1010=d,110,3
set d2422=d,253,3
set d3024=d,295,3
set d3030=d,330,3
set d3230=d,341,3
set d3228=d,330,3
set d3224=d,305,3
set d3028=d,319,3
set d2016=d,197,3
set d2222=d,242,3
set d2220=d,231,3
set d2822=d,273,3
set d3232=d,352,12
set d4436=d,438,8
set exch=g,.7,500,.8,600
set filter=g,2,500,3,600
set Tin=T,5:<
set Tout=T,18
set Texch=T,22:<
set Tflr1=T,22:<
set Tflr2=T,22:<
set Tflr3=T,22:<
set qiN=s,-8:q
set qiS=s,8:q
set qoN=s,8:q
set qoS=s,-8:q
com set rN=g,.5,30,.6,50:h
com set rS=g,.5,30,.6,50:h
set rN=g,10,40,60,100:h
set rS=g,10,22,50,50:h
com set koll=h?-35.5
com set rN=e,50:h
com set rS=e,50:h
set TF=h?-562
set FF=h,0
com fan TF 25:155 21:200 12:300 1:400
com fan TF 11:400 10:562 9:700
com fan FF 11:400 10:562 9:700
set sp1=e,47
set sp2=e,13
set sp3=e,0.01
set sp4=e,40
set sp5=e,30
```

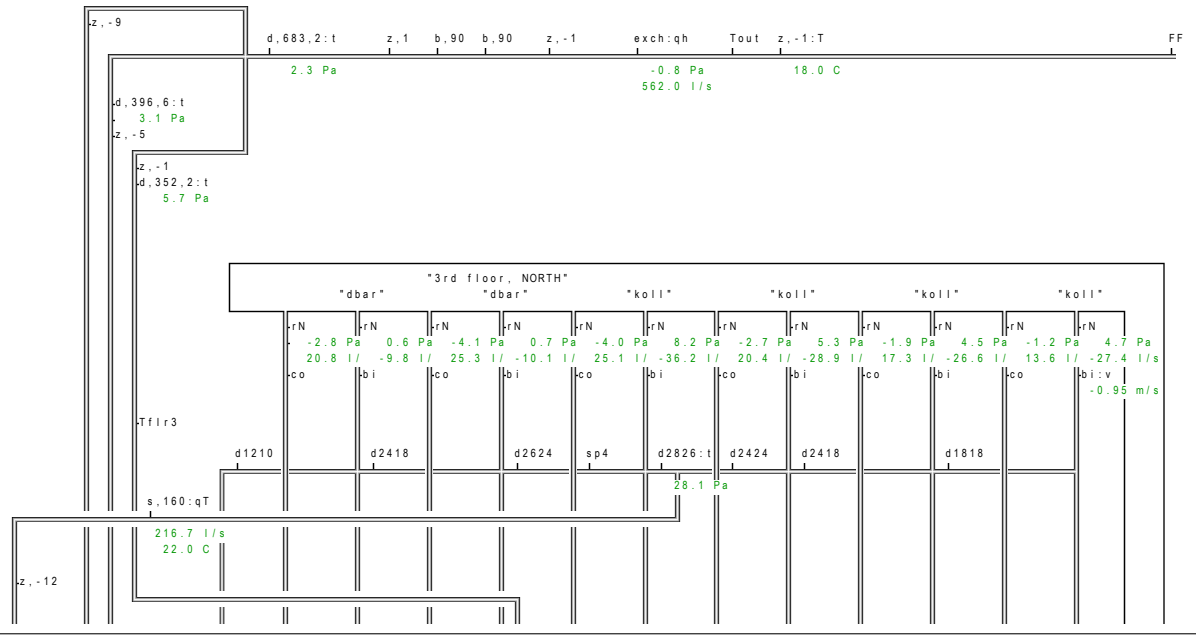

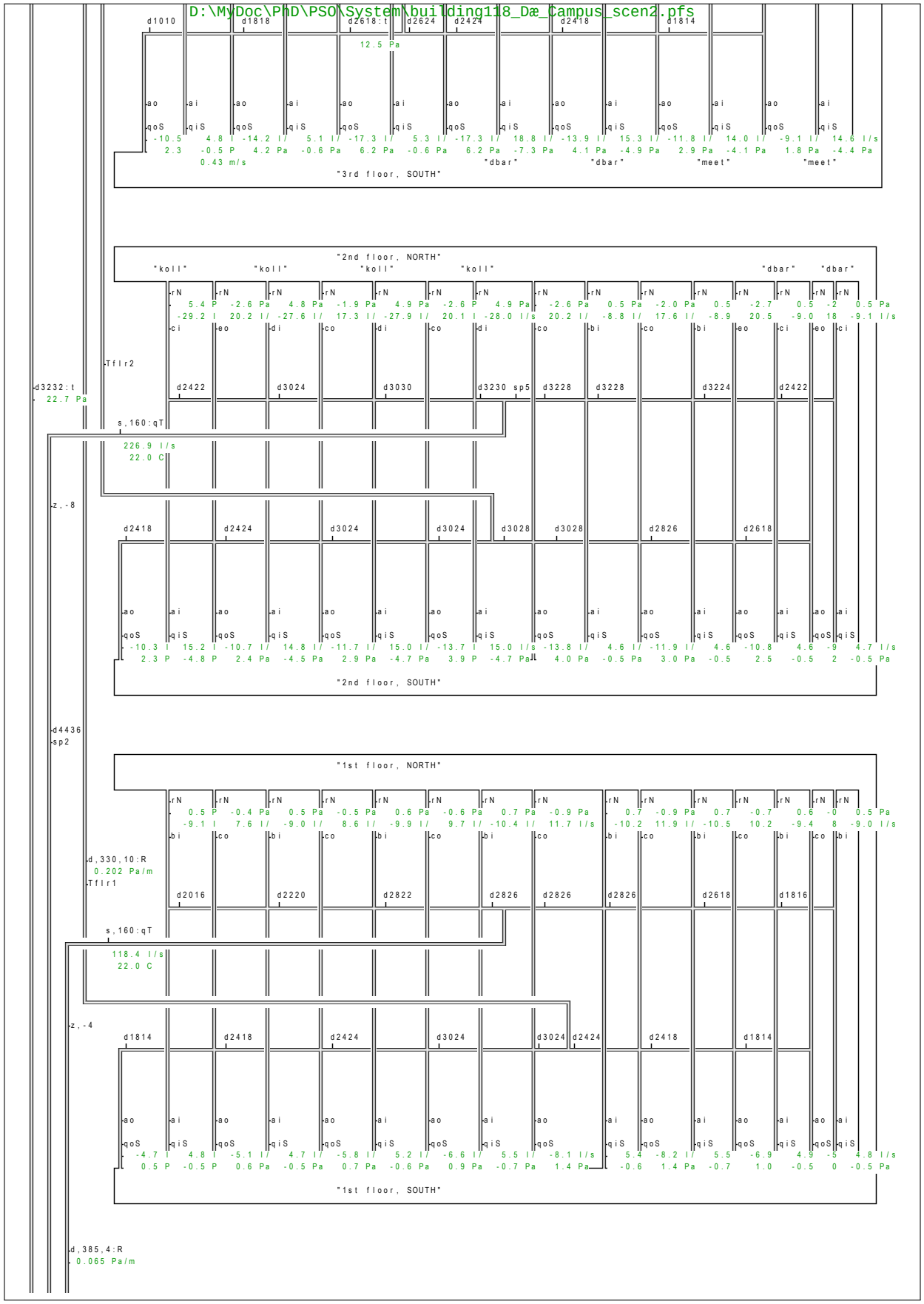
D:\MyDoc\PhD\PSO\System\building118_Dæ_Campus_scen2.pfs
d1010
d1818
d2618:t
d2624
d2424
d2418
d1814
12.5 Pa
"3rd floor, SOUTH"
"dbar"
"meet"
"2nd floor, NORTH"
"koll"
"dbar"
Tflr2
d3232:t
22.7 Pa
d2422
d3024
d3030
d3230 sp5
d3228
d3224
s,160:qT
226.9 l/s
22.0 C
z,-8
d2826
d2618
"2nd floor, SOUTH"
d4436
sp2
"1st floor, NORTH"
d,330,10:R
0.202 Pa/m
Tflr1
d2016
d2220
d2822
d1816
118.4 l/s
z,-4
"1st floor, SOUTH"
d,385,4:R
0.065 Pa/m

D:\MyDoc\PhD\PSO\System\building118_Dæ_Campus_scen2.pfs

```
d,683,2:hR
   0.1 Pa
  0.057 Pa/m


Texch

exch:h
   0.8 Pa

b,90


filter:hv
   2.7 Pa
 -1.53 m/s

z,3

Tin

h?-562:tsdqh<
 -33.6 Pa
  33.6 Pa
  32.2 Pa
   1.4 Pa
 -33.6 Pa
-562.0 l/s


end 1  1 system  562 elements  0 errors  75 observations  2009-07-30  10.24.19
```

## D.3 Scenario 3

D:\MyDoc\PhD\PSO\System\building118_Dæ_Campus_scen3.pfs

```
com
begin
date                2009-07-30  10.25.15
flow l/s
pressure Pa
format  v 2  q 1 R 3
com 5C=denz1.27 0C=denz1.29 20C=denz1.2
control bend=1  duct=16 con=1 dim=1 denz=1.27 dencase=1 cp=1006
set ai=d,119,1.5
set ao=d,138,1.5
set bi=d,192,1.5
set bo=d,192,1.5
set ci=d,215,1.5
set co=d,132,1.5
set di=d,165,1.5
set do=d,253,1.5
set eo=d,209,1.5
set d1814=d,175,3
set d1816=d,187,3
set d1818=d,198,3
set d2418=d,228,3
set d2424=d,264,3
set d2624=d,275,3
set d2618=d,237,3
set d1210=d,121,3
set d2826=d,297,3
set d1010=d,110,3
set d2422=d,253,3
set d3024=d,295,3
set d3030=d,330,3
set d3230=d,341,3
set d3228=d,330,3
set d3224=d,305,3
set d3028=d,319,3
set d2016=d,197,3
set d2222=d,242,3
set d2220=d,231,3
set d2822=d,273,3
set d3232=d,352,12
set d4436=d,438,8
set d315=d,347,3
set d400=d,441,3
set d450=d,496,3
set d500=d,551,3
set d550=d,606,3
set koll=d,347,0.5
set exch=g,.7,500,.8,600
set filter=g,2,500,3,600
set Tin=T,20:<
set Tout=T,20
set Texch=T,20:<
set Tflr1=T,20:<
set Tflr2=T,20:<
set Tflr3=T,20:<
set qiN=s,8:q
set qiS=s,-8:q
set qoN=s,-8:q
set qoS=s,8:q
com set rN=g,1,5,4,20:h
com set rS=g,1,5,4,20:h
set rN=g,10,40,60,100:h
set rS=g,10,22,50,50:h
com set rN=e,50:h
com set rS=e,50:h
set ceil=g,0.9,24.5,2,45:hn
com set TF=h,-0.01
com set TF=h?-450
set TF=h?-311
set FF=h,0
com fan TF 25:155 21:200 12:300 1:400
com fan TF 11:400 10:562 9:700
com fan FF 11:400 10:562 9:700
set sp1=e,40
set sp2=e,10
set sp3=e,0
set sp4=e,12
set sp5=e,3
set spdb1=e,0
set spdb2=e,0
```

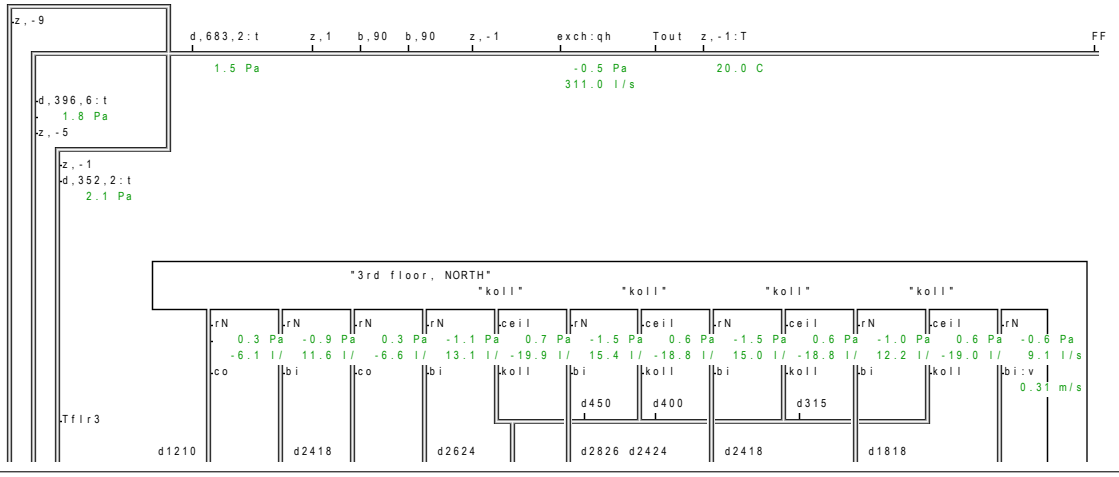

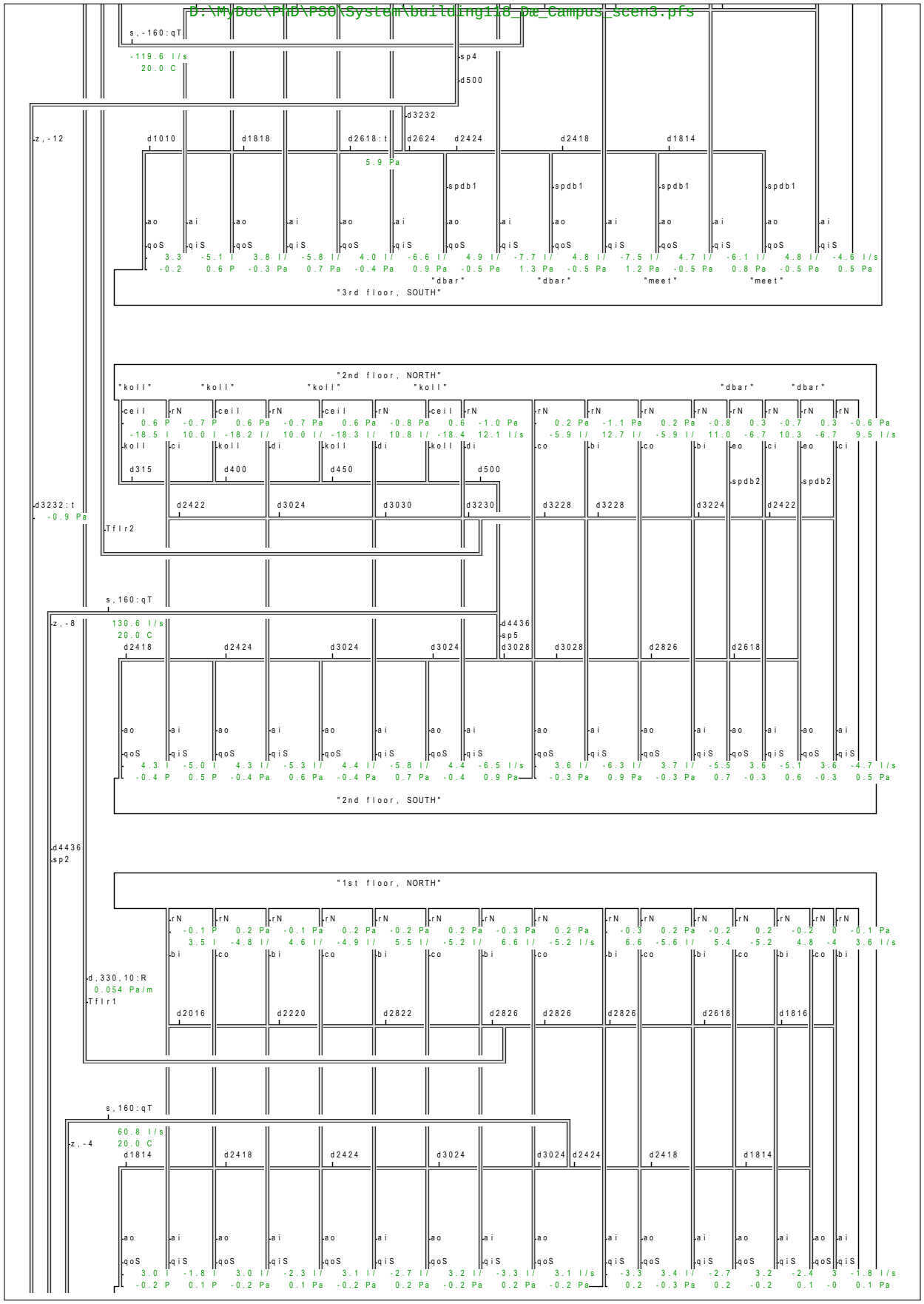
D:\MyDoc\PhD\PSO\System\building118_Pæ_Campus_Scen3.pfs
s,-160:qT
-119.6 l/s
20.0 C
sp4
d500
d3232
z,-12
d1010
d1818
d2618:t
5.9 Pa
d2624
d2424
d2418
d1814
spdb1
ao
ai
qoS
qiS
3.3 -5.1 l 3.8 l/ -5.8 l/ 4.0 l/ -6.6 l/ 4.9 l/ -7.7 l/ 4.8 l/ -7.5 l/ 4.7 l/ -6.1 l/ 4.8 l/ -4.6 l/s
-0.2 0.6 P -0.3 Pa 0.7 Pa -0.4 Pa 0.9 Pa -0.5 Pa 1.3 Pa -0.5 Pa 1.2 Pa -0.5 Pa 0.8 Pa -0.5 Pa 0.5 Pa
"dbar"
"meet"
"3rd floor, SOUTH"
"2nd floor, NORTH"
"koll"
"dbar"
ceil
rN
0.6 P -0.7 P 0.6 Pa -0.7 Pa 0.6 Pa -0.8 Pa 0.6 -1.0 Pa 0.2 Pa -1.1 Pa 0.2 Pa -0.8 0.3 -0.7 0.3 -0.6 Pa
-18.5 l 10.0 l -18.2 l/ 10.0 l/ -18.3 l/ 10.8 l/ -18.4 12.1 l/s -5.9 l/ 12.7 l/ -5.9 l/ 11.0 -6.7 10.3 -6.7 9.5 l/s
koll
ci
di
co
bi
eo
d315
d400
d450
d500
spdb2
d3232:t
-0.9 Pa
d2422
d3024
d3030
d3230
d3228
d3224
d2422
Tflr2
s,160:qT
z,-8
130.6 l/s
20.0 C
d4436
sp5
d2418
d2424
d3024
d3028
d2826
d2618
4.3 l -5.0 l 4.3 l/ -5.3 l/ 4.4 l/ -5.8 l/ 4.4 -6.5 l/s 3.6 l/ -6.3 l/ 3.7 l/ -5.5 3.6 -5.1 3.6 -4.7 l/s
-0.4 P 0.5 P -0.4 Pa 0.6 Pa -0.4 Pa 0.7 Pa -0.4 0.9 Pa -0.3 Pa 0.9 Pa -0.3 Pa 0.7 -0.3 0.6 -0.3 0.5 Pa
"2nd floor, SOUTH"
d4436
sp2
"1st floor, NORTH"
-0.1 P 0.2 Pa -0.1 Pa 0.2 Pa -0.2 Pa 0.2 Pa -0.3 Pa 0.2 Pa -0.3 0.2 Pa -0.2 0.2 -0.2 0 -0.1 Pa
3.5 l -4.8 l/ 4.6 l/ -4.9 l/ 5.5 l/ -5.2 l/ 6.6 l/ -5.2 l/s 6.6 -5.6 l/ 5.4 -5.2 4.8 -4 3.6 l/s
d,330,10:R
0.054 Pa/m
Tflr1
d2016
d2220
d2822
d2826
d2826
d2826
d2618
d1816
s,160:qT
z,-4
60.8 l/s
20.0 C
d1814
d2418
d2424
d3024
d3024
d2424
d2418
d1814
3.0 l -1.8 l 3.0 l/ -2.3 l/ 3.1 l/ -2.7 l/ 3.2 l/ -3.3 l/ 3.1 l/s -3.3 3.4 l/ -2.7 3.2 -2.4 3 -1.8 l/s
-0.2 P 0.1 P -0.2 Pa 0.1 Pa -0.2 Pa 0.2 Pa -0.2 Pa 0.2 Pa -0.2 Pa 0.2 -0.3 Pa 0.2 -0.2 0.1 -0 0.1 Pa

D:\MyDoc\PhD\PSO\System\building118_Dæ_Campus_scen3.pfs
"1st floor, SOUTH"

-d,385,4:R
0.018 Pa/m

-d,683,2:hR
0.0 Pa
0.018 Pa/m

-Texch

-exch:h
0.5 Pa

-b,90

-filter:hv
0.7 Pa
-0.85 m/s

-z,3

-Tin

-TF:tsdqh<
-3.2 Pa
3.2 Pa
2.8 Pa
0.4 Pa
-3.2 Pa
-311.0 l/s

end 1 1 system 593 elements 0 errors 47 observations 2009-07-30 10.25.19

## D.4 Scenario 4

D:\MyDoc\PhD\PSO\System\building118_uden_fans_Dæ.pfs

```
com Ventilation is driven by thermal buoyancy and pressure
com Porous ceilings in teaching rooms
com Ducts are resized to supply teaching rooms
begin
date                  2009-07-30  10.28.09
flow l/s
pressure Pa
format  o 2  q 1 R 3 v 3
com 5C=denz1.27 0C=denz1.29 20C=denz1.2
control       bend=1 duct=16 con=1 dim=1 denz=1.27 dencase=1 cp=1006
set ai=d,119,1.5
set ao=d,138,1.5
set bi=d,192,1.5
set bo=d,192,1.5
set ci=d,215,1.5
set co=d,132,1.5
set di=d,165,1.5
set do=d,253,1.5
set eo=d,209,1.5
set d1814=d,175,3
set d1816=d,187,3
set d1818=d,198,3
set d2418=d,228,3
set d2424=d,264,3
set d2624=d,275,3
set d2618=d,237,3
set d1210=d,121,3
set d2826=d,297,3
set d1010=d,110,3
set d2422=d,253,3
set d3024=d,295,3
set d3030=d,330,3
set d3230=d,341,3
set d3228=d,330,3
set d3224=d,305,3
set d3028=d,319,3
set d2016=d,197,3
set d2222=d,242,3
set d2220=d,231,3
set d2822=d,273,3
set d3232=d,352,12
set d4436=d,438,8
set koll=d,347,0.5
set d315=d,347,3
set d400=d,441,3
set d450=d,496,3
set d500=d,551,3
set d550=d,606,3
set exch=g,.7,500,.8,600
set filter=g,2,500,3,600
set Tin=T,5:<
set Tout=T,18
set Texch=T,22:<
set Tflr1=T,22:<
set Tflr2=T,22:<
set Tflr3=T,22:<
set qiN=s,-8:q
set qiS=s,8:q
set qoN=s,8:q
set qoS=s,-8:q
set rN=g,.5,30,.6,40:h
set rS=g,.5,30,.6,40:h
com set rN=g,10,40,60,100:n
com set rS=g,10,22,50,50:n
com set rN=e,50:h
com set rS=e,50:h
set ceil=g,0.9,24.5,2,45:hn
set TF=h,-0.01
com set TF=h?-562
set FF=h,0
com fan TF 25:155 21:200 12:300 1:400
com fan TF 11:400 10:562 9:700
com fan FF 11:400 10:562 9:700
set sp1=e,30
set sp2=e,10
set sp3=e,0.01
set sp4=e,0
set sp5=e,5
set spdb1=e,999
set spdb2=e,999
```

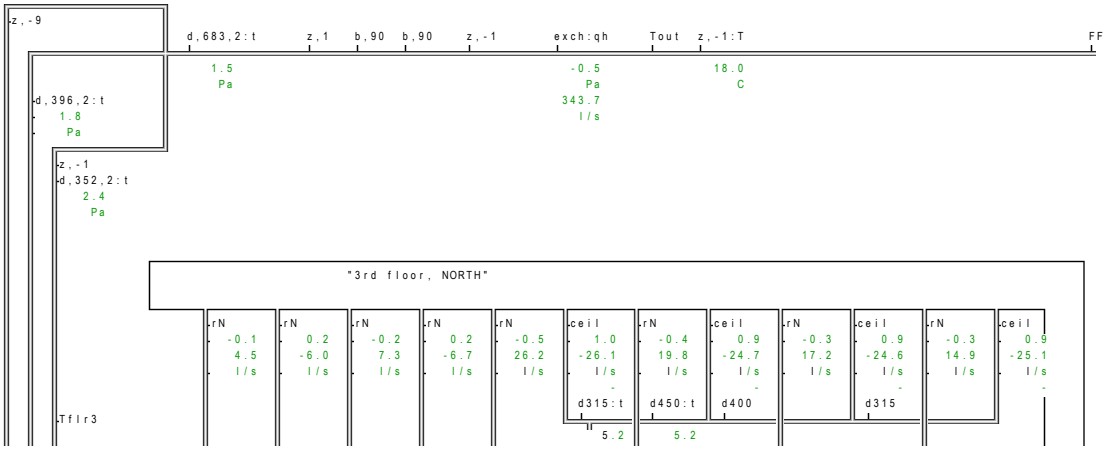

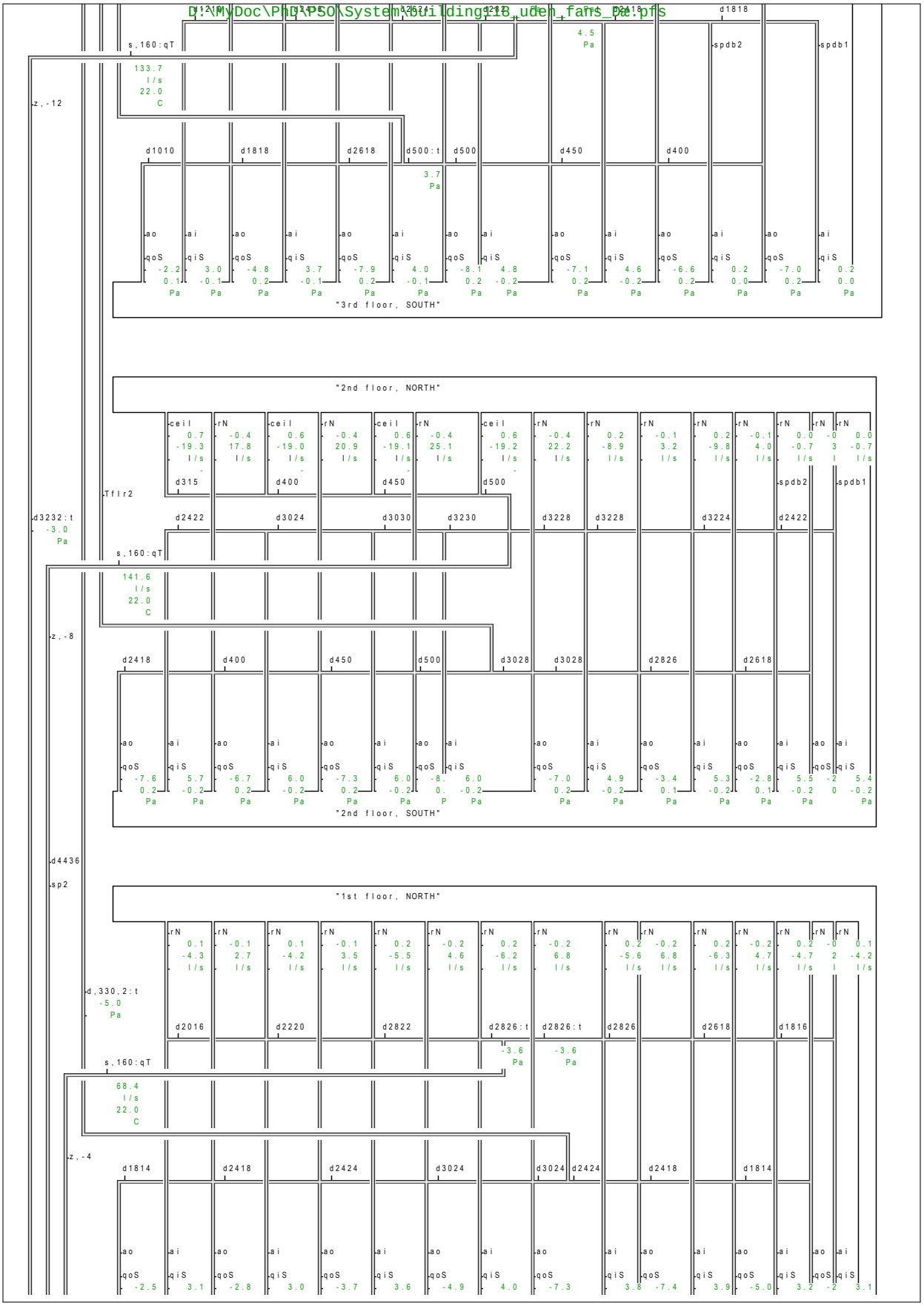
D:\MyDoc\PhD\PSO\System\Building18_udem_fans_Pa.prfs
d1818
4.5
Pa
s,160:qT
133.7
l/s
22.0
C
z,-12
d1010
d1818
d2618
d500:t
d500
d450
d400
3.7
Pa
spdb2
spdb1
ao
ai
qoS
qiS
-2.2 0.1 Pa
3.0 -0.1 Pa
-4.8 0.2 Pa
3.7 -0.1 Pa
-7.9 0.2 Pa
4.0 -0.1 Pa
-8.1 0.2 Pa
4.8 -0.2 Pa
-7.1 0.2 Pa
4.6 -0.2 Pa
-6.6 0.2 Pa
0.2 0.0 Pa
-7.0 0.2 Pa
0.2 0.0 Pa
"3rd floor, SOUTH"
"2nd floor, NORTH"
ceil
rN
0.7 -19.3 l/s
-0.4 17.8 l/s
0.6 -19.0 l/s
-0.4 20.9 l/s
0.6 -19.1 l/s
-0.4 25.1 l/s
0.6 -19.2 l/s
-0.4 22.2 l/s
0.2 -8.9 l/s
-0.1 3.2 l/s
0.2 -9.8 l/s
-0.1 4.0 l/s
0.0 -0.7 l/s
-0 3 l
0.0 -0.7 l/s
d315
d400
d450
d500
Tflr2
d3232:t
-3.0
Pa
d2422
d3024
d3030
d3230
d3228
d3228
d3224
d2422
s,160:qT
141.6
l/s
22.0
C
z,-8
d2418
d400
d450
d500
d3028
d3028
d2826
d2618
-7.6 0.2 Pa
5.7 -0.2 Pa
-6.7 0.2 Pa
6.0 -0.2 Pa
-7.3 0.2 Pa
6.0 -0.2 Pa
-8. 0. P
6.0 -0.2 Pa
-7.0 0.2 Pa
4.9 -0.2 Pa
-3.4 0.1 Pa
5.3 -0.2 Pa
-2.8 0.1 Pa
5.5 -0.2 Pa
-2 0 Pa
5.4 -0.2 Pa
"2nd floor, SOUTH"
d4436
sp2
"1st floor, NORTH"
0.1 -4.3 l/s
-0.1 2.7 l/s
0.1 -4.2 l/s
-0.1 3.5 l/s
0.2 -5.5 l/s
-0.2 4.6 l/s
0.2 -6.2 l/s
-0.2 6.8 l/s
0.2 -5.6 l/s
-0.2 6.8 l/s
0.2 -6.3 l/s
-0.2 4.7 l/s
0.2 -4.7 l/s
-0 2 l
0.1 -4.2 l/s
d,330,2:t
-5.0
Pa
d2016
d2220
d2822
d2826:t
d2826:t
d2826
d2618
d1816
-3.6
Pa
-3.6
Pa
s,160:qT
68.4
l/s
22.0
C
z,-4
d1814
d2418
d2424
d3024
d3024
d2424
d2418
d1814
-2.5 3.1
-2.8 3.0
-3.7 3.6
-4.9 4.0
-7.3 3.8
-7.4 3.9
-5.0 3.2
-2 3.1

end 1 1 system 587 elements 0 errors 79 observations 2009-07-30 10.28.12

## D.5 Scenario 5

C:\Users\Gahv\Documents\Research\PhD\PSO\System\building118_Dæ_FINAL_max_flowrate.pfs

```
com REALIZED system in building 118
com including extra 315 mm duct to room 225
com Min flow rate 490 l/s
com 109 l/s to floor1, 230 l/s to floor2
com Bagfilter
begin
date                  2013-01-12  21.12.06
flow l/s
pressure Pa
format  v 2  q 1 R 3
com 5C=denz1.27 0C=denz1.29 20C=denz1.2
com Replace denz value in following line to set outdoor temp
control bend=1  duct=16 con=1 dim=1 denz=1.27  dencase=1 cp=1006
set ai=d,119,1.5
set ao=d,138,1.5
set bi=d,192,1.5
set bo=d,192,1.5
set ci=d,215,1.5
set co=d,132,1.5
set di=d,165,1.5
set do=d,253,1.5
set eo=d,209,1.5
set d1814=d,175,3
set d1816=d,187,3
set d1818=d,198,3
set d2418=d,228,3
set d2424=d,264,3
set d2624=d,275,3
set d2618=d,237,3
set d1210=d,121,3
set d2826=d,297,3
set d1010=d,110,3
set d2422=d,253,3
set d3024=d,295,3
set d3030=d,330,3
set d3230=d,341,3
set d3228=d,330,3
set d3224=d,305,3
set d3028=d,319,3
set d2016=d,197,3
set d2222=d,242,3
set d2220=d,231,3
set d2822=d,273,3
set d3232=d,352,12
set d4436=d,438,8
set newdu=d,315,3
set exch=g,.7,500,.8,600
set filter=g,9.0,490,15.6,650
set Tin=T,5:<
set Tout=T,18
set Texch=T,22:<
set Tflr1=T,22:<
set Tflr2=T,22:<
set Tflr3=T,22:<
set qiN=s,-8:q
set qiS=s,8:q
set qoN=s,8:q
set qoS=s,-8:q
com set rN=g,.5,30,.6,50:h
com set rS=g,.5,30,.6,50:h
set rN=g,2,10,3,20:h
set rS=g,2,10,3,20:h
com set koll=h?-35.5
com set rN=e,50:h
com set rS=e,50:h
set TF=h?-490
set FF=h,0
com fan TF 25:155 21:200 12:300 1:400
com fan TF 11:400 10:562 9:700
com fan FF 11:400 10:562 9:700
set sp1=e,102
set sp2=e,33
com set sp1=e,47
com set sp2=e,13
set sp3=e,0.01
com set sp4=e,0
set sp5=e,5
com set sp6=e,0
diagram sp4 (ipq) 10:100:5.8 40:10:58 60:20:346 90:12:576
diagram sp6 (ipq) 10:100:7.3 40:10:72.8 60:20:436 90:12:728
```

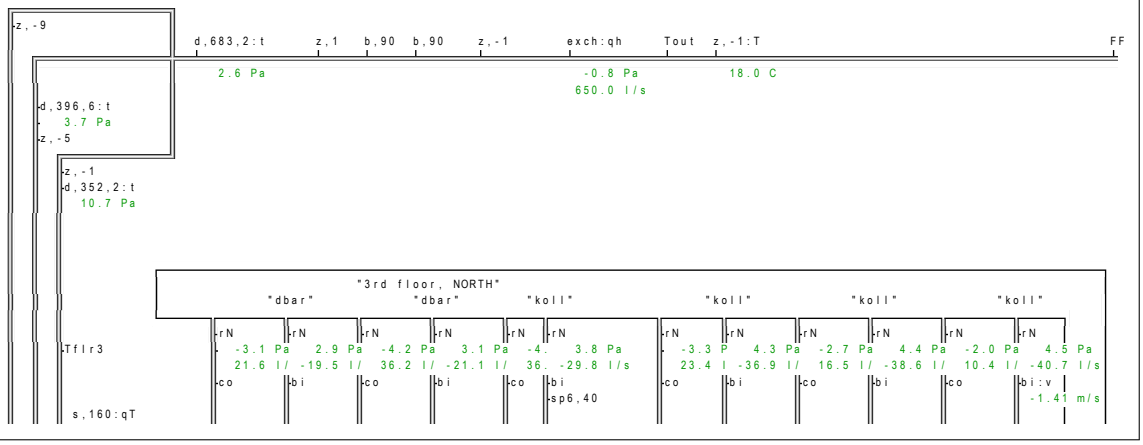

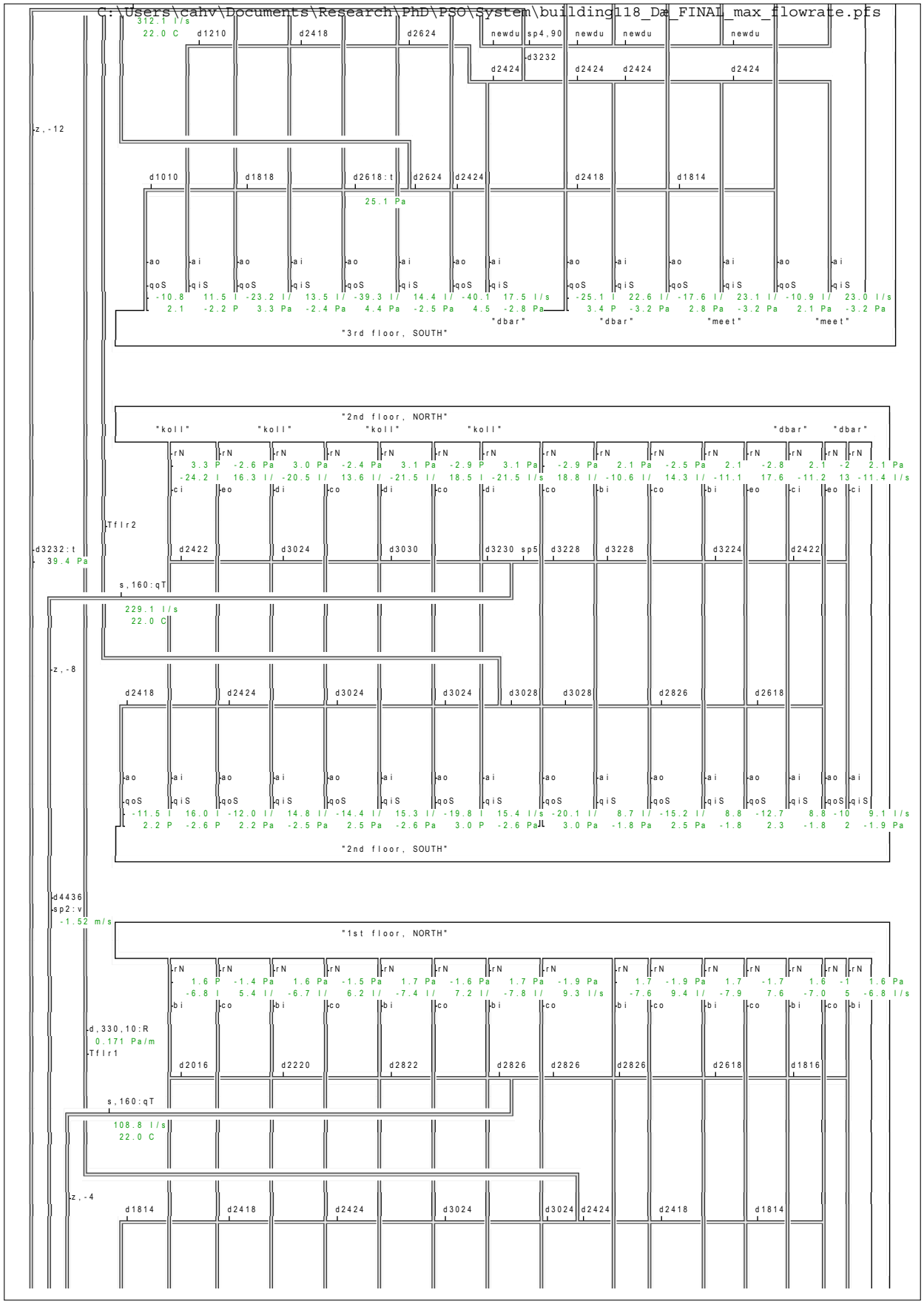
C:\Users\cahv\Documents\Research\PhD\PSO\System\building118_Dæ_FINAL_max_flowrate.pfs
"3rd floor, SOUTH"
"2nd floor, NORTH"
"2nd floor, SOUTH"
"1st floor, NORTH"
"koll"
"dbar"
"meet"
z,-12
z,-8
z,-4
Tflr2
Tflr1
d3232:t
39.4 Pa
s,160:qT
229.1 l/s
22.0 C
108.8 l/s
d4436
sp2:v
-1.52 m/s
d,330,10:R
0.171 Pa/m
312.1 l/s
25.1 Pa

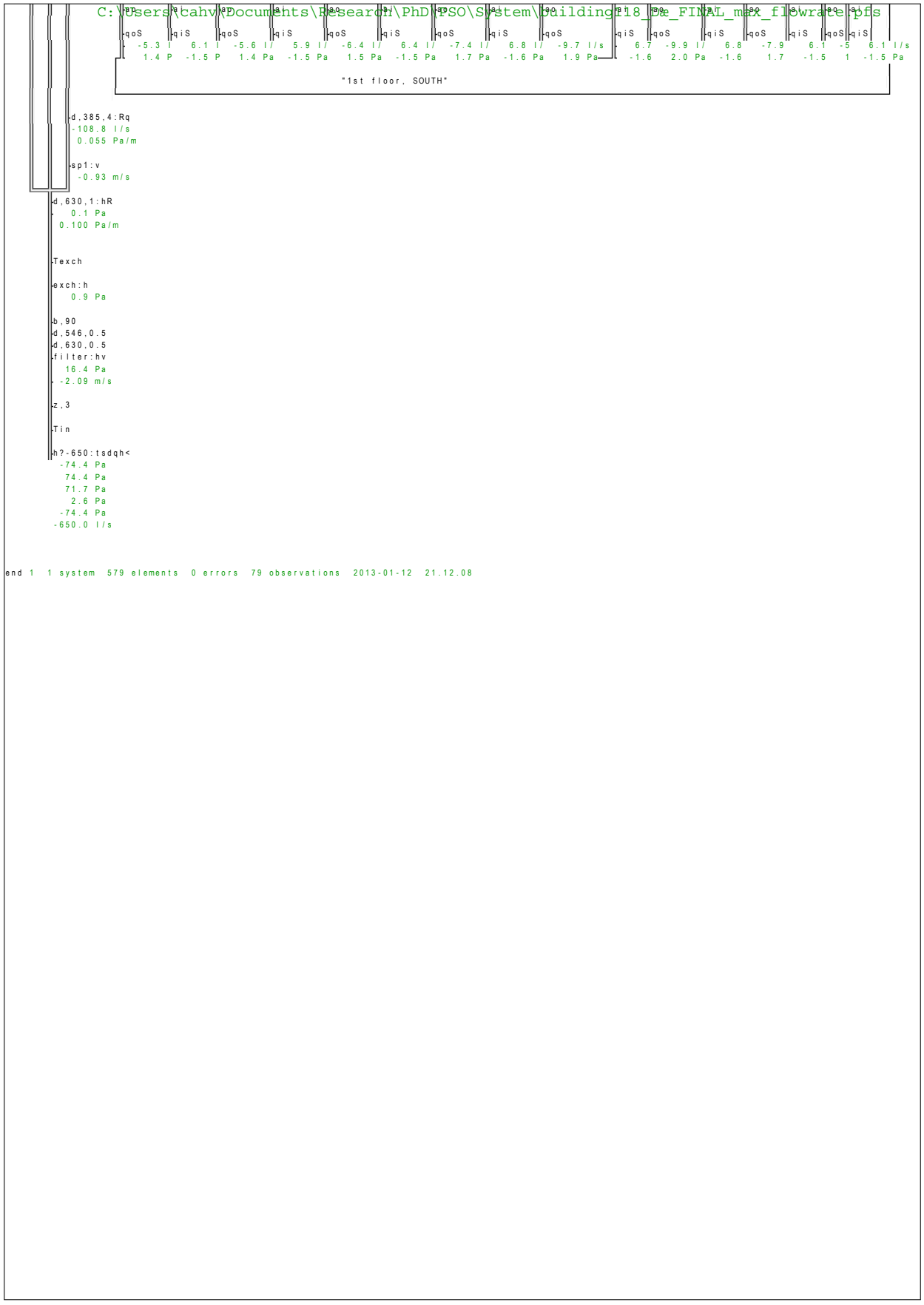
C:\Users\cahv\Documents\Research\PhD\PSO\System\Building18_De_FINAL_max_flowrate.pfs
qoS qiS qoS qiS qoS qiS qoS qiS qoS qiS qoS qiS qoS qiS qoS qiS qoS qiS
-5.3 l 6.1 l -5.6 l/ 5.9 l/ -6.4 l/ 6.4 l/ -7.4 l/ 6.8 l/ -9.7 l/s 6.7 -9.9 l/ 6.8 -7.9 6.1 -5 6.1 l/s
1.4 P -1.5 P 1.4 Pa -1.5 Pa 1.5 Pa -1.5 Pa 1.7 Pa -1.6 Pa 1.9 Pa -1.6 2.0 Pa -1.6 1.7 -1.5 1 -1.5 Pa
"1st floor, SOUTH"
d,385,4:Rq
-108.8 l/s
0.055 Pa/m
sp1:v
-0.93 m/s
d,630,1:hR
0.1 Pa
0.100 Pa/m
Texch
exch:h
0.9 Pa
b,90
d,546,0.5
d,630,0.5
filter:hv
16.4 Pa
-2.09 m/s
z,3
Tin
h?-650:tsdqh<
-74.4 Pa
74.4 Pa
71.7 Pa
2.6 Pa
-74.4 Pa
-650.0 l/s
end 1 1 system 579 elements 0 errors 79 observations 2013-01-12 21.12.08

# Appendix E

# Schematics of original ventilation

This appendix comprises schematics of the original ventilation system in building 118, DTU. Four almost identical supply and exhaust systems each ventilate 1/4 of the building. Only the quarter in question is shown. The shown systems are:

1. Supply with three main ducts to each floor
2. Exhaust with three main ducts from each floor

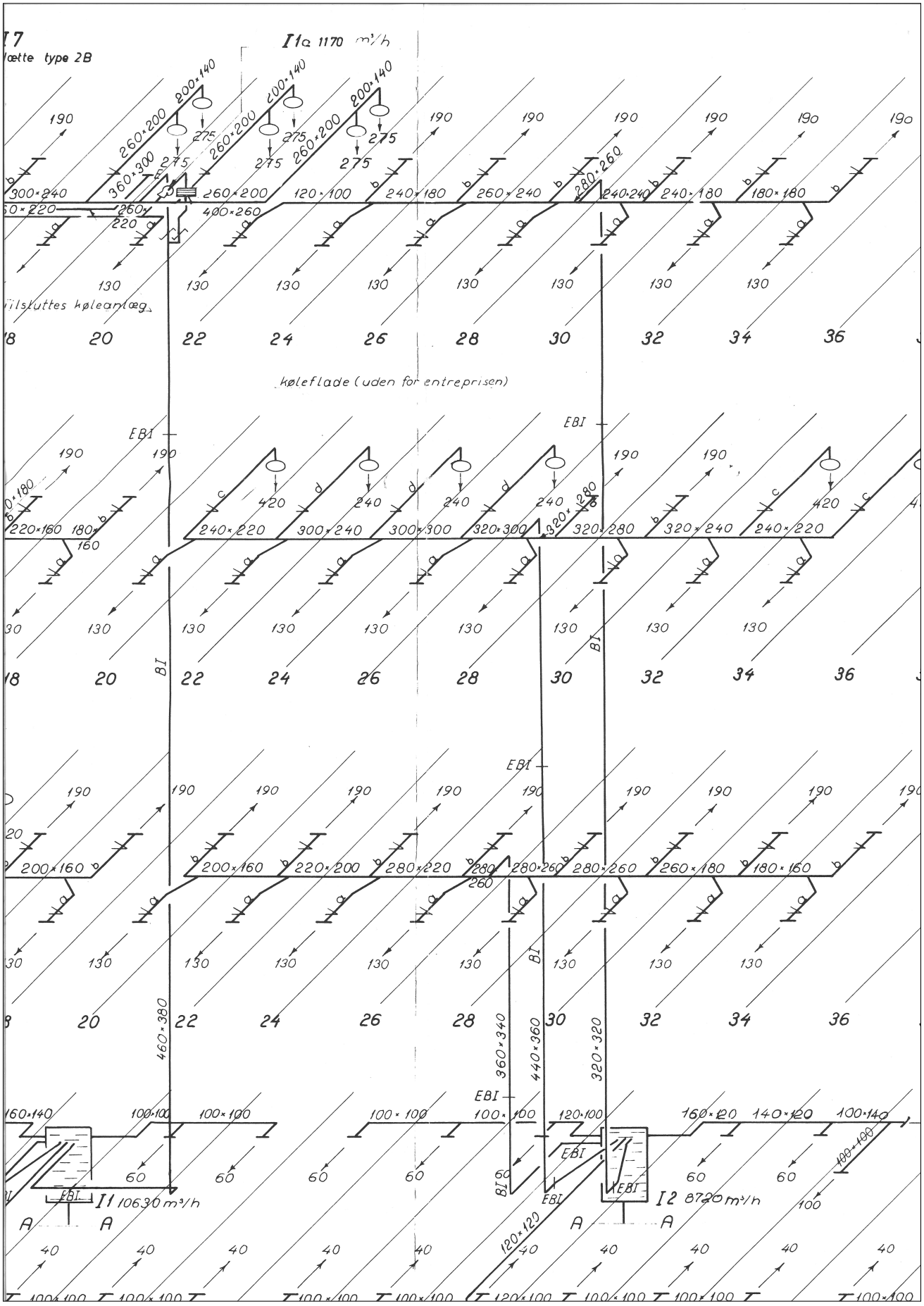
I7
Iła 1170 m³/h
type 2B
190
200×140
260×200
275
360×300
300×240
260×200
120×100
240×180
260×240
280×260
240×240
180×180
400×260
130
18
20
22
24
26
28
30
32
34
36
køleflade (uden for entreprisen)
EBI
BI
220×160
240×220
300×240
300×300
320×300
320×280
420
240
200×160
220×200
280×220
280×260
260×180
180×160
460×380
360×340
440×360
320×320
160×140
100×100
120×100
160×120
140×120
100×140
60
40
120×120
I1 10630 m³/h
I2 8720 m³/h
A
A

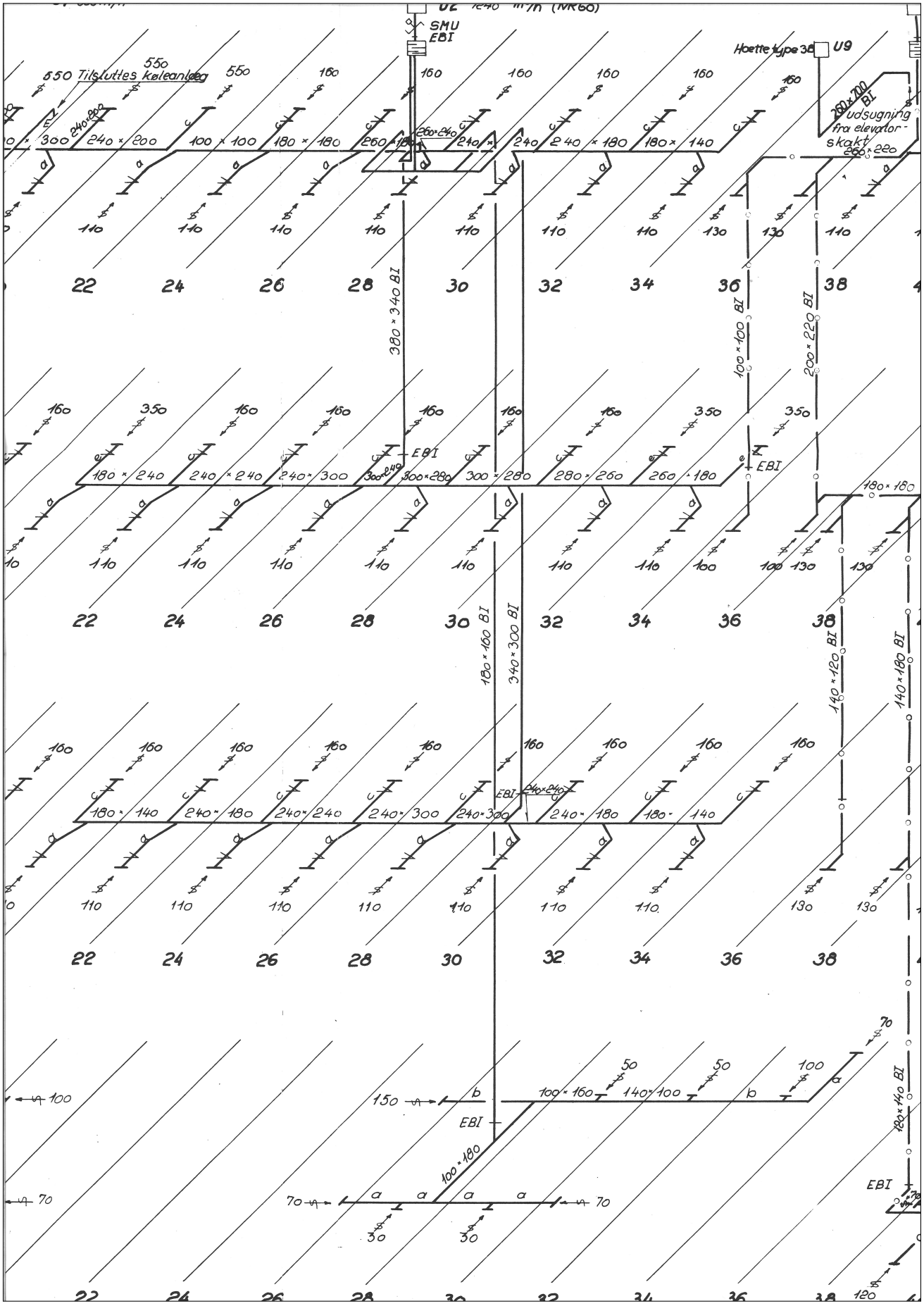
SMU
EBI
Tilsluttes køleanlæg
Hætte type 38
U9
udsugning fra elevator-skakt
EBI
22
24
26
28
30
32
34
36
38

# List of Symbols

# List of Figures

# List of Tables